論文 / 著書情報
Article / Book Information

題目(和文)	
Title(English)	Physical tar removal using oil-based absorption in venturi scrubber producing syngas microbubble for biomass gasification
著者(和文)	ウンヤパン シリワット
Author(English)	Siriwat Unyaphan
出典(和文)	学位:博士(工学), 学位授与機関:東京工業大学, 報告番号:甲第10655号, 授与年月日:2017年9月20日, 学位の種別:課程博士, 審査員:吉川 邦夫,竹下 健二,日野出 洋文,高橋 史武,時松 宏治,梶谷 史朗
Citation(English)	Degree:Doctor (Engineering), Conferring organization: Tokyo Institute of Technology, Report number:甲第10655号, Conferred date:2017/9/20, Degree Type:Course doctor, Examiner:,,,,,
学位種別(和文)	博士論文
Type(English)	Doctoral Thesis

PHYSICAL TAR REMOVAL USING OIL-BASED ABSORPTION IN VENTURI SCRUBBER PRODUCING SYNGAS MICROBUBBLE FOR BIOMASS GASIFICATION

Siriwat Unyaphan

Supervisor: Professor Kunio Yoshikawa

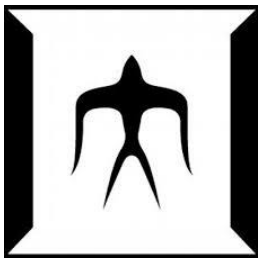

A doctoral dissertation submitted to

Department of Environmental Science and Technology

Interdisciplinary Graduate School of Science and Engineering

Tokyo Institute of Technology

Yokohama, Japan

September 2017

ACKNOWLEDGEMENTS

Firstly and most importantly, I would like to express my gratitude to Professor Kunio Yoshikawa, as the supervisor, for giving me the precious opportunity to study in Japan including his wisdom and motivation providing to me during the study.

I would like to express my gratitude to Associate Professor Fumitake Takahashi and Associate Professor Koji Tokimatsu for their valuable guidance and suggestion on this doctoral dissertation and one-on-one meeting which greatly improve the quality of my research. I would further like to express my gratitude to the dissertation committees, Professor Kenji Takeshita, Professor Hirofumi Hinode and Professor Shiro Kajitani for their valuable suggestions, constructive criticisms and thorough reviews.

I would like to acknowledge the Innovative Science and Technology Initiative for Security, ATLA, Japan, the Ministry of Defense, Japan and the Siam Cement Public Company Limited (SCG), Thailand for providing the research financial and facility support. I gratefully acknowledge the Ministry of Education, Culture, Sports, Science and Technology (MEXT), Japan for the five-year financial support during my study in Japan.

This dissertation would not be completed without all unwavering supports from Assistant Professor Kiyoshi Tsuji, Dr. Thana Phuphuakrat, Dr. Muhammad Kunta Biddinika, Dr. Thanyawan Tarnpradab, Mrs. Eriko Ohno, Mr. Alex Obrero Mosqueda, Mr. Chanatip Kupradit, Mr. Vitid Assavarut and all of Yoshikawa-Takahashi-Tokimatsu Laboratory's members

I would also like to thank Assistant Professor Wichai Siwakosit, Kasetsart University, Thailand for his recommendation to study in Yoshikawa laboratory.

Finally, I am greatly indebted to my parents, sister and Pupipatphol family for their eternity love and unconditional support. I would like to express my special gratitude to Tarnpradab family for their encouragement and support as well.

Siriwat Unyaphan

August 15, 2017

ABSTRACT

Biomass gasification process produces not only the syngas but also some undesirable products especially tar, which causes the blocking and fouling in piping systems and downstream components. This research aims to develop a low cost and high efficiency physical tar removal by absorption technique. Three main aspects were investigated; absorbent characteristic, scrubber type and absorbent regeneration. Firstly, the characteristic of emulsified absorbent was studied to maximize the tar removal efficiency for both polar and non-polar tar. Secondly, the venturi scrubber producing syngas microbubble was investigated based on various parameters; the size distribution, the mean microbubble diameter, the number density, the specific absorption surface area, Reynolds number and the mass transfer modelling. Then, the tar removal efficiency of the pilot gasifier was conducted by a venturi scrubber. Finally, the study of air-blown stripping for absorbent regeneration was investigated comparing with the filtration and the centrifugal sedimentation.

CONTENTS

LIST OF FIGURES

LIST OF TABLES

Chapter 1

Introduction

1.1 Background

For past several decades, energy is a necessary and fundamental factor in daily life, business and industry such as transportation, telecommunication, entertainment, manufacturing and so forth. For this reason, the world energy demand is continuously growing. Figure 1.1 illustrates the history and projection of world energy demand between 1990 and 2040 released by U.S. Energy Information Administration (EIA) [1.1]. It can be seen that the world energy consumption will grow by 48% between 2012 and 2040. Therefore, energy security is the challenging issues. A reliable energy should be supplied with sufficient quality, high quality and economical prices. Nevertheless, the fossil fuels like crude oil, natural gas and coal are non-renewable energy resources, which take several million year to reproduce. They also have significant impacts on the environment leading to greenhouse gas emission and climate change. Furthermore, the unstable price of crude oil in the world market has had a huge effect on the economy of several countries, especially in Asia. As a result, several countries supported the utilization of renewable energy to promote energy security and environmental conservation. It can be observed from Figure 1.1 that renewable energy is expected to increase by an average 2.6% per year through 2040.

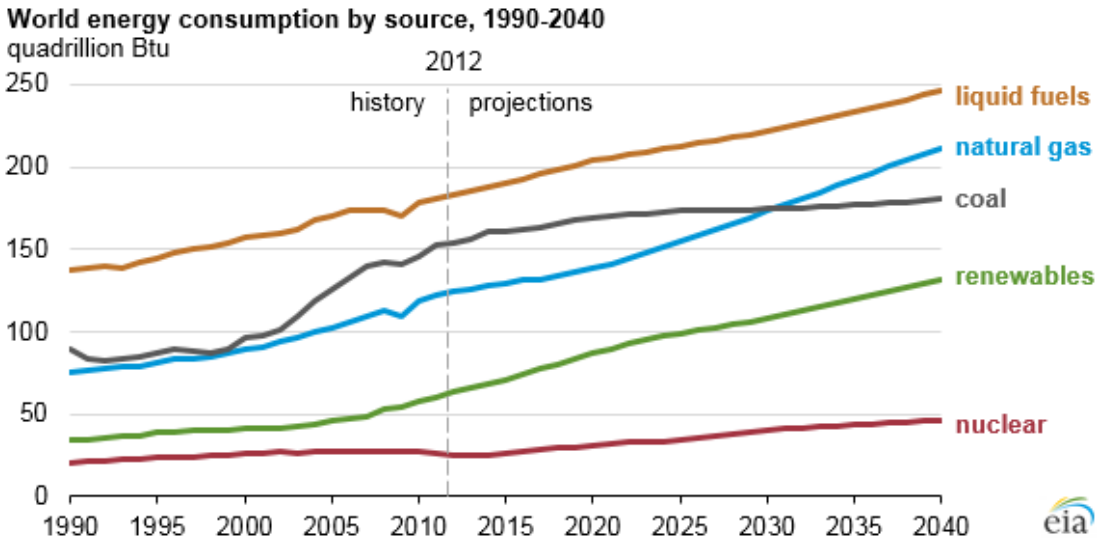

Figure 1.1. History and projection world energy consumption between 1990 and 2040

As developing country that heavily imported fossil fuels for power generation, Thailand has already experienced rampant impacts of energy crisis which could become major obstacles for the country's future development. Moreover, carbon dioxide emissions from electricity generation in Thailand increased by 16.5% from 1993 to 2008 [1.2]. Figure 1.2 illustrates histogram of carbon dioxide emission from electricity generation in Thailand during 1986-2008. It was found that the average growth of carbon dioxide emission was 3.2% per year. Therefore, the revised power development plan for the next decades is to mainly increase higher proportion of renewable energy utilization [1.3]. The renewable energy is technologies which can produce heat or electricity without burning fossil fuels and constantly renewed such as solar energy [1.4], wind energy [1.5], geothermal energy [1.6], hydropower energy [1.7] and biomass energy [1.8,1.9]. These technologies will support not only the growth of energy demand but also reduce the uncertainty of imported fossil fuels prices.

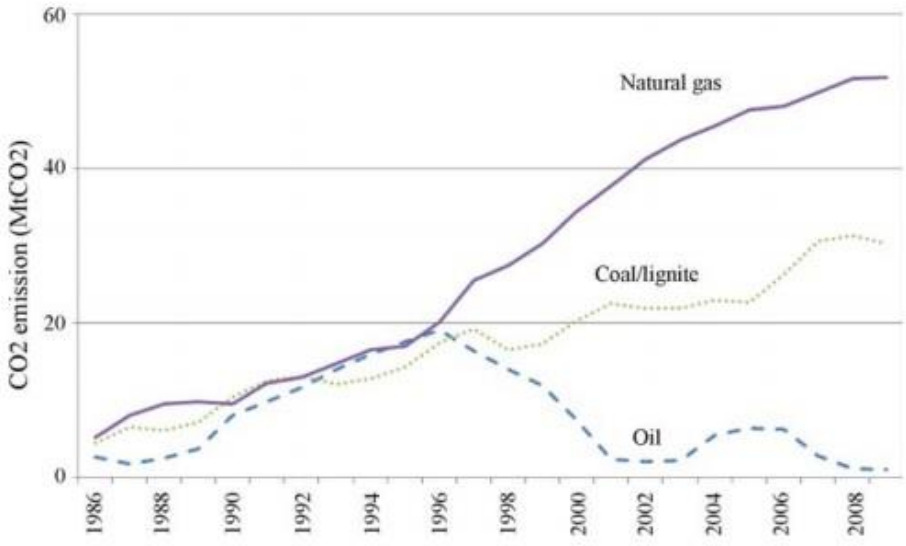

Figure 1.2. Carbon dioxide emissions from electricity generation in Thailand (Ministry of Energy, Thailand)

Biomass is one of the most interesting candidates as a renewable energy resources. There is no CO_2 emission released to the atmosphere due to its carbon neutrality. Three main biomass sources in Thailand are from agricultural residues, forest industry and residential sector. Agriculture is a major business in Thailand. There are high potentials for all types of renewable energy sources produced by agricultural products such as rice, sugarcane, rubber, palm, cassava and so forth. The process of these agricultural products produced large amount of residues, which could be used as fuels. Table 1.1 concludes the evaluation of biomass potential of Thailand in 2004 [1.10].

Table 1.1. Evaluation of biomass potential of Thailand in 2004 Unit: (1,000 tons per year)

Biomass	Production	Residue	Crop-residue ratio	Amount	Surplus availability factor	Unused residue
Sugar cane	70,101	Bagasse	0.291	20,399	0.207	4,223
		Trash	0.302	21,171	0.986	20,874
Rice	26,841	Rice husk	0.230	6,173	0.493	3,044
			0.447	11,998	0.684	8,207
		Rice straw				
Palm	4,903	EFB	0.250	1,226	0.584	716
		Fiber	0.147	721	0.134	97
		Shells	0.049	240	0.037	9
		Fronds	2.604	12,767	1.000	12,767
Total				**74,695**		**49,936**

There are two main technologies to convert biomass to energy that is the biochemical [1.11] and the thermochemical process [1.12]. However, biochemical techniques have some difficulties on feedstock variability, expensive and specific cellulosic enzymes, microorganism requirement, low biofuel yield and expensive pretreatment cost [1.13,1.14]. Thermochemical techniques are more feasible for energy transformation, higher yield production and compatible with the existing technologies utilized for fossil fuel as well. There are various thermochemical conversion pathways of biomass such as pyrolysis, liquefaction, gasification and combustion [1.12]. The stored energy in biomass could be directly released as heat by combustion or transformed to solid (charcoal and ash), liquid (bio-oil) and gaseous products (syngas) by pyrolysis, liquefaction and gasification. Figure 1.3 illustrates the thermochemical process for biomass energy production and their products.

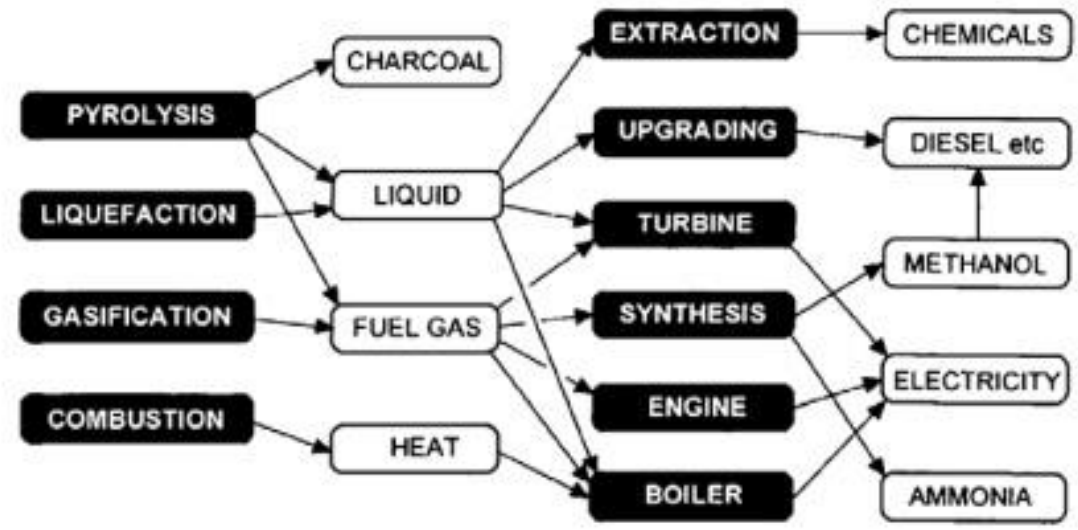

Figure 1.3. Thermochemical process for biomass energy production and their products

1.1.1 Combustion

Combustion is the most widely used technology for the thermochemical conversion among others. The thermal decomposition process that takes place when biomass is burnt in an excess of oxygen is the complete combustion. Over 97% of biomass energy production utilized this technology due to its operational simplicity. There are three main processes occurred during biomass combustion that is drying, pyrolysis and combustion of volatile gases and solid char [1.15]. 70% of the overall heat generation come from the combustion of volatile gases. The combustion of volatile gases commonly take place above the bed with yellow flames, while the combustion of solid chars take place at the bed with small blue flames [1.15,1.16]. There are three main types of combustion system that is the fixed bed, the fluidized bed and the entrained flow combustor [1.17]. For the fixed bed combustor, it is widely used for biomass combustion. It consists of one combustion room with a grate. When feeding biomass to the combustion room, it is pyrolyzed into volatile gases and chars. A primary air is supplied at under the grate for combustion of chars, while a greater secondary air is supplied at above the grate for combustion of volatile gases due to the high content of volatile matter in biomass. The heat from char combustion is responsible for pyrolysis of newly fed biomass. The operational temperature of fixed bed combustor is around 850-1400°C [1.15]. For the fluidized bed combustor, the combustion efficiency is higher than the fixed bed combustor. It is suitable to implement in the commercial scale. The fluidized bed combustor employs silica sand, limestone, dolomite or other non-combustible materials as the bed material in order to behave like the heat transfer media fluidized by the air flow from the bottom. Biomass intermixed with the moving bed material has a high combustion

efficiency. It is able to be further classified into the bubbling fluidized bed (BFB) and the circulating fluidized bed (CFB). The operational temperature of the fluidized bed combustor is around 700-1000°C. For the entrained flow combustor, it is well known for the coal combustion process. The operational temperature of the entrained flow combustor is around 1200-1500°C

1.1.2 Pyrolysis

Pyrolysis is a thermal decomposition that takes place in the absence of oxygen so as to convert the biomass into chars, bio-oils and volatized gases. There are three main processes occurred during biomass pyrolysis that is the pre-pyrolysis process, the main pyrolysis process and the continuous char de-volatilization [1.18–1.20]. The pyrolysis process can be further classified into the fast pyrolysis and the slow pyrolysis. For the fast pyrolysis, it is the pyrolysis process with a high heating rate and a short residence time. The main product of the fast pyrolysis is bio-oils consisted of an aqueous phase containing various light organo-oxygen compounds and a non-aqueous phase (tar). Bio-oils from the fast pyrolysis have a potential to be utilized as liquid fuel. A fine biomass particle size (<1 mm) is required in this process. The most common pyrolyzer for the fast pyrolysis is the bubbling fluidized bed, the circulating fluidized bed and the entrained flow reactor [1.21]. The operational conditions of the fast pyrolysis are the temperature in the range of 450-550°C, the high heating rate (>200°C/s) and the short residence time (<4 s). For the slow pyrolysis, it is a pyrolysis process with a low heating rate and a long residence time. The main product of the slow pyrolysis is char which can be utilized in various applications such as activated carbon, adsorbent, soil condition, pharmaceutical and so forth. The biomass with higher lignin contents and lower hemicellulose contents can be pyrolized into a higher yield of char product. The most common pyrolyzer for the slow pyrolysis is the rotary kiln or the moving bed pyrolyzer.

1.1.3 Liquefaction

Liquefaction is a thermal decomposition that takes place in a low temperature and a high pressure so as to break down the biomass into fragments of small molecules in water or another suitable solvents. The product of liquefaction can be re-polymerized into oily compounds as bio-oil [1.22]. The most widely used types of biomass for bio-oil production in the liquefaction process are lignocellulosic biomass. The main process occurred during the biomass liquefaction is de-polymerization into monomer (decomposition). These monomers may re-polymerized or condensed into solid char, which is undesirable product. A solvent is generally added to slow down the higher solid phase reactions resulting in reducing the detrimental condensation reactions. Comparing to the pyrolysis process, this process is similar to pyrolysis in terms of the target products, which is liquid products. However, the operational conditions of liquefaction are in a lower reaction temperature but

in a higher pressure than pyrolysis. Drying of the biomass do not required for liquefaction, but it is a necessary step for pyrolysis.

1.1.4 Gasification

Gasification is a thermal decomposition that converts carbonaceous biomass into combustible gases or syngas such as H_2, CO, CO_2 and CH_4, which takes place in the presence of a partial oxygen. The gasification process is similar to the combustion process, but it is considered as a partial combustion process. Table 1.2 summarizes the comparison of gasification and combustion [1.23]. It can be seen that the purpose of combustion focuses on heat generation, while gasification focuses on gaseous production. The syngas from the gasification process can be further utilized such as direct combustion for heat generation, gaseous fuel for electricity production, chemical products and so forth. In terms of the specific heating values and the industrial application, syngas can be classified into four groups as summarized in Table 1.3 [1.23].

Table 1.2. Comparison of gasification and combustion

Features	Gasification	Combustion
Purpose	Creation of valuable, environmental friendly, usable products from waste or lower value material	Generation of heat or destruction of waste
Process type	Thermal and chemical conversion using no/limited oxygen	Complete combustion using excess oxygen (air)
Gas composition	H2, CO, H_2S, NH_3, and particulates	
Gas cleanup	- Syngas cleanup at atmosphereic to high pressures depending on the gasifier design	- Flue gas cleanup at atmospheric pressure
	- Treated syngas used for chemical, fuels, or power generation	- Treated flue gas is discharged to atmosphere
Solid byproducts	Char or slag	Bottom and fly ashes
Ash/char or slag handling	- Low temperature processes produce a char that can be sold as fuel - High temperature processes produce a slag, a nonleachable, non-hazardous material suitable for use as construction materials	Bottom ash and fly ash are collected, treated, and disposed as hazardous waste in most cases or can be sold as a material for making concrete

	- Fine particulates are recycled to gasifier	
Pressure	Atmospheric to high	Atmospheric

Table 1.3. Heating values and application of four types of syngas

Type of syngas	Typical heating value (MJ/m^3)	Application in industry
Low heating value gas	3.5 - 10	Gas turbine fuel, boiler fuel and fuel for smelting
Medium heating value gas	10 - 20	Gas turbine fuel, hydrogen production, fuel cell feed, chemical and fuel synthesis and substitute natural gas with methanation process
High heating value gas	20 - 35	Gas turbine fuel, SNG and hydrogen production, fuel cell feed and chemical and fuel synthesis
Substitute natural gas (SNG)	>35	Substitute for natural gas, hydrogen and chemical production, fuel cell feed

During the biomass gasification process, the biomass is heated up with a gasifying agent like air, oxygen, steam, carbon dioxide or the mixture of these gasifying agents to produce the syngas in the partial combustion condition. The main processes occurring during the biomass gasification consist of drying, pyrolysis, combustion and reduction as shown in Figure 1.4 [1.24].

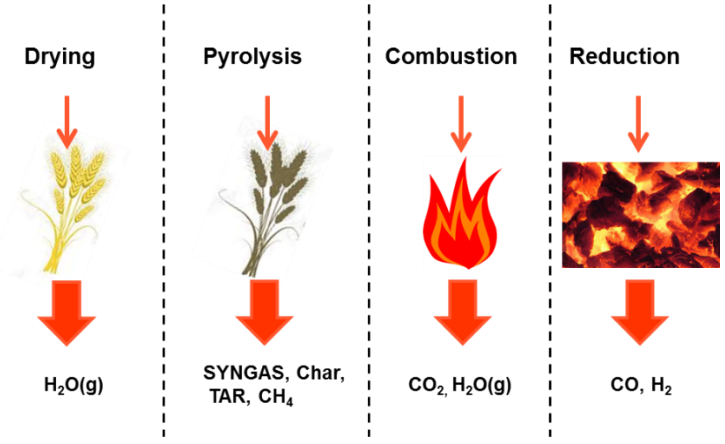

Figure 1.4. Main processes during biomass gasification

In the drying process, all of moisture contained in biomass is vaporized by the thermal energy from the oxidation process up to 150°C. After that, the pyrolysis process takes place in the temperature range of 200-700°C. Carbon dioxide and acetic acid are firstly produced in the temperature range of 200-280°C. Then, large quantities of tar and volatile gases are mainly produced in the temperature range of 280-500°C. From 500°C to 700°C, the gaseous products are still produced with only a small portion, but hydrogen is produced in this temperature range. Generally, non-volatile biomass during the pyrolysis process constitutes about 5% - 25% by weight, which is called as “char”. In the combustion or oxidation process, heat is the main product to produce the energy driving the whole process of gasification. The mixture of CO, CO_2, and H_2O is the by-product from this process. Finally, all products in the pyrolysis and oxidation process is reacted in the reduction process. The reduction temperature is the key parameter of the overall process and used to optimize the char and syngas characteristics, which is illustrated in Figure 1.5. In addition, the major and minor reactions occurring in the gasifier is summarized in Table1.4.[1.25].

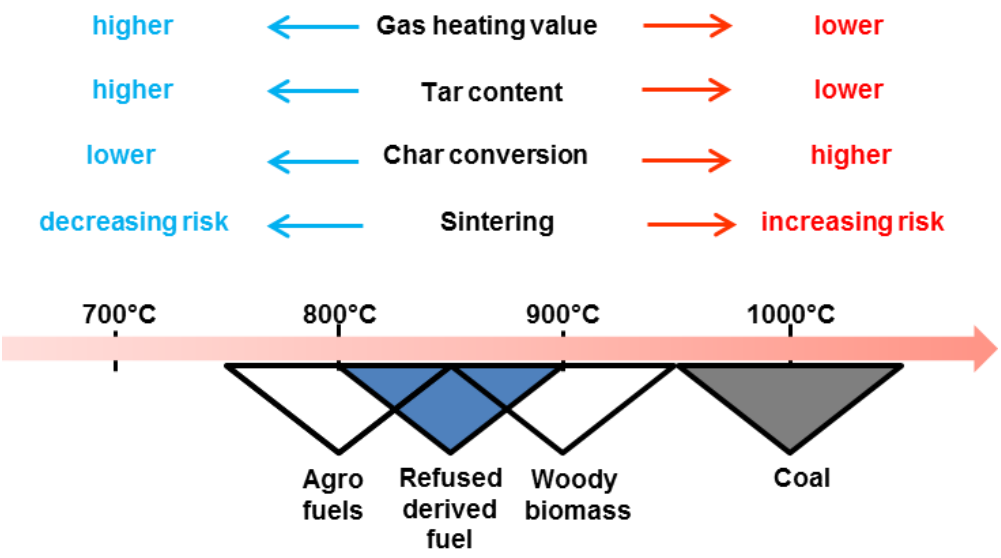

Figure 1.5. Influence of the temperature change on the critical process characteristics

The types of the gasification system is the same as the combustion system that is the fixed bed (updraft and downdraft), the fluidized bed (bubbling and circulating type) and the entrained flow gasifier [1.26]. The advantages and disadvantages of each gasifier are summarized in Table 1.5 [1.27].

Table 1.4. Major and minor reactions in biomass gasification

Major reaction		**$\Delta H°_{298}$(kJ/mol)**	**Name**
$C + 1/2O_2 = CO$	**R1**	**-110.5**	Partial oxidation reaction (or gasification with oxygen)
$C + O_2 = CO_2$	**R2**	**-393**	Complete oxidation reaction (or combustion with oxygen)
$C + CO_2 = 2CO$	**R3**	**+172**	Boudourd reaction (Gasification with carbon dioxide)
$C + H_2O = CO + H_2$	**R4**	**+131.4**	Water gas reaction (Gasification with stream)
Minor reaction		**$\Delta H°_{298}$(kJ/mol)**	**Name**
$C + 2H_2 = CH_4$	**R5**	**-74.8**	Hydrogasification reaction (Gasification with hydrogen)
$CO + H_2O = CO_2 + H_2$	**R6**	**-40.9**	Water gas shift reaction
$CO + 3H_2 = CH_4 + H_2O$	**R7**	**-205**	Methanation

Table 1.5. Advantages and disadvantages of different gasifier design

Type	**Advantages**	**Disadvantages**
Updraft	- Simple construction - High thermal efficiency - High carbon conversion - Usable with high ash content feedstock	- High tar content - Limited for scaling up
Downdraft	- Simple construction - High carbon conversion - Usable with high ash content feedstock - Low tar content	- Low moisture content feedstock required - Limited for scaling up
Bubbling Fluidized bed	- High gas-solid mixing - Moderate tar content - High conversion efficiency - Potential for scaling-up	- High ash content - Ash molten problem in some feedstock

Circulating Fluidized bed	- High carbon conversion - Moderate tar content - High conversion efficiency - Potential for scaling-up	- High ash content - Ash molten problem in some feedstock - High energy consumption
Entrained Flow	- Potential for scaling-up - Low tar content	- Particle size limits - Large amount of carrier gas - High particle load

1.2 Tars in biomass syngas

Although the biomass gasification is one of the promising conversion technologies to overcome the global warming issues and the depletion of fossils fuels and its gaseous products called “syngas” is widely applicable to various applications such as heat and power generation and chemical production, where the main obstacle of the syngas utilization is the blocking and fouling by tar in piping systems and downstream components due to its condensation and polymerization at the temperature below 350°C [1.28]. In this study, the purpose of the syngas utilization is mainly focused on the power generation in the internal combustion engines. In order to prevent the gas engine breakdown, the tar content in the syngas must be lower than 100 mg/Nm3, while the tar content in fluidized bed gasifiers (10,000–40,000 mg/Nm3) is often much higher than the limitation [1.29,1.30]. Therefore, it is essential to reduce the tar concentration to expand the syngas utilization.

The definition of tar is a complex mixture of secondary and tertiary products (mostly aromatic hydrocarbon) from the thermal decomposition or partial oxidation of organic material. According to the Energy Research Center of the Netherland (ECN) [1.31], tar consists of various organic aromatic ring hydrocarbon, which can be classified into five classes based on composition, delectability, water solubility and condensation behavior of individual compounds as summarized in Table 1.6. It is found that the tar class 1 or the gravimetric tar is the heaviest tar among the others. The gravimetric tar starts to condense at around 300-350°C. In addition, Figure 1.6 illustrates the relationship between the light tar (class 2-5) dew point and the concentration of the different classes, which can be concluded as following. Tar dew point increases with an increase of tar concentration because the condensation of tar is an integral of all tar classes. When the tar vapor pressure exceeds the saturation pressure, it leads to condensation of saturated vapor. The tar dew point of the class 3 is the lowest, while the classes 2, 4 and 5 are relatively high, which results in fouling and blocking in downstream components. Therefore, the removal of the class 1, the class 2, the class 4 and the class 5 is mainly concerned.

Table 1.6. Classification of tar

Tar classification	Definition
Class 1	GC undetectable tar: It contains heavy poly-aromatic hydrocarbon, which is more than 7 rings. It could be called heavy tar or gravimetric tar as well.
Class 2	Heterocyclic compounds: It is highly water soluble hydrocarbon such as phenol.
Class 3	Aromatic compounds: It is one-ring aromatic hydrocarbon, which does not cause condensation and solubility problem such as benzene, toluene, xylene, and styrene.
Class 4	Light poly-aromatic compounds: It is two and three rings aromatic hydrocarbon, which condense at relatively high concentration at moderate temperature, such as indene, naphthalene, phenanthrene and anthracene.
Class 5	Heavy poly-aromatic compounds: It is from four to seven rings aromatic hydrocarbon, which condense at low concentration at high temperature such as pyrene, fluoranthene, chrysene.

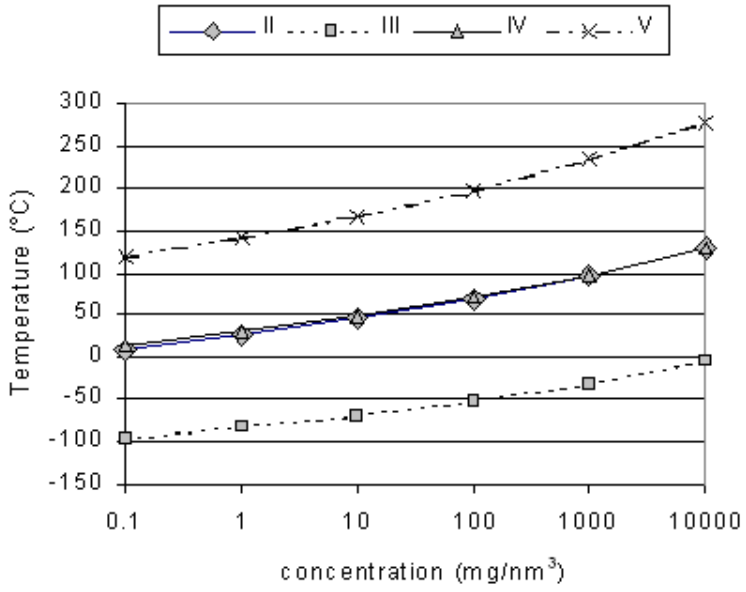

Figure 1.6. Relationship between the tar dew point and the concentration of the different classes

Currently, there are two methods to remove tar components [1.32]. One method is the chemical removal, where tar is destructed or converted to permanent gases or smaller molecules, by employing the thermal, the catalytic cracking and so forth [1.33,1.34]. The chemical methods can be done either

in the gasifier itself or outside the gasifier. However, these advanced techniques require a very high-temperature operation (>1,000°C) [1.35,1.36], modification of conventional gasifiers [1.37] and expensive catalysts [1.38]. Thus, the main consideration in this study is the employment of a low cost and highly effective tar removal method. The other method is the physical removal, where tar is simply trapped or captured without any chemical reactions, such as scrubbing and so forth [1.39–1.42]. The physical methods can be done only outside of the gasifier. The advantages of this technique are the operation of gasifier at a lower temperature specifically 800°C, no modification of conventional gasifiers, no usage of catalyst, highly effective tar removal and uncomplicated and economical operation in the commercial scale [1.43]. Among the physical methods, the absorption technique performed the best tar removal performance. Therefore, the physical tar removal by the scrubbing technique has been studied in this work. Table 1.7 summarizes the tar removal techniques of chemical and physical methods.

Table 1.7. Tar removal techniques of chemical and physical methods

Chemical method	Physical method
- Thermal cracking	- Cyclone
- Reforming	- Filter (baffle, fabric, ceramic, granular beds)
- Catalytic cracking	- Electrostatic precipitator
- Plasma reactor (Pyroarc, Corona, Glidare)	- Scrubber (absorption)
- Use of catalytic bed material	- Adsorbers

1.3 Literature reviews on tar removal by absorption technique

In the industrial sector, wet scrubbers have been widely used since 18th century in order to control the concentration of particles and other impurities in gases. It could be classified into two major application; the particle collection and the gas absorption. The particle collection relies on three main inertial forces; impaction, interception and diffusion, while the gas absorption relies on the absorbent selection, the creation of large absorption surface area through the variety of mechanical methods (scrubber type) and absorbent regeneration [1.44]. Therefore, the study on tar removal by absorption technique is divided into three main aspects that is absorbent selection, scrubber type and absorbent regeneration.

For absorbent selection, various types of absorbents for tar removal have been investigated previously. With Japanese cedar as a feed stock, the study on polar absorbents and non-polar absorbents found that water, which is a conventional absorbent and polar substance, removed only

31.8% of the gravimetric tar, whereas 60.4% gravimetric tar was removed by vegetable oil which is non-polar [1.39]. In addition, with sewage sludge as feed stock, the gravimetric tar removal performance of water was just 10.3% while that of vegetable oil was 60.2% [1.41]. Therefore, vegetable oil (non-polar substance) is a more appropriate tar absorbent than water (polar substance). However, due to the high price of vegetable oil, the tar absorption performance was compared between waste cooking oil and vegetable oil focusing on the effect of the mixing speed. Previous research on tar absorption mainly focused on polar and non-polar absorbents separately, and there is no combination of polar and non-polar absorbents for tar removal. As it is well-known that the main proportion of tar is non-polar but some are polar ones, an emulsified oil (mixture of oil and water) is investigated in this study in order to maximize the tar removal performance in the absorbent selection aspect.

For the scrubber type, the bubbling scrubber was generally studied in laboratory scale, however, the absorption surface area between tar and absorbent was relatively low. The tar removal efficiency of vegetable oil in conventional bubbling scrubber was about 60.4% [1.39]. Then, the modified bubbling scrubber with a magnetic stirrer was utilized to increase the turbulent mixing and found that the tar removal efficiency increased compared to conventional one [1.40]. However, the tar concentration in the treated syngas is still higher than limitation. This is because most of the syngas bubbles were still visually observed leading to a low absorption surface area, where a number of tar molecules in a large syngas bubble diameter were escaped from the scrubber. Therefore, the bubbling scrubber is not appropriate for real implementation. Then, the performance of vegetable oil in packed bed scrubber was investigated and the tar removal efficiency was about 75.0%, where the tar concentration could be lower than 100 mg/Nm3 as long as the inlet tar concentration is lower than 600 mg/Nm3 [1.45]. However, the tar concentration in general air-blown biomass gasifiers was between 10,000 and 150,000 mg/Nm3 [1.29]. The similar result was also confirmed in other study, where the absorbent type, the column bed height, the absorbent temperature and the absorbent flow rate were varied [1.46]. In addition, previous study reported the potential for tar removal of venturi scrubber could be in the range from 50% to 90% [1.47]. It was also confirmed that the tar removal efficiency of water in a venturi scrubber was up to 81%, where the increasing water flow rate enhanced the efficiency [1.48]. Therefore, in order to completely remove tar by scrubbers, one of the possibility to achieve the target is to increase the turbulent mixing in a venturi scrubber. The increase of the turbulent mixing should improve the syngas bubbles getting smaller until it become microbubbles, which resulted in the increase of the absorption surface area and that gave more area for tar to be absorbed. Therefore, a venturi scrubber was mainly studied in this aspect.

For the absorbent regeneration, previous research investigated the absorbent regeneration by the centrifugal sedimentation and filtration techniques [1.49]. It was found that, during 10 hours of the experiment without regeneration of the used oil, only 48% of the gravimetric tar could be removed as a result of solid particle and tar accumulation in the oil obstructing the oil absorbability. 16.6 g of the gravimetric tar could be absorbed in 1 liter of canola oil. With the regeneration of the used oil, the tar removal efficiency was able to be improved to 78 and 83% by the filtration and the centrifugal sedimentation, respectively. The tar removal capacity was shown to be increased to 160 and 175% by the filtration and the centrifugal sediment, respectively, compared to non-regenerated oil. In addition, OLGA tar removal technology reported the absorbent regeneration technique by the stripping. The absorbent was regenerated in the stripper by using air to trip the tar. However, the tar removal capacity and the efficiency of this technique was not reported. Therefore, the performance of the air-blown stripping for the absorbent regeneration was mainly studied in this aspect.

1.4 Objective and outline of the thesis

This research aims to develop a low cost and high efficiency tar removal technique for electricity generation in the biomass gasification process. The physical tar removal method by the absorption technique is utilized in order to achieve the acceptable limitation of the tar content for utilizing the synthesis gas in electricity generation. The tar removal performance of oil-based absorbent in a venturi scrubber producing syngas microbubble is investigated in both the laboratory and the pilot scale during the pyrolysis/gasification of biomass. This thesis is divided into three main aspects that are the absorbent selection, the scrubber type and the absorbent regeneration. The content has been divided into six chapters as below.

Chapter 1. Introduction

In this chapter, the basic background of the biomass gasification technology and the problems of tar formation in downstream components are introduced, respectively. The tar removal techniques are also reviewed, where the attention is paid to the physical method for tar removal by absorption. Then, the literature reviews on the development of tar removal are shown in three main aspects; the absorbent selection, the scrubber type and the absorbent regeneration. Finally, the objectives and the originality of this research are stated.

Chapter 2. Effect of emulsified absorbent for tar removal in biomass gasification process

The objective of this study is to maximize the tar removal performance for both polar and non-polar tar components by comparing between the emulsified oil (EO) and the pure vegetable oil (VO). Real tar produced by the pyrolysis of Japanese cedar is introduced in a scrubber and tar is removed

by the pure vegetable oil and the emulsified oil with varying water content from 2.5% to 15%. The study can be divided into two parts; the gravimetric tar removal performance of EO compared with VO and the light tar removal performance of EO compared with VO.

Chapter 3. Improvement of tar removal performance of oil scrubber by producing syngas microbubbles

This study first presents a fundamental investigation on the microbubbles formation utilizing the venturi scrubber. Vegetable oil is selected as the absorbent in this study. In the laboratory scale experiment, the venturi tubes with various throat diameter ratios (0.17, 0.42 and 0.67) and inverter frequencies (40, 50 and 60 Hz) are tested. Based on various venturi tube designs, the microbubble size distribution, the mean microbubble diameter, the number density and the specific absorption surface area are investigated for each condition. Then, the effect of the specific absorption surface area on the gravimetric and light tar removal performance is investigated in the laboratory scale experiment. Finally, the venturi scrubber producing syngas microbubbles are demonstrated in the pilot scale 650 kW_{th} air blown bubbling fluidized bed gasifier.

Chapter 4. Comparative performance of oil and emulsified absorbent in scrubber producing syngas microbubbles

In this study, the tar removal performance of VO and 7.5%EO in a venturi scrubber enhancing the turbulent mixing by producing syngas microbubbles is investigated, where the Reynolds number is the parameter to measure the level of turbulence. The Reynolds number is determined based on the assumption of multiphase flow of syngas-absorbent. This study first presents a fluid behavior of syngas and absorbent (VO and 7.5%EO) in the bubbling scrubber and venturi scrubber. Then, the effect of Reynolds number on the gravimetric and the light tar removal performance is determined in laboratory scale. Finally, based on the experimental data, the mass transfer modelling is studied to observe the overall volumetric liquid-side mas-transfer coefficient.

Chapter 5. Performance of absorbent regeneration by a series of filtration and air-blown stripping for tar removal in biomass gasification

In this study, the objective is to investigate the possibility of the increase of the tar removal capacity of oil-based absorbent by a series of the filtration and the air-blown stripping regeneration compared with the centrifugation and filtration techniques. The combination of the bubbling type scrubber with the oil regeneration system is evaluated for treating the biomass gaseous tar in order to prolong the absorbent lifetime and reduce the waste oil produced after reaching its saturation. This study first presents the fundamental of air-blown stripping for tar removal, stripping performance and

10 hours test for tar removal performance by a series of the filtration and the air-blown stripping. Finally, the comparison of non-regenerated oil and the regenerated oil (the filtration, the centrifugal sedimentation and a series of the filtration and the air-blown stripping techniques) is discussed in terms of the tar removal capacity and efficiency.

Chapter 6. Conclusion and recommendation

This chapter summarizes the important concluding remarks of this thesis. In view of these, some recommendations are also proposed to improve the tar removal performance.

1.5 Reference

[1.1] EIA US. International energy outlook 2016. US Energy Inf Adm 2016.

[1.2] Sawangphol N, Pharino C. Status and outlook for Thailand's low carbon electricity development. Renew Sustain Energy Rev 2011;15:564–73.

[1.3] Energy Policy and Planning Office E. Summary of Thailand power development plan 2012-2030 (PDP2010). Minist Energy Bangkok, Thail 2012.

[1.4] Chimres N, Wongwises S. Critical review of the current status of solar energy in Thailand. Renew Sustain Energy Rev 2016;58:198–207.

[1.5] Chingulpitak S, Wongwises S. Critical review of the current status of wind energy in Thailand. Renew Sustain Energy Rev 2014;31:312–8.

[1.6] Bakhtyar B, Sopian K, Sulaiman MY, Ahmad SA. Renewable energy in five South East Asian countries: Review on electricity consumption and economic growth. Renew Sustain Energy Rev 2013;26:506–14.

[1.7] Aroonrat K, Wongwises S. Current status and potential of hydro energy in Thailand: a review. Renew Sustain Energy Rev 2015;46:70–8.

[1.8] Wianwiwat S, Asafu-Adjaye J. Modelling the promotion of biomass use: A case study of Thailand. Energy 2011;36:1735–48.

[1.9] Roni MS, Chowdhury S, Mamun S, Marufuzzaman M, Lein W, Johnson S. Biomass co-firing technology with policies, challenges, and opportunities: A global review. Renew Sustain Energy Rev 2017;78:1089–101.

[1.10] Papong S, Yuvaniyama C, Lohsomboon P, Malakul P. Overview of biomass utilization in Thailand. Meet. LCA ASEAN Biomass Proj. Japan, vol. 28, 2004.

[1.11] Gaurav N, Sivasankari S, Kiran GS, Ninawe A, Selvin J. Utilization of bioresources for sustainable biofuels: A Review. Renew Sustain Energy Rev 2017;73:205–14.

[1.12] Zhang L, Xu CC, Champagne P. Overview of recent advances in thermo-chemical conversion of biomass. Energy Convers Manag 2010;51:969–82.

[1.13] Park J-H, Kim S-H, Park H-D, Lim DJ, Yoon J-J. Feasibility of anaerobic digestion from bioethanol fermentation residue. Bioresour Technol 2013;141:177–83.

[1.14] Lin Y, Tanaka S. Ethanol fermentation from biomass resources: current state and prospects. Appl Microbiol Biotechnol 2006;69:627–42.

[1.15] Bioenergy IEA. Biomass combustion and co-firing: An Overview. IEA Bioenergy Task, vol. 32, 2004.

[1.16] Quaak P, Knoef H, Stassen HE. Energy from biomass: a review of combustion and gasification technologies. vol. 23. World Bank Publications; 1999.

[1.17] Nussbaumer T. Combustion and co-combustion of biomass: fundamentals, technologies, and primary measures for emission reduction. Energy & Fuels 2003;17:1510–21.

[1.18] Maschio G, Koufopanos C, Lucchesi A. Pyrolysis, a promising route for biomass utilization. Bioresour Technol 1992;42:219–31.

[1.19] Marsh R, Hewlett S, Griffiths T, Williams K. Advanced thermal treatment for solid waste--a waste manager's guide. Proceeding 22nd Int. Conf. solid waste Manag. Technol. Philadelphia, 2007.

[1.20] Demirba\cs A. Biomass resource facilities and biomass conversion processing for fuels and chemicals. Energy Convers Manag 2001;42:1357–78.

[1.21] Mohan D, Pittman CU, Steele PH. Pyrolysis of wood/biomass for bio-oil: a critical review. Energy & Fuels 2006;20:848–89.

[1.22] Zhong C, Wei X. A comparative experimental study on the liquefaction of wood. Energy 2004;29:1731–41.

[1.23] Rezaiyan J, Cheremisinoff NP. Gasification technologies: a primer for engineers and scientists. CRC press; 2005.

[1.24] Molino A, Chianese S, Musmarra D. Biomass gasification technology: The state of the art overview. J Energy Chem 2016;25:10–25.

[1.25] Mondal P, Dang GS, Garg MO. Syngas production through gasification and cleanup for downstream applications—Recent developments. Fuel Process Technol 2011;92:1395–410.

[1.26] Sansaniwal SK, Pal K, Rosen MA, Tyagi SK. Recent advances in the development of biomass gasification technology: A comprehensive review. Renew Sustain Energy Rev 2017;72:363–84.

[1.27] Warnecke R. Gasification of biomass: comparison of fixed bed and fluidized bed gasifier. Biomass and Bioenergy 2000;18:489–97.

[1.28] Bergman PCA, van Paasen SVB, Boerrigter H. The novel “OLGA” technology for complete tar removal from biomass producer gas. Pyrolysis Gasif. biomass waste, Expert Meet. Strasbourg, Fr., vol. 30, 2002.

[1.29] Hasler P, Nussbaumer T. Gas cleaning for IC engine applications from fixed bed biomass gasification. Biomass and Bioenergy 1999;16:385–95.

[1.30] Gómez-Barea A, Ollero P, Leckner B. Optimization of char and tar conversion in fluidized bed biomass gasifiers. Fuel 2013;103:42–52.

[1.31] Kiel JHA, Van Paasen SVB, Neeft JPA, Devi L, Ptasinski KJ, Janssen F, et al. Primary measures to reduce tar formation in fluidised-bed biomass gasifiers. ECN, ECN-C-04-014 2004.

[1.32] Abdoulmoumine N, Adhikari S, Kulkarni A, Chattanathan S. A review on biomass gasification syngas cleanup. Appl Energy 2015;155:294–307.

[1.33] Phuphuakrat T, Namioka T, Yoshikawa K. Tar removal from biomass pyrolysis gas in two-step function of decomposition and adsorption. Appl Energy 2010;87:2203–11.

[1.34] Shen Y, Yoshikawa K. Recent progresses in catalytic tar elimination during biomass gasification or pyrolysis - A review. Renew Sustain Energy Rev 2013;21:371–92.

[1.35] Tsuboi Y, Ito S, Takafuji M, Ohara H, Fujimori T. Development of a regenerative reformer for tar-free syngas production in a steam gasification process. Appl Energy 2017;185:1217–24.

[1.36] Wiinikka H, Wennebro J, Gullberg M, Pettersson E, Weiland F. Pure oxygen fixed-bed gasification of wood under high temperature (>1000°C) freeboard conditions. Appl Energy

2017;191:153–62.

[1.37] Zeng X, Wang F, Li H, Wang Y, Dong L, Yu J, et al. Pilot verification of a low-tar two-stage coal gasification process with a fluidized bed pyrolyzer and fixed bed gasifier. Appl Energy 2014;115:9–16.

[1.38] Shen Y, Zhao P, Shao Q, Takahashi F, Yoshikawa K. In situ catalytic conversion of tar using rice husk char/ash supported nickel--iron catalysts for biomass pyrolytic gasification combined with the mixing-simulation in fluidized-bed gasifier. Appl Energy 2015;160:808–19.

[1.39] Phuphuakrat T, Namioka T, Yoshikawa K. Absorptive removal of biomass tar using water and oily materials. Bioresour Technol 2011;102:543–9.

[1.40] Paethanom A, Nakahara S, Kobayashi M, Prawisudha P, Yoshikawa K. Performance of tar removal by absorption and adsorption for biomass gasification. Fuel Process Technol 2012;104:144–54.

[1.41] Chen H, Namioka T, Yoshikawa K. Characteristics of tar, NOx precursors and their absorption performance with different scrubbing solvents during the pyrolysis of sewage sludge. Appl Energy 2011;88:5032–41.

[1.42] Tarnpradab T, Unyaphan S, Takahashi F, Yoshikawa K. Tar removal capacity of waste cooking oil absorption and waste char adsorption for rice husk gasification. Biofuels 2016;7:401–12.

[1.43] Paethanom A, Bartocci P, D'alessandro B, D'Amico M, Testarmata F, Moriconi N, et al. A low-cost pyrogas cleaning system for power generation: Scaling up from lab to pilot. Appl Energy 2013;111:1080–8.

[1.44] Schifftner KC, Hesketh HE. Wet scrubbers 1983.

[1.45] Bhave AG, Vyas DK, Patel JB. A wet packed bed scrubber-based producer gas cooling-cleaning system. Renew Energy 2008;33:1716–20.

[1.46] Bhoi PR, Huhnke RL, Kumar A, Payton ME, Patil KN, Whiteley JR. Vegetable oil as a solvent for removing producer gas tar compounds. Fuel Process Technol 2015;133:97–104.

[1.47] Hasler P, Buehler R, Nussbaumer T. Evaluation of Gas Cleaning Technologies for Small Scale Biomass Gasifiers: Biomass Programme; Final Report. Bundesamt für Energiewirtschaft; 1997.

[1.48] Surjosatyo A, Vidian F. Tar Content Evaluation of Produced Gas in Downdraft Biomass Gasifier. Iran J Energy Environ 2012;3:210–2.

[1.49] Tarnpradab T, Unyaphan S, Takahashi F, Yoshikawa K. Improvement of the biomass tar removal capacity of scrubbing oil regenerated by mechanical solid--liquid separation. Energy & Fuels 2017.

Chapter 2

Effect of emulsified absorbent for tar removal in biomass gasification process

Abstract

Tar contained in syngas produced by biomass gasification causes a problem for utilization in downstream applications due to its condensation. According to the tar property, it is a complex and various compound hydrocarbons. Some of them are good-dissolved and removed in non-polar substance like oily material while some are in polar substance like water. In this chapter, a mixture of water and emulsified oil, consisting of vegetable oil from canola seed and water without any pretreatment method, is investigated in order to maximize the tar removal performance of both non-polar and polar absorbents. The tar removal performances of the emulsified oil and pure vegetable oil were compared by wet and dry tar analysis methods. The results showed that 76.6% of the gravimetric tar was removed by pure vegetable oil whereas the best performance was 87.6% of removal in the case of 7.5% water content emulsified oil. For light tar, phenol and naphthalene are mainly trapped due to its high condensation point. For light tar removal, there was no significant difference between pure vegetable oil and 7.5% water content emulsified oil. Therefore, the emulsified oil can enhance the gravimetric tar removal performance with no significant change of the light tar removal efficiency compared with pure vegetable oil.

2.1 Background

As outlined in the introduction, the tar removal efficiency of conventional absorbent mainly focused on polar and non-polar absorbents separately, and there is no combination of polar and non-polar absorbents for tar removal. In this chapter, the tar removal performance of the emulsified oil (mixture of oil and water) is investigated in order to maximize the tar removal performance in absorbent selection aspect.

Emulsified oil is a thermodynamically stable and translucent fluid. It is widely used for cleaning application [2.1]. The absorbent mainly removes tar by dissolution and condensation. Firstly, the tar components with high boiling point will condense when directly contact with the lower temperature absorbent. Then, the tar components with the low boiling point will be dissolved in the absorbent. Tar is a complex hydrocarbon, in terms of polarity, so it can be both polar (hydrophilic)

and non-polar (hydrophobic) depending on the structure and the elemental bonding in the molecule. Using the 'like dissolves likes' principle, polar solutes dissolve in polar solvents, non-polar solutes dissolve in non-polar solvents and polar solutes do not dissolve in non-polar solvents. Therefore, in this chapter, a mixture of vegetable oil and water absorbent (emulsified oil) without any additive was selected to be the absorbent. Vegetable oil is expected to eliminate non-polar tar components while water is expected to eliminate polar ones. The emulsified oil was produced by well-mixing of oil and water at 1,000 rpm by a magnetic stirrer for homogeneously controlling the emulsion state and uniform distribution of oil and water [2.2,2.3]. The objective of this study is to maximize tar removal performance for both polar and non-polar tar components by comparing the emulsified oil (EO) and the pure vegetable oil (VO). Real tar produced by the pyrolysis of Japanese cider was introduced in an absorber and tar was removed by the pure vegetable oil and the emulsified oil with varying water content from 2.5% to 15%. The study can be divided into two parts; gravimetric tar removal performance of EO compared with VO and light tar removal performance of EO compared with VO. Real tar produced by the pyrolysis of Japanese cider was introduced in an absorber and tar was removed by the pure vegetable oil and the emulsified oil with varying water content from 2.5% to 15%. The study can be divided into two parts; gravimetric tar removal performance of EO compared with VO and light tar removal performance of EO compared with VO.

2.2 Material and experimental setup

2.2.1 Raw material

The feedstock was Japanese cedar with a mesh size between 0.5 mm and 1 mm dried at 105°C for 10 hours to remove moisture content. The proximate and ultimate analysis results are shown in Table 2.1.

Table 2.1. The proximate and ultimate analysis of Japanese cedar

	Japanese cedar
Proximate analysis (wt.% dry basis)	
Volatile matter	84.1
Fixed carbon	15.6
Ash	0.3
HHV (MJ/kg)	20.0
Ultimate analysis (wt% dry ash free basis)	
C	50.4
H	6.3
N	0.1
O	43.2
S	<0.1
Cl	<0.1

Cedar was packed in a screw feeder with the feed rate of 0.6 g/min. Nitrogen was used as a carrier gas by controlling the flow rate at 0.8 l/min. The pyrolysis reactor was covered by an electric heater and its temperature was controlled at 800°C. After running the feeder for 30 minutes to reach the steady state, the synthesis gas with tar content was introduced into a gas cleaning unit. Finally, it was introduced to wet and dry tar measurement units in order to measure the amount of tar remaining. A schematic diagram of the synthesis gas generation part and the cleaning unit are shown in Figure 2.1.

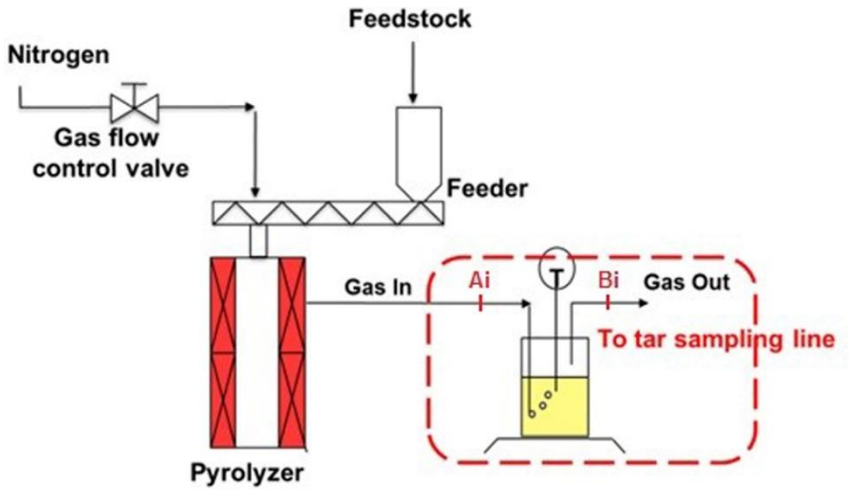

Figure 2.1. Schematic diagram of the experimental setup

2.2.2 Absorbent used

Vegetable oil (100% canola oil) was purchased in a supermarket while water was supplied from an untreated tap water line. Eight absorbents were utilized in this study for tar removal that were pure oil, pure water and 2.5%, 5%, 7.5%, 10%, 12.5% and 15% by volume of water in oil (emulsified oil). The total absorbent volume was fixed at 500 ml.

2.2.3 Scrubber

The pure vegetable oil, the pure water and the emulsified oil were contained in a 500 ml Woulff glass bottle, three-neck flask sealed with silicone gums, as a scrubber with a magnetic stirrer. The investigated stirring speed was 1,000 rpm at the room temperature as per previous research

[2.4]. The emulsified oil was produced by well-mixing of oil and water without any additive at 1,000 rpm stirring speed for 30 minutes before conducting the experiment to homogeneously control the emulsion state and uniform distribution of oil and water.

2.2.4 Tar sampling and analysis methods

Tar measurement was done by both wet and dry methods. The wet method can measure the gravimetric tar concentration by weight while the dry method can measure the light tar by GC-FID. Both methods are described below.

2.2.4.1 Wet method

The wet method from VTT Energy guideline was used for analyzing the gravimetric tar [2.5]. The procedure of the sampling method is shown in Figure 2.2. The wet method consisted of 10 impingers connected in series. The first two impingers were packed with glass beads to increase the retention time of the syngas. They were put in a water bath kept at 25°C. The remaining eight impingers were put in a salt, water and ice mixture bath kept at 3°C where the first three impingers were filled with 100 ml of water while the last five impingers were filled with 100 ml of IPA. The impingers packed with glass beads were installed aiming at capturing high boiling point tar while those filled with water and IPA were installed aiming at capturing polar tar and non-polar tar, respectively. The gas sampling was done for 60 minutes. After that, tar was separated from water and IPA by the rotary evaporator in a water bath kept at 40°C. The residue was the gravimetric tar whose amount was measured by weight.

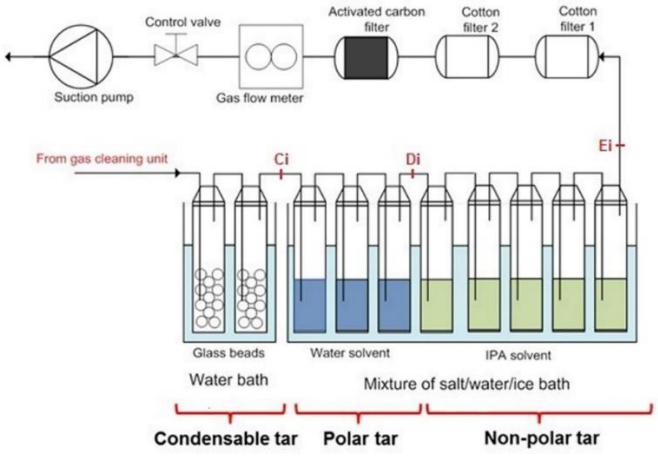

Figure 2.2. Illustration of the gravimetric tar sampling method

2.2.4.2 Dry method

The dry method was used for analyzing the light tar [2.6]. The procedure of this sampling method is shown in Figure 2.3. The sampling line consists of a 6 mm ID charcoal tube (containing 150 g of activated carbon) connected in series with an 8 mm ID silica gel tube (containing 780 mg of silica gel) purchased from Sibata Scientific Technology Ltd. It was connected at the points Ai (inlet gas) and Bi (exit gas) to compare light tar concentration before and after the scrubbing. This method can analyze the light tar composition such as benzene, toluene, xylene, styrene, naphthalene, and phenol. The sampling line was connected with a cotton filter, an activated carbon filte, a gas flow meter and a suction pump. Light tar was sampled at a constant flow rate (0.5 l/min) for 3 min. It was repeatedly sampled every 24 minutes at the point Ai and every 4 min at the point Bi for 72 minutes. After finishing the tar sampling, gas chromatography flame ionization detector (GC-FID) was utilized to detect light tar components and their concentrations. Carbon disulfide and acetone are used as solvents for the charcoal tube and the silica gel tube, respectively.

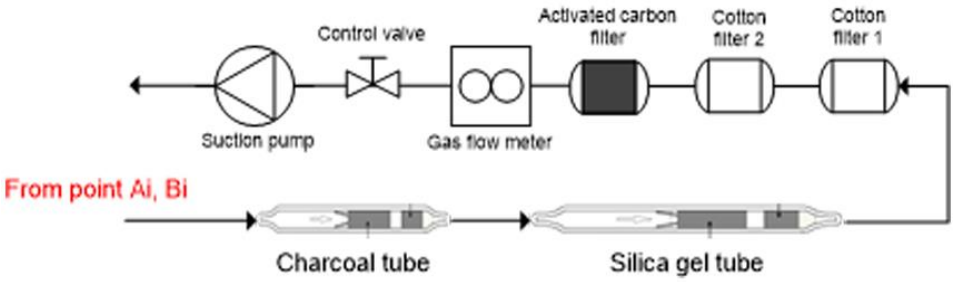

Figure 2.3. Illustration of the light tar sampling method

2.3 Result and discussion

2.3.1 Gravimetric tar formation and removal performance of emulsified oil absorbent (EO) compared with pure vegetable oil absorbent (VO) and pure water

2.3.1.1 Gravimetric tar formation of Japanese cedar

Figure 2.4 presents the gravimetric tar contained in the synthesis gas at the exit of the reactor. It can be seen that the synthesis gas from Japanese cedar contained 69.8 g/m^3 of gravimetric tar. It could be divided into three groups; non-polar, polar and condensable tars. Non-polar tar was in a large proportion among other gravimetric tar which contributed 60% (42.3 g/m^3) of the total. The

second was the condensable tar which contributed 25% (17.3 g/m^3). It can be both non-polar and polar tars but condenses at the room temperature. Finally, 15% (10.2 g/m^3) was polar tar.

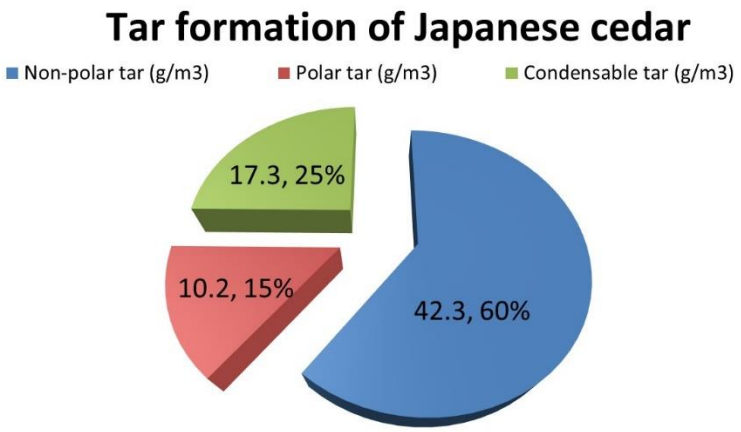

Figure 2.4. Gravimetric tar formation of Japanese cedar

2.3.1.2. Gravimetric removal performance of water and emulsified oil absorbent (EO) compared with pure vegetable oil absorbent (VO)

Figure 2.5 illustrates the gravimetric tar concentration at the exit of the scrubber and the tar removal efficiency for three tar groups (condensable, polar and non-polar). The results confirmed that the tar removal efficiency of water absorbent was lower than the others. The total gravimetric tar remained was 36.9 g/m^3 (47.2% of the tar removal efficiency). In addition, all polar tar components were completely removed due to dissolubility, while 28.8% of the non-polar tar was removed by water. This can be explained by these reasons. Although most of the non-polar tar components have no solubility in water, they can be condensed as a separate liquid in the water, where 61.0% of condensable tar was removed by water. Due to the fact that the condensable tar can be both polar and non-polar, the accumulation of the non-polar tar in the condensable tar might have dissolved the non-polar tar. Therefore, water absorbent could slightly remove the non-polar tar. The gravimetric tar removal performance of the emulsified oil absorbent (EO) compared with the pure vegetable oil absorbent (VO) was explained as below.

For the condensable tar, it is the heaviest tar which is easily condensable under the room temperature and was captured in the glass bead impingers. It can be both polar and non-polar. This tar is very dangerous due to its liquid form in a high operating temperature. When there was no

absorbent in the scrubber, the condensable tar captured was 17.3 g/m^3 (25% of the total tar). The concentration was reduced by scrubbing with VO and EO. VO could remove the condensable tar by 75.0% while EO performed better with all of water content ratios (2.5-15%). The tar removal performance increased from 2.5% EO (86.2% of the removal efficiency) to the highest performance at 7.5% EO (89.3% of the removal efficiency). However, from 10% EO to 15% EO, the tar removal performance slightly dropped. Thus, there are positive and negative mechanisms for adding water to absorbent. For positive aspects, adding from 2.5% to 7.5% water content showed desirable results for tar removal. The increase of water has a correlation between the viscosity and the syngas bubble size. Table 2.2 indicates that the viscosity of the emulsified oil directly decreased with increasing the water content. The viscosity decrease has a favor to the syngas bubble size. The lower the viscosity, the smaller the bubble produced [2.7]. Luo et al. shows the model of overall force balance on a bubble which can be written as Equation 2.1 [2.8].

$$F_B + F_M = F_D + F_\sigma + F_{BA} + F_{I,g} + F_C + F_{I,m} \quad (2.1)$$

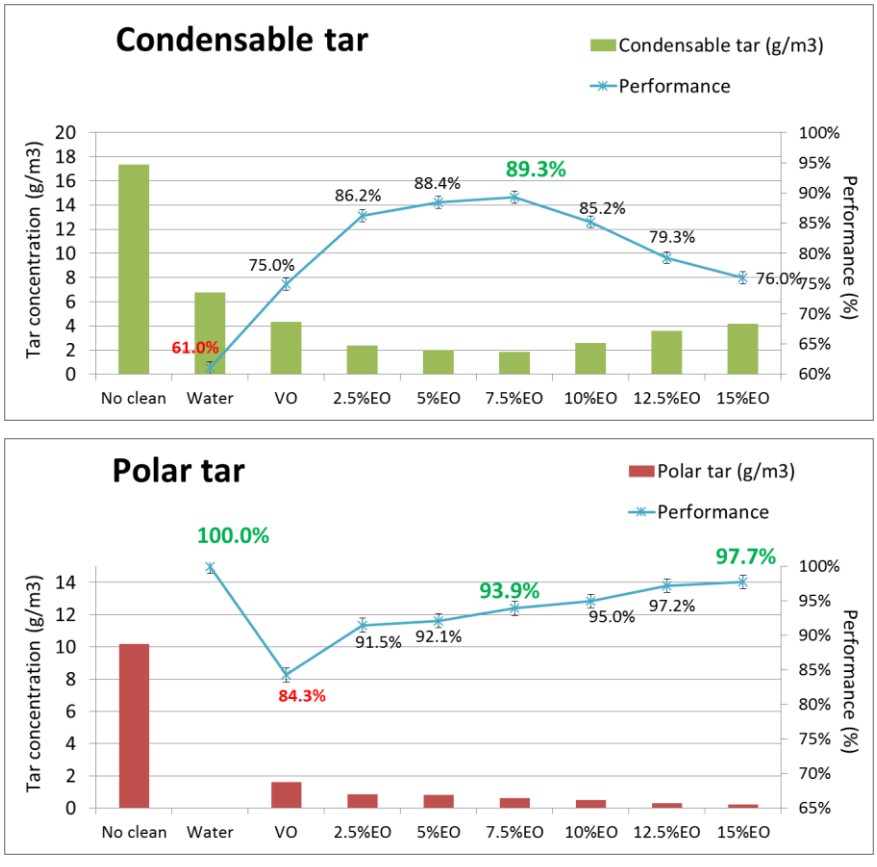

Figure 2.5. Gravimetric tar concentration and tar removal efficiency

(c)

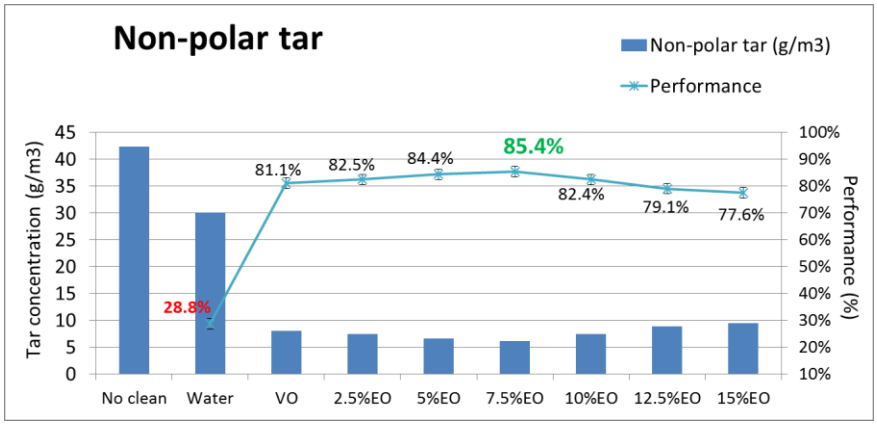

(d)

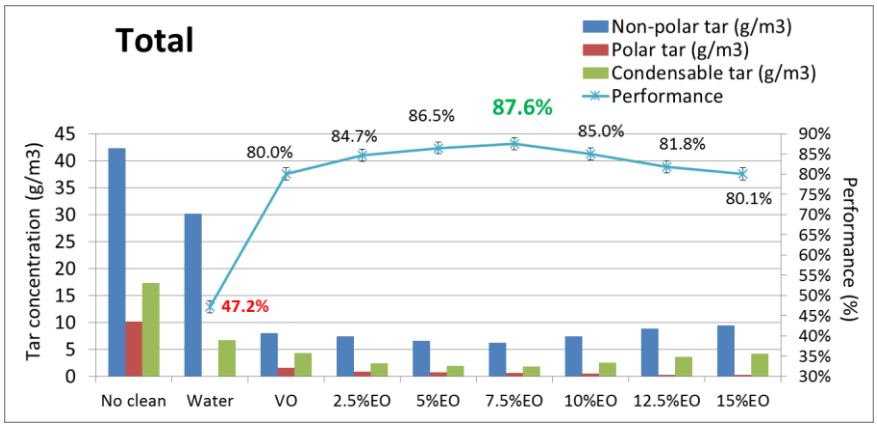

Figure 2.5. (Continued)

Table 2.2. Viscosity of vegetable oil (VO) and emulsified oil (EO)

	VO	2.5%EO	5%EO	7.5%EO	10%EO	12.5%EO	15%EO
Viscosity (cSt)	66.1	65.8	65.0	63.9	63.3	62.5	61.7

According to the equation, a lower viscosity oil contributes a lower liquid drag force (F_D) and surface tension force (F_s). It is profitable to the buoyancy force (F_B) getting small value due to the Equation 2.1. The bubble size becomes smaller with the direct variation of the buoyancy force as in Equation 2.2.

$$F_B = \frac{\pi}{6} d_b^3 (\rho_l - \rho_g) g \quad (2.2)$$

Smaller bubbles increase the contact area between the bubble and the absorbent. Figure 2.6 illustrates that tar bubble size was slightly decreased from VO to 15% EO with the increase of the number of tar bubbles by the viscosity effect. The contact area increased as the number of bubbles increased, assuming no tar volume flow rate changes into the scrubber. Moreover, more water contained in EO improved the polar tar removal. In the emulsion stage, water droplets were homogenously dispersed into vegetable oil which was a continuous phase. While VO can mainly dissolve non-polar tar, EO can dissolve both non-polar and polar tars. However, 10-15% water content showed undesirable results for tar removal. Figure 2.6c shows the contacting area of oil and water droplet intensity to the gas bubble. It was found that the number of water droplet increased with an increase of the water content. While adding water increased the polar-tar and the water contacting area, it simultaneously decreased the non-polar tar and the oil contacting area. Due to the fact that most of the tar was non-polar, when the water content is too high (more than 10%), the contacting area between the oil and the non-polar tar is significantly decreased by replacing of water droplet. This leads to a decrease in the non-polar tar removal efficiency. According to the positive and negative mechanisms, 7.5% EO was the balance condition to effectively remove condensable polar and non-polar tar.

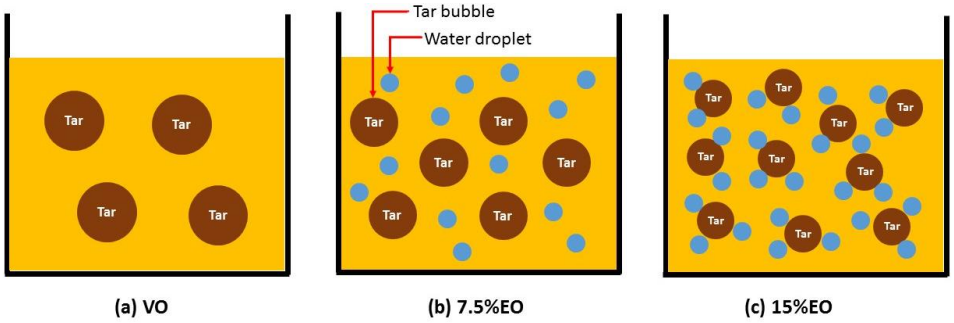

Figure 2.6. Gravimetric tar removal mechanism and phenomenon

For the polar tar, it was captured by the water impingers. The total polar tar contained in the synthesis gas was 10.2 g/m^3 (14.4% of the total tar). EO performed better than VO, where 84.3% of the polar tar could be removed by VO while all of EO showed the tar removal efficiency higher than 90%. The highest performance was obtained by 15% EO which showed 97.7% of the removal efficiency. From this result, it could be explained that VO also absorbed the polar tar because of fatty acids contained in the vegetable oil, where 7% of fatty acid was saturated and polyunsaturated acids which predominated in polar lipids while others were monounsaturated fatty acids which

predominated in non-polar lipids [2.9,2.10]. The majority of polar lipids in canola oil were palmitic acid (3.8%), stearic acid (1.9%), arachidic acid (0.6%), behenic acid (0.4%), lignoceric acid (0.1%) and miristic acid (0.1%) [2.10]. These polar lipids played an important role for the polar tar removal in VO. Turning to EO, Figure 2.7 shows the total polar tar removed (green line), the polar tar removed by polar lipids from vegetable oil (blue lines) and the polar tar removed by water (red line). It was assumed that reducing the amount of vegetable oil had a direct linear variation to the tar removal efficiency by polar lipids effect and the difference of the total polar tar removed and the polar tar removed by vegetable oil was the polar tar removed by water. The polar tar removed by water proportionally rose with increasing the water content due to the dissolution principle. However, it was found that there was a marked increase of the polar tar removed by water between VO (0 g/m^3) and 2.5% EO (0.9 g/m^3). The linear equation of the polar tar removed by water was assumed and is shown in Equation 2.3.

$$Y = 0.1655X + 0.3027 \quad (2.3)$$

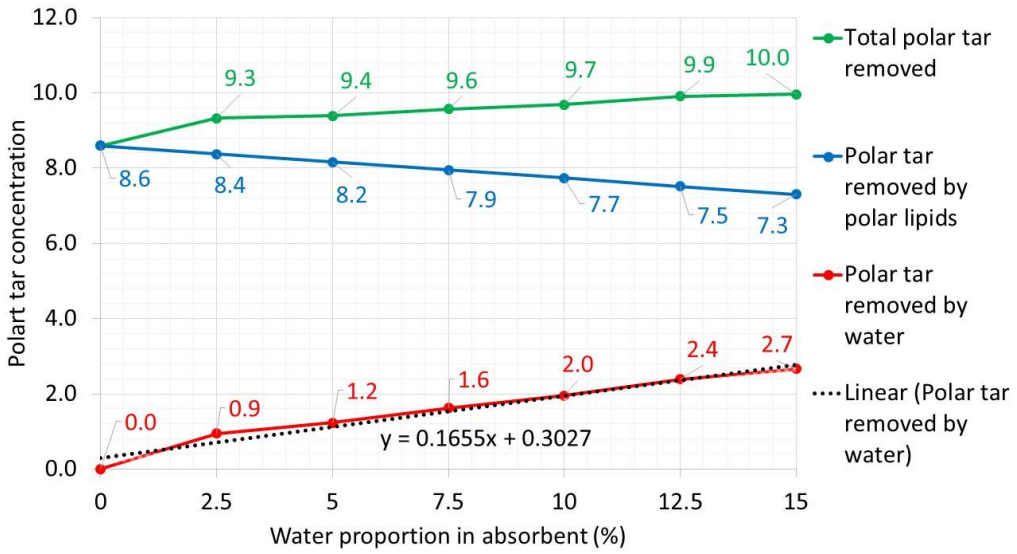

Figure 2.7. Polar tar concentration removed by vegetable oil (VO) and emulsified oil (EO) with consideration of polar lipids and water.

Y-axis is the polar tar removed by water and X-axis is the water content percentage in EO. Theoretically, when the effects of polar lipids are indiscriminate, VO is not able to remove polar tars (X=0, Y=0). However, according to the linear equation, at point Y=0, X equals to -1.829. It was implied

that there was some water adding to VO during one hour of gravimetric tar measurement experiment. Inherent moisture in feedstock could become water steam in reactor and condensed in VO scrubber. This finding was also observed from fast pyrolysis of Eucalyptus grandis by Joubert et al [2.11]. Therefore, 1.829% of the inherent moisture contained in VO during the experiment could remove 0.30 g/m^3 of the polar tar. Either the water contained in EO or the inherent water contained in VO had a strong influence on removing the polar tar due to the dissolution principle.

For non-polar tar, the concentration without the absorbent was 42.3 g/m^3 which was the largest proportion among these three groups (60.6%). 81.1% of the non-polar tar was removed by VO while, from 2.5% EO to 7.5% EO, the performance was slightly enhanced until reaching the highest at 85.4%. This is because the emulsion state increased the contacting area between the non-polar tar and the oil as previously mentioned. In addition, these oil and water absorbents are immiscible phases. In this experiment, oil was the continuous phase and water was the dispersed phase. The droplet of water dispersed in oil lead to an increase in the contacting area. Therefore, a small amount of water content can improve the non-polar tar removal. However, with more water content, the tar removal efficiency dropped to just only 77.6% at 15% EO due to the unbalance between the oil and water. Too much water content reduced the non-polar tar removal efficiency but increased the polar tar removal efficiency as described above.

As described in the previous section, there was a similar mechanism between the condensable tar and the nonpolar tar for tar removal. This is because the condensable tar contained both polar and non-polar. Compared between VO and EO, 14.3% (2.5 g/m^3) of the removal efficiency could be improved by 7.5% EO for the condensable tar while just only 4.3% (1.8 g/m^3) of the removal efficiency could be improved by 7.5% EO for the non-polar tar. This could be explained that both the contacting area and the polarity of water had influences to remove the condensable tar while the non-polar tar was removed only by the effect of the contacting area enhancement. Thus, the removal efficiency improvement of the condensable tar was higher than the non-polar tar. After that, the removal performance for the condensable tar and the non-polar decreased due to too much water content in EO. Compared between VO and EO, 1.0% (0.2 g/m^3) of the removal efficiency can be improved by 15% EO for the condensable tar while 3.5% (1.5 g/m^3) of dropped performance was found by 15% EO for the non-polar tar. Due to the fact that although the unbalance of the water content had unfavorable effect on the non-polar tar removal in the condensable tar, while the polar tar in the condensable tar was increasingly removed with the water portion increased. Thus, there was a slight increase of the condensable tar removal efficiency compared to VO. However, adding too much water had direct inferior effect on the non-polar removal. That led to lower non-polar tar removal efficiency compared to VO.

In conclusion, EO performed better than VO in all water content proportions. VO was able to remove gravimetric tar down to 14.0 g/m^3 with the 80.0% removal efficiency, however EO removed more than 80% of the gravimetric tar. The best water proportion in EO was 7.5%, where the gravimetric tar could be removed down to 8.7 g/m^3 with 87.6% removal efficiency due to gas to liquid contacting area enhancement and the polarity of water.

2.3.2 Light tar removal performance of emulsified oil absorbent (EO) compared with pure vegetable oil absorbent (VO) and pure water

The light tar removal performances for benzene, toluene, xylene, styrene, phenol, indene and naphthalene were studied. Their properties are shown in Table 2.3. From Table 2.3, we can see that naphthalene and phenol are of interest in this experiment because they have a tendency to become a solid phase at an ambient temperature leading to the blockage in the piping system. Phenol, which is a polar tar, is appropriate to dissolve in water while naphthalene and other light tars are appropriate to dissolve in vegetable oil.

Table 2.3. Light tar properties

	Formula	Freezing point (°C)	Solubility in water
Benzene	C_6H_6	5.5	1.79 g/L
Toluene	C_7H_8	-95.0	0.47 g/L
Xylene	C_8H_{10}	13.0	insoluble
Styrene	C_8H_8	-30.0	0.29 g/L
Phenol	C_6H_6O	40.5	83 g/L
Indene	C_9H_8	-5.0	insoluble
Naphthalene	$C_{10}H_8$	80.3	0.03 g/L

2.3.2.1 Classification of light tar

The combination between wet and dry methods for light tar analysis is utilized for proving the light tar classification. Benzene, toluene, xylene, styrene, indene and naphthalene are non-polar tars while phenol is a polar tar. The non-polar substances are highly dissolved in IPA impingers while the polar substance is highly dissolved in water impingers. However, both of these are possible to be markedly removed by glass bead impingers owing to the effect of a high condensation point itself.

In this experiment, light tar concentrations were measured by the dry method at the points of Ai (total light tar formation), Ci (after glass beads impinger), Di (after water impinger) and Ei (after IPA

impinger) as shown in Figure 2.2. The results in the case without absorbent are summarized in Table 2.4.

Table 2.4. Light tar removal by the wet method in the case without absorbent

	Ai		Ci		Di		Ei	
	g/m³	%	g/m³	%	g/m³	%	g/m³	%
Benzene	25.1		14.5	42.1	9.7	61.3	-	100.0
Toluene	3.7		3.3	12.9	2.6	31.4	-	100.0
Xylene	0.4		0.1	61.4	0.1	62.9	-	100.0
Styrene	0.6		0.3	56.4	0.1	75.0	-	100.0
Phenol	0.2		0.1	76.3	-	100.0	-	100.0
Indene	0.1		0.1	11.8	0.1	28.1	-	100.0
Naphthalene	0.7		0.1	81.5	<0.1	97.9	-	100.0

From Table 2.4, we can see that phenol and naphthalene were highly condensed in glass beads impingers, 76.3 and 81.5%, respectively. Moreover, from Table 2.3, we can see that the freezing points of naphthalene and phenol are higher than those of other light tars (80.3 and 40.5°C, respectively). Therefore, phenol and naphthalene can be categorized in the condensable tar groups based on the test results and their condensation in a higher temperature than the ambient temperature (25°C). However, phenol can be classified in the polar tar group as well owing to 100% removal in water impingers. This is because the polar tar is soluble in water (polar solvent) and phenol has highly water soluble properties (83 g/L) while only 16.4% of naphthalene was removed when passing through water impingers. After passing IPA impingers, benzene, toluene, xylene, styrene, indene and naphthalene were completely removed because non-polar tars can be removed in IPA impingers. Therefore, these can be categorized in the non-polar tar groups. The light tar classification is summarized in Figure 2.8.

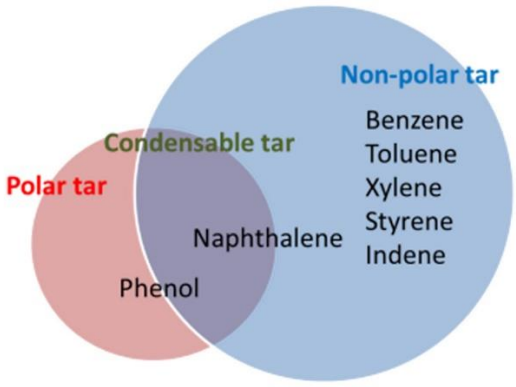

Figure 2.8. Summary of light tar classification by condensation and polarity

2.3.2.2 Light tar removal performance of emulsified oil absorbent (EO) compared with pure vegetable oil absorbent (VO) and pure water

Figure 2.9 illustrates the time change of the light tar concentration measured at the inlet (A_i) and the exit (B_i) of the scrubber filled with VO and EO. The results in each graph show the concentration change of benzene, toluene, xylene, styrene, phenol, indene and naphthalene for 72 minutes. Table 2.5 summarizes the light tar removal efficiency for VO and EO.

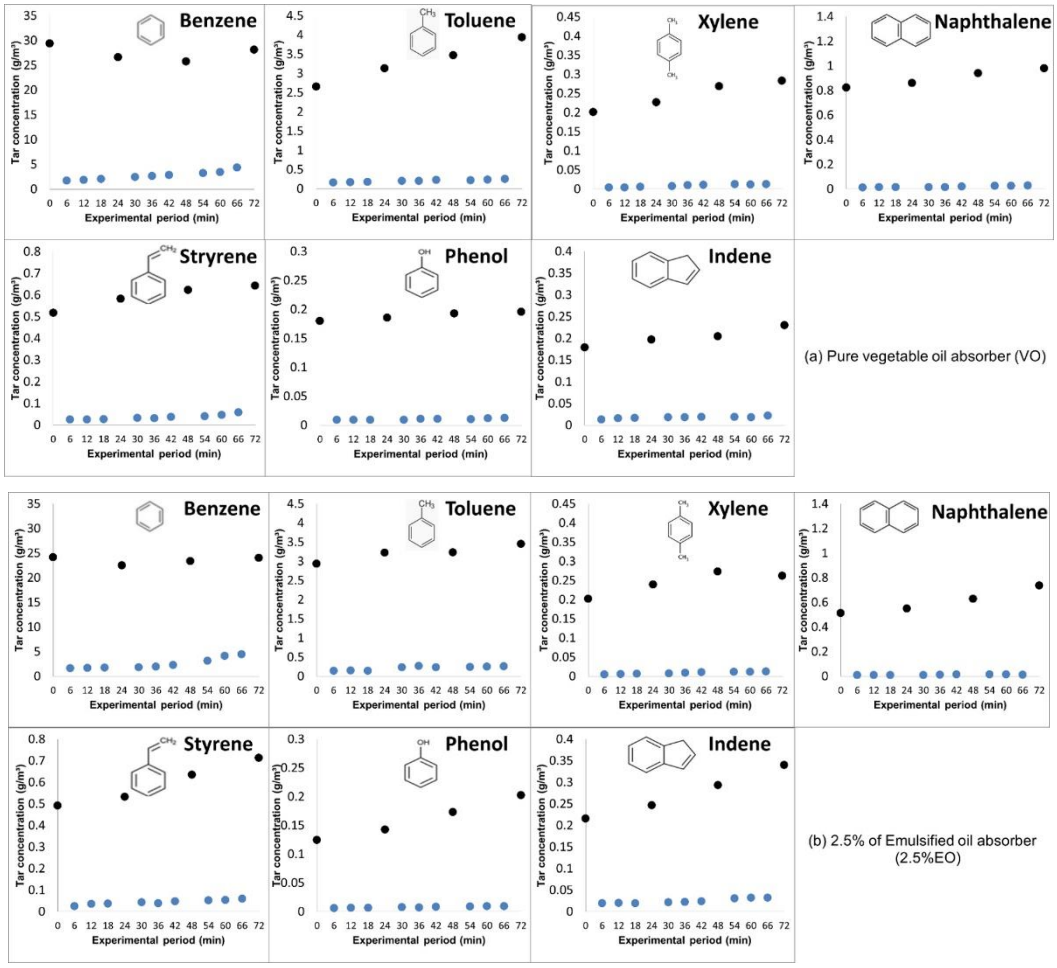

Figure 2.9. Time change of light tar concentration measured at inlet (A_i) and outlet (B_i) of the scrubber filled with VO and EO

● represents the concentration at the inlet of the scrubber (A_i) ● represents the concentration at the exit of the scrubber (B_i)

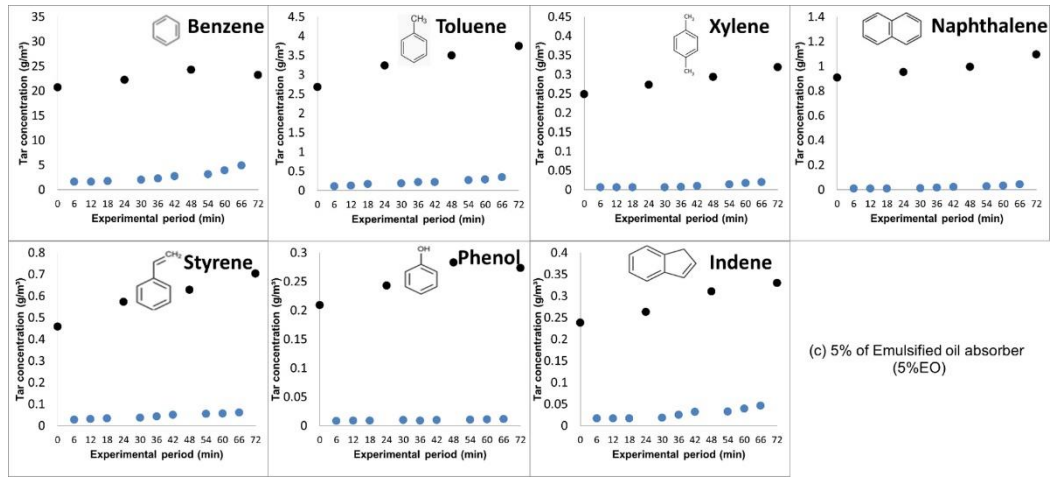

(c) 5% of Emulsified oil absorber (5%EO)

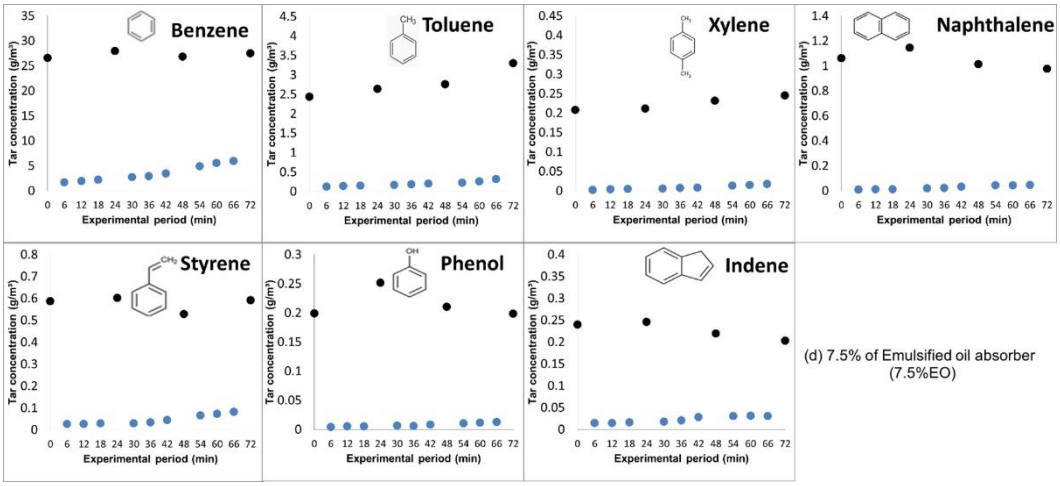

(d) 7.5% of Emulsified oil absorber (7.5%EO)

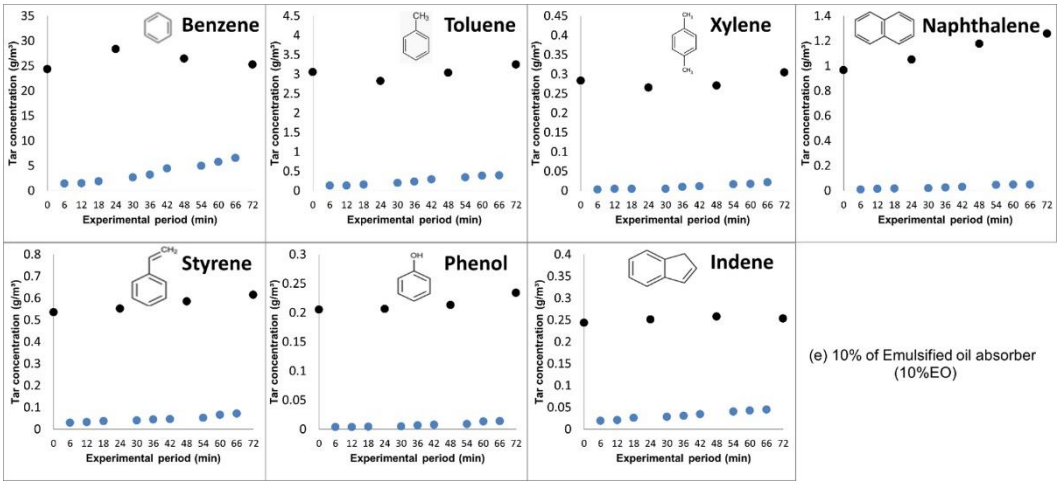

(e) 10% of Emulsified oil absorber (10%EO)

Figure 2.9. (Continued)

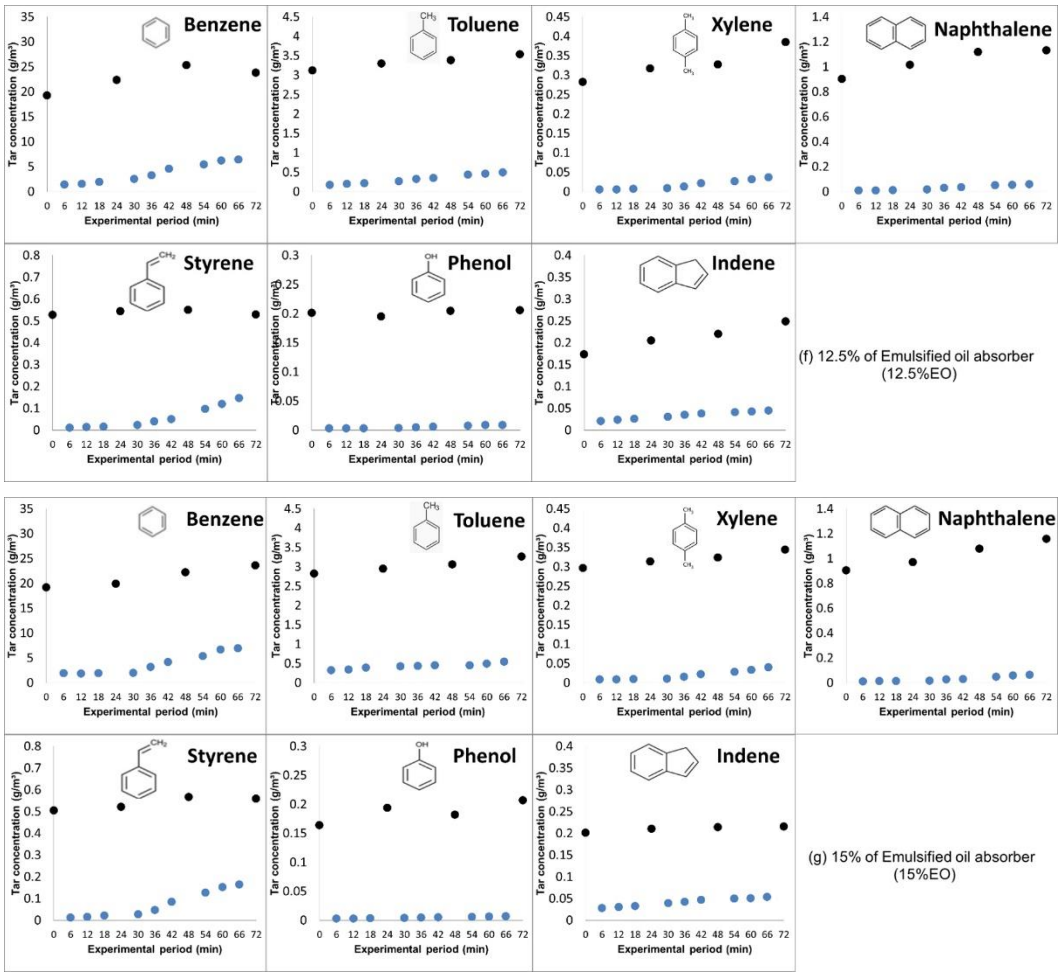

Figure 2.9. (Continued)

Table 2.5. Summary of light tar removal efficiency for VO and EO

	Benzene	Toluene	Xylene	Styrene	Phenol	Indene	Naphthalene
Water [2.12]	24.1%	22.5%	22.1%	23.5%	92.8%	28.2%	38.9%
VO	90.1%	93.8%	96.4%	94.0%	94.6%	91.2%	97.9%
2.5% EO	89.2%	93.4%	96.4%	92.7%	95.2%	91.0%	98.1%
5% EO	88.2%	93.5%	96.4%	92.6%	96.2%	90.5%	98.0%
7.5% EO	87.2%	93.0%	96.3%	92.1%	96.4%	90.0%	97.5%
10% EO	86.2%	91.8%	96.3%	91.8%	96.6%	87.3%	97.4%
12.5% EO	83.7%	90.3%	94.8%	89.4%	97.3%	84.2%	97.0%
15% EO	82.2%	85.8%	93.9%	86.5%	97.5%	80.2%	97.0%

The light tar removal efficiency was calculated by the numerical method (Equation 2.4), where f(x) and g(x) express the polynomial equations of the light tar concentration at the inlet and the exit of the scrubber derived from Figure 2.9, respectively. X stands for the experimental period (minutes).

$$\frac{\int_0^{72} f(x)dx - \int_0^{72} g(x)dx}{\int_0^{72} f(x)dx} \times 100 \quad (2.4)$$

For water absorbent, according to Phuphuakrat et al. [2.12], it can be observed that water could mainly remove only phenol, while it could slightly remove other light aromatic hydrocarbon tars (benzene, toluene, xylene, styrene, indene and naphthalene). This is because phenol is a polar tar (hydrophilic compound) having weak tendency to lose the H+ ion from the hydroxyl group, whereas benzene, toluene, xylene, styrene, and indene are non-polar tar (hydrophobic compounds) [2.12,2.13]. Therefore, phenol has a high solubility in water, but benzene, toluene, xylene, styrene, indene and naphthalene are slightly insoluble in water. The light tar removal performance of emulsified oil absorbent (EO) compared with pure vegetable oil absorbent (VO) was explained as below.

For light tar removal, low viscosity absorbent was not affected by the non-polar and polar light tar. Benzene, toluene, xylene, styrene, indene and naphthalene had decreased trends with the increase of the water proportion. It was a drawback of adding water to the absorbent because increasing the water portion reduces the amount of vegetable oil at the same time. For phenol, when the water content in the emulsified oil increases, the viscosity of the emulsified oil decreases. In the term of the mass transfer, the decrease in the viscosity decreases the tar removal efficiency. However, in the case of phenol (polar tar), the increasing water content (polar absorbent) in the emulsified oil is beneficial for phenol removal according to “like dissolves likes” principle. It is a positive (phenol dissolution in water) and negative (low viscosity oil) effect of the emulsified oil for phenol removal. Therefore, the phenol removal was almost the same. However, with the use of VO and EO as the absorbent, it can be seen that there is no significant change of light tar removal performance between VO and 2.5-7.5% EO (less than 3% performance difference).

In view of preventing the fouling, blocking or breaking of downstream components in the gasification process, the condensation of tar under the normal operation temperature should be focused [2.14–2.16]. Therefore, phenol and naphthalene which have a high tendency to condense and change to solid phase at 40 and 80°C, respectively, are mainly concerned in this study. Comparing VO and 7.5% EO (the best gravimetric tar removal performed), VO can remove 94.6% of phenol and 97.9% of naphthalene while 7.5% EO can remove 96.4% of phenol and 97.5% of

naphthalene Therefore, in terms of light tar removal performance, 7.5% EO showed the similar performance with VO.

2.4 Conclusion

The objective of the study in this chapter was to investigate the tar removal performance of emulsified oil compared with pure oil absorbent. According to their properties, although most of tar components are good dissolved in non-polar substance like oily material, some of them are polar tar that should be well removed by polar substance. In this study, pure vegetable oil and the emulsified oil of water and vegetable oil mixtures were used for testing tar removal performance in a laboratory scale. The synthesis gas containing tar was produced by Japanese cedar fed to the pyrolyzer and then was introduced into absorbents. There were eight absorbents utilized for investigating the tar removal performance which were pure vegetable oil (VO), pure water and 2.5%, 5%, 7.5%, 10%, 12.5% and 15% by volume of water in oil (emulsified oil or EO). After cleaning in the scrubber, the remaining tar in the synthesis gas was measured by both the gravimetric (wet) and the light tar (dry) measurement methods.

For the gravimetric tar, it was able to be sub-categorized into three groups: the condensable tar, the polar tar and the non-polar tar. Without absorbent, the total gravimetric tar produced was 69.8 g/m3, which could be divided into 17.3 g/m^3 (25%), 10.2 g/m^3 (15%) and 42.3 g/m^3 (60%) for the condensable tar, the polar tar and the non-polar tar, respectively. Comparing VO and 7.5% EO (showing the best gravimetric tar removal among EO absorbents) for condensable tar, it was shown that VO could remove 75.0% while 7.5% EO could remove 89.3% because VO can mainly dissolve the non-polar tar while EO can dissolve both the non-polar and the polar tars. For the polar tar removal, 7.5% EO performed much better than VO. Only 60.7% of the polar tar could be removed by VO while 7.5% EO performed 93.9% tar removal efficiency. For the non-polar tar, 81.1% was removed by VO while 7.5% EO could remove 85.4% because the emulsion state increased the contacting area between the non-polar tar and oil. EO performed better tar removal than VO in all water content proportions investigated. VO was able to remove the gravimetric tar down to 16.4 g/m^3 with 76.6% removal efficiency while 7.5% EO could remove the gravimetric tar down to 8.7 g/m^3 with 87.6% removal efficiency.

Among the light tar, phenol and naphthalene were categorized in the condensable tar due to their high condensation temperatures. However, phenol was classified into the polar tar group and naphthalene was classified into the non-polar tar group. The others (benzene, toluene, xylene, styrene and indene) were categorized in the non-polar tar group. Comparing VO and EO as the absorbent, it could be seen that there was no significant difference in the light tar removal

performance between VO and 2.57.5% EO (less than 3% removal efficiency difference). With a higher water content, VO performed slightly better for the non-polar tar removal while EO performed slightly better for the polar tar removal.

In summary, compared with pure vegetable oil, the emulsified absorbent mainly enhanced the gravimetric tar removal performance by increasing the polar tar removal efficiency with no significant decrease in the light tar removal efficiency.

2.5 Reference

[2.1] Quintero L, Carnahan NF. Microemulsions for Cleaning Applications. Dev Surf Contam Clean Methods Clean Cleanliness Verif 2013;6:65.

[2.2] Leal-Calderon F. Emulsified lipids: formulation and control of end-use properties. Oléagineux, Corps Gras, Lipides 2012;19:111–9.

[2.3] Emulsion Stability and Testing. Part Sci: Tech Brief. 2011;2.

[2.4] Paethanom A, Nakahara S, Kobayashi M, Prawisudha P, Yoshikawa K. Performance of tar removal by absorption and adsorption for biomass gasification. Fuel Process Technol 2012;104:144–54.

[2.5] Ståhlberg P, Lappi M, Kurkela E, Simell P, Oesch P, Nieminen M. Sampling of contaminants from product gases of biomass gasifiers. Tech Res Cent Finl 1998.

[2.6] Van Paasen SVB, Kiel JHA, Neeft JPA, Knoef HAM, Buffinga GJ, Zielke U, et al. Guideline for sampling and analysis of tar and particles in biomass producer gases. Energy Res Cent Netherlands, ECN-C-02-090 2002.

[2.7] Zhang W. Evaluation of effect of viscosity changes on bubble size in a mechanical flotation cell. Trans Nonferrous Met Soc China 2014;24:2964–8.

[2.8] Luo X, Yang G, Lee DJ, Fan L-S. Single bubble formation in high pressure liquid—solid suspensions. Powder Technol 1998;100:103–12.

[2.9] Parcerisa J, Richardson DG, Rafecas M, Codony R, Boatella J. Fatty acid distribution in polar and nonpolar lipid classes of hazelnut oil (Corylus avellana L.). J Agric Food Chem 1997;45:3887–90.

[2.10] Zambiazi RC, Przybylski R, Zambiazi MW, Mendonca CB. Fatty acid composition of vegetable oils and fats. B Ceppa, Curitiba 2007;25:111–20.

[2.11] Joubert J-E, Carrier M, Dahmen N, Stahl R, Knoetze JH. Inherent process variations between fast pyrolysis technologies: A case study on Eucalyptus grandis. Fuel Process Technol 2015;131:389–95.

[2.12] Phuphuakrat T, Namioka T, Yoshikawa K. Absorptive removal of biomass tar using water and oily materials. Bioresour Technol 2011;102:543–9.

[2.13] Chen H, Namioka T, Yoshikawa K. Characteristics of tar, NOx precursors and their absorption performance with different scrubbing solvents during the pyrolysis of sewage sludge. Appl Energy 2011;88:5032–41.

[2.14] Bergman PCA, van Paasen SVB, Boerrigter H. The novel “OLGA” technology for complete tar removal from biomass producer gas. Pyrolysis Gasif. biomass waste, Expert Meet. Strasbourg, Fr., vol. 30, 2002.

[2.15] Hasler P, Nussbaumer T. Gas cleaning for IC engine applications from fixed bed biomass gasification. Biomass and Bioenergy 1999;16:385–95. doi:10.1016/S0961-9534(99)00018-5.

[2.16] Gómez-Barea A, Ollero P, Leckner B. Optimization of char and tar conversion in fluidized bed biomass gasifiers. Fuel 2013;103:42–52.

Chapter 3

Improvement of tar removal performance of oil scrubber by producing syngas microbubbles

Abstract

This chapter investigated the feasibility of a low-cost and highly effective tar removal technique using venturi oil scrubber enhancing the absorption surface area by producing microbubbles for tar removal in biomass pyrolysis/gasification processes. The basic experiment was carried out by utilizing a laboratory-scale fixed bed pyrolyzer, and then the achievements were implemented in a pilot-scale bubbling fluidized bed gasifier. In the laboratory-scale experiment, the absorption surface area was evaluated based on the mean diameter and the number density. The venturi tubes with various throat diameter ratios (0.17, 0.42 and 0.67) and inverter frequencies (40, 50 and 60n Hz) were tested to show that the throat diameter ratio of 0.42 and the inverter frequency of 60 Hz were the optimum conditions. Furthermore, it was found that up to 97.7% of the gravimetric tar was removed by the venturi scrubber, while naphthalene and phenol were completely removed, which markedly improved the performance comparing with other conventional scrubbers. The 20-hour operation of the pilot-scale gasifier also showed that the gravimetric tar removal efficiency of the venturi scrubber was 87.1% on average and there were no naphthalene and phenol observed at the exit of the venturi scrubber as well. Totally, 99.2% of the gravimetric tar was removed by using only physical methods comprised of the following: a series of cyclone, ceramic filter, air cooler, water coolers, venturi scrubber and packed bed adsorber, which achieved the syngas quality requirement for internal combustion engines.

3.1 Background

Syngas microbubbles are the syngas bubbles with the diameter range from one to several hundred micrometers, which should significantly increase the absorption surface area compared with the previous study done by employing bubbling scrubbers. Micro-bubbling technique is widely used to improve the efficiency in various applications, such as in water treatment processes, washing processes, plant cultivation and so forth [3.1–3.4]. However, to the best of our knowledge, there was no report on the usage of microbubbles for tar removal. Four main techniques can be used in order to produce microbubbles; the bubble breakup [3.5–3.7], the ultrasonic wave [3.8], the

microfluidics/MEMS [3.9] and the pressurized dissolution techniques [3.10]. This study focused on the bubble breakup technique because the principle of this technique is similar to a venturi scrubber, which has scale up potential. The investigation of microbubble generator, based on air-water mixture, found that the bubble breakup of air increased linearly with an increase of the water flow rate [3.5]. The venturi type microbubble generator easily generated tiny bubbles of about 100 μm in the diameter and the dependence of the bubble size distribution on the different liquid flow rates had a favorable effect on the highest water flow rate [3.6]. An image processing technique was mainly utilized for determining the mean bubble diameter and bubble size distribution [3.7]. However, previous researches mainly focused on air-water mixture and no studies were found on syngas-oil mixture. The originalities of this chapter are not only the fundamental study of microbubbles formation of syngas-oil mixture but also investigating effect of syngas microbubbles produced by a venturi scrubber on the tar removal efficiency, where the relationship between the syngas microbubble formation and the absorption surface area for tar removal did not exist as well.

This study first presents a fundamental investigation on the microbubbles formation utilizing a venturi scrubber. Based on various venturi tube designs, the microbubble size distribution, the mean microbubble diameter, the number density and the specific absorption surface area were investigated for each condition. Then, the effect of the specific absorption surface area on the gravimetric and light tar removal performance was investigated in the laboratory-scale experiment. Finally, the venturi scrubber producing syngas microbubbles were demonstrated in a 650 kWth of pilot-scale bubbling fluidized bed gasifier to confirm the utilization of the real applications.

3.2 Principle of the syngas microbubble formation by venturi scrubber

Figure 3.1 illustrates the venturi tube consisting of a convergent, a throat and a divergent part. The pressurized fluid like water or oil is introduced into the convergent part of the venturi tube. According to the conservation of mass and energy, the fluid velocity at the throat position,V_2, becomes higher than the inlet velocity, V_1, while the pressure there, P_2, becomes lower than the inlet pressure, P_1, as shown in Eq. (3.1).

$$\frac{1}{2}\rho V_1^2 + \rho g Z_1 + P_1 = \frac{1}{2}\rho V_2^2 + \rho g Z_2 + P_2 \quad (3.1)$$

In this equation, Z_1 and Z_2 are the elevation of the point above a reference plane, which can be neglected, ρ is the density of the fluid and g is the gravity acceleration. Under such a condition of

the throat position, the syngas is able to be sucked into the liquid stream in the lower pressure region of the venturi tube. The sucked syngas is well-broken into numerous microbubbles by the action of a highly-turbulent shear flow called “the bubble breakup mechanism” [3.5].

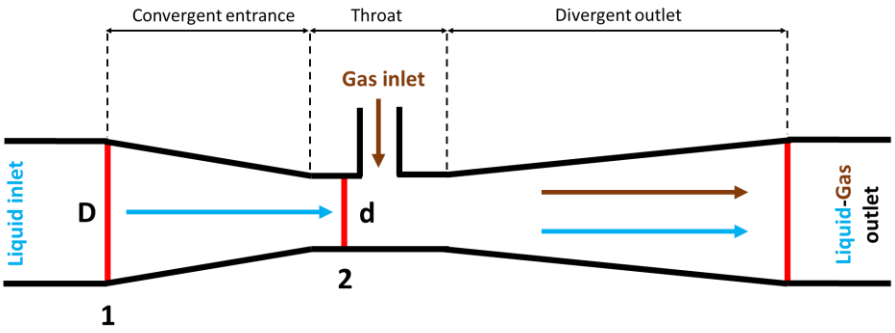

Figure 3.1. Illustration of a venturi tube

3.3. Experimental setup

3.3.1 Microbubble size measurement

A schematic diagram of the microbubble size measurement is shown in Figure 3.2. According to the opaqueness of the syngas whose microbubble size is difficult to measure, 1 l/min of air was supplied into the venturi scrubber instead. After placing the venturi tube at the bottom of the acrylic tank, whose volume is approximately 6 liters (300×300×80 mm), 2 litters of canola oil purchased in a Japanese supermarket was introduced into the venturi tube by a magnetic pump (SL-20S, As-one Co., Ltd., Japan). The oil circulation rate was measured and adjusted by a digital flow meter (DigiFlow 6700M, As-one Co., Ltd., Japan) and an inverter (FR-FS2-0.8K, Mitsubishi Electric Co., Ltd., Japan), respectively. In order to measure the microbubble diameter and the number density, a high frame rate digital microscope with 960×720 pixel resolution (MSP-3080, As-one Co., Ltd., Japan) was used for recording the bubble breakup mechanism and the images of the microbubbles at the location of 0.1 m above the bottom of the tank. The microbubble detection and quantification consisted of three steps as shown in Figure 3.3. Figure 3.3a) illustrates an original image. As shown in Figure 3.3b), a threshold function was implemented to inspect the microbubbles and convert the original image into the binary format, where the black is the detected microbubbles, while the white is the background. The core of microbubbles have some white regions as same as its background due to the backlit shadow graph as can be seen in Figure 3.3a). Then, the next image processing was conducted by using the watershed transformation as shown in Figure 3.3c). Finally, the arithmetic mean diameter

of the equal volume spherical microbubble (D_{10}) is utilized to calculate the equivalent microbubble diameter of more than 100 microbubbles and number density (n) is the total number of specified microbubbles ($N_{b,i}$) per specific unit volume taken by a digital microscope (V) as shown in Eqs. (3.2) and (3.3), respectively. In addition, the standard deviation (S.D.), which is a measure of the data dispersion, is defined in Eq. (3.4).

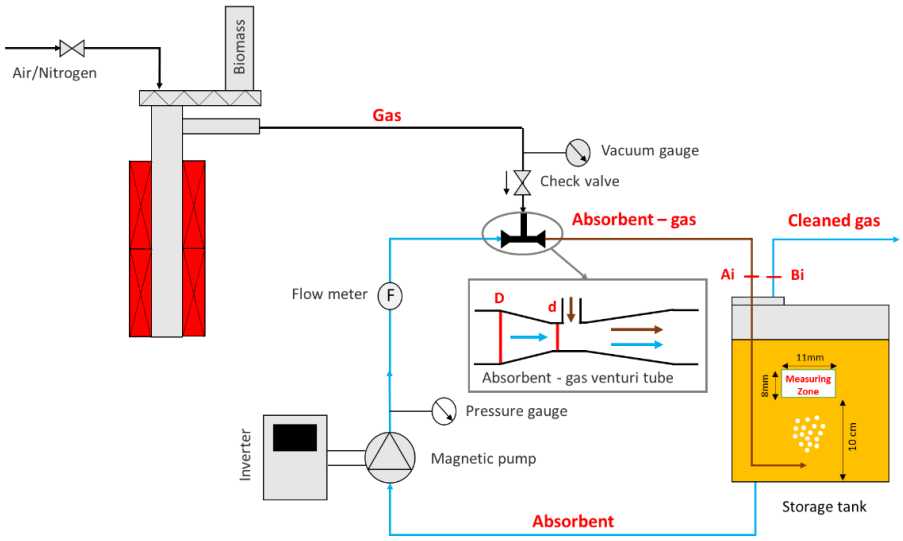

Figure 3.2. Schematic diagram of the microbubble size measuring and the laboratory-scale experimental setup

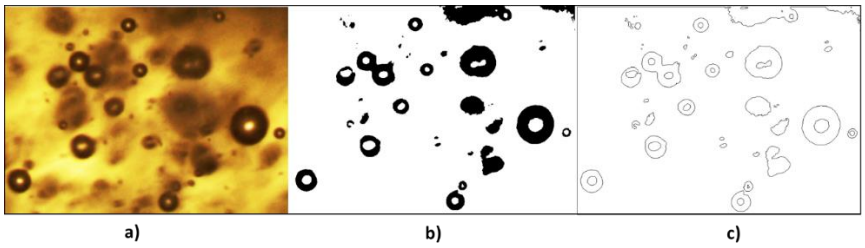

Figure 3.3. Image processing sequences for measuring the equivalent microbubble diameter

$$D_{10} = \frac{\sum_{i=1}^{n} D_{b,i}}{n} \tag{3.2}$$

$$\mathrm{n} = \frac{\sum_{i=1}^{n} N_{b,i}}{V} \tag{3.3}$$

$$S.D. = \sqrt{\frac{1}{n-1}\sum_{i=1}^{n}(D_{b,i} - D_{10})^2} \tag{3.4}$$

In order to find the optimum design of the venturi tube for microbubble production, the experiments were organized as shown in Table 3.1 in which the throat diameter ratio (d/D) and the inverter frequency were varied at three different levels. A fixed tube diameter of D = 12 mm was tested with different venturi tube diameters, d = 2, 5 and 8 mm, and different inverter frequencies, 40, 50 and 60 Hz, to study the influence of the throat velocity on the microbubble formation.

Table 3.1. Experimental setup for microbubble size measurement

Venturi tube			Inverter frequency (Hz)
Tube diameter (D, mm)	Venturi diameter (d, mm)	d/D (-)	
12	2	0.17	40, 50, 60
12	5	0.42	40, 50, 60
12	8	0.67	40, 50, 60

3.3.2 Laboratory-scale experiment

Real tar from pyrolysis gasification were produced using Japanese cedar as biomass feedstock. The Japanese cedar was pre-treated by crushing and sieving with a mesh size between 0.5 and 1 mm. The sample was dried at 105°C for 10 hours to reduce its moisture content. It was then stored in an enclosed container at the room temperature and humidity. As for scrubbing absorbent, canola oil was utilized. Its density and kinematic viscosity at 30°C scrubbing temperature was 0.9 g/cm^3 and 50.7 cSt, respectively. The characteristics of Japanese cedar and canola oil are summarized in Table 3.2.

Table 3.2. Proximate and ultimate analysis of Japanese cedar, rice husk, palm oil and canola oil

	Japanese cedar	Thai rice husk	Canola oil	Palm oil
Proximate analysis (wt.% dry basis)				
Volatile matter	84.1	59.7	-	-
Fixed carbon	15.6	11.9	-	-
Ash	0.3	28.4	-	-
LHV (MJ/kg)	16.4	14.3	-	-
Ultimate analysis (wt% dry ash free basis)				
C	50.4	32.2	77.5	76.3
H	6.3	4.3	12.7	12.3
N	0.1	0.8	0.2	0.1
O	43.2	62.3	9.6	11.3
S	<0.1	<0.4	<0.1	<0.1
Cl	<0.1	<0.4	<0.1	<0.1

Laboratory experiments were conducted using the fixed bed pyrolysis reactor made from stainless steel (SUS306) with an inner diameter and a height of 30 mm and 280 mm, respectively. The reactor was heated to 800°C by an electrical heater. Nitrogen was used as carrier gas by controlling the flow rate at 0.8 l/min. After an isothermal retention time of 30 minutes, the feedstock was continuously fed into the reactor by a screw feeder at the constant feed rate of 0.6 g/min. Then, the syngas and tar produced by the thermal decomposition were introduced into the venturi scrubber. The workflow of the venturi scrubber was the same as the one of microbubble size measurement. The tar content in the syngas before and after the scrubbing was analyzed by both wet and dry methods. A schematic diagram of the syngas generation part and the gas cleaning unit is shown in Figure 3.2 and the experiments were organized as shown in Table 3.3.

Table 3.3. Laboratory-scale experimental setup

Initial experimental set up		
Feedstock		Japanese cedar
- Feed rate (g/min)		0.6
- Mesh size (mm)		0.5 - 1
Carrier gas		Nitrogen
- Flow rate (l/min)		0.8
Pyrolyzer temperature (°C)		800
Absorbent		Canola oil
- Volume (liters)		2
Experimental no.	d/D (-)	Inverter frequency (Hz)
1	0.17	40
2	0.17	50
3	0.17	60
4	0.42	40
5	0.42	50
6	0.42	60
7	0.67	40
8	0.67	50
9	0.67	60

3.3.3 Pilot-scale experiment

In this study, Thai rice husk without any pretreatment process was utilized as feedstock and 50 liters of palm oil was used as scrubbing absorbent because it is abundant in the same region. Its density and the kinematic viscosity at 30°C scrubbing temperature was 0.9 g/cm^3 and 47.5 cSt, respectively. The characteristics of Thai rice husk and palm oil are also summarized in Table 3.2.

Figure 3.4 shows the schematic diagram of the pilot-scale bubbling fluidized bed gasifier (BFBG) designed by Siam Cement Public Company Limited (SCG), Thailand. There are two main parts in the gasifier section; the biomass feeding system and the gasifier. At the beginning, the gasifier was preheated by natural gas until the thermocouples at point T_1 and T_2 reached the temperature of 850°C and 800°C, respectively. After that, rice husk was continuously fed into the gasifer by the three series of screw feeder at the constant feed rate of 260 kg/h. The air flow rate was set at 375 Nm^3/h so as to control the equivalence ratio = 0.35. Silica sand was used as a bed material. The gasifer temperatures were approximately controlled at 800°C. Five thermocouples (K-type) were installed for monitoring the temperature inside the gasifier as shown in Figure 3.4. After the syngas was produced, it was introduced into the physical gas cleaning system consisting of a cyclone, a ceramic filter, an air cooler, two water coolers, a venturi scrubber and a packed bed adsorber. A schematic diagram of the gas cleaning unit is shown in Figure 3.4. The d/D and the oil throat velocity of venturi scrubber were fixed at 0.41 and 0.6 m/s, respectively. Finally, the tar removal efficiency of the venturi scrubber was analyzed by the wet and dry methods during the 20-hour operation. The experiments were organized as shown in Table 3.4.

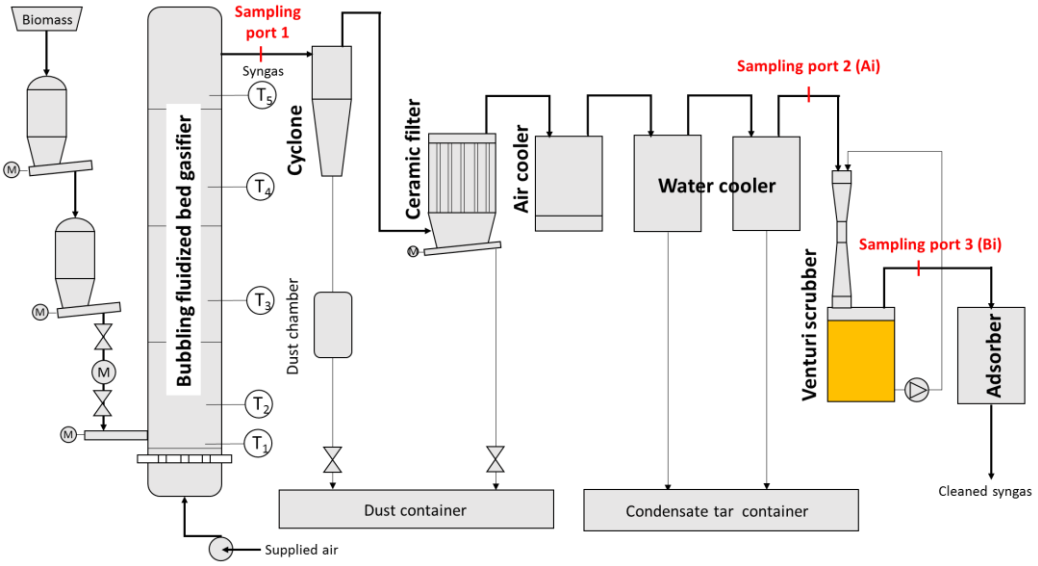

Figure 3.4. Schematic diagram of the pilot-scale bubbling fluidized bed gasifier (BFBG) and the physical gas cleaning unit

Table 3.4. Pilot-scale gasifier experimental setup

Experimental set up	
Feedstock	Rice husk
- Feed rate (kg/hr)	260
Carrier gas	Air
- Flow rate (Nm^3/hr)	375
Equivalence ratio	0.35
Gasifier temperature (°C)	800
Bed material	Silica sand
Venturi scrubber	
- Absorbent	Palm oil
- Volume (liters)	50
- d/D (-)	0.41
- Oil throat velocity (m/s)	0.6
Durations (hrs)	20

3.3.4 Tar sampling

According to the Energy Research Center of the Netherland (ECN) [3.11], tar consists of various organic aromatic ring hydrocarbons and can be classified into five classes based on the composition, the delectability, the water solubility and the condensation behavior of individual compounds as summarized in Table 3.5. It is found that the class 1 tar or gravimetric tar is the heaviest tar among all classes. The gravimetric tar starts to condense at around 300-350°C. In addition, ECN also reported the relationship between the light tar (class 2-5) dew point and the concentration of the different classes, which could be concluded as following. The tar dew point increases with an increase in the tar concentration because the condensation of tar is an integral of all tar classes. When the tar vapor pressure exceeds the saturation pressure, it leads to condensation of saturated vapor. The tar dew point of the class 3 tar is the lowest, while those of the class 2, 4 and 5 tars are relatively high, which results in fouling and blocking in downstream components. Therefore, the removal of the gravimetric tar (class 1), phenol (class 2) and naphthalene (class 4) was mainly investigated in this study.

Table 3.5. Classification of tar

Tar classification	Definition
Class 1	GC undetectable tar: It contains heavy poly-aromatic hydrocarbon, which is more than 7 rings. It could be called heavy tar or gravimetric tar as well.
Class 2	Heterocyclic compounds: It is highly water soluble hydrocarbon such as phenol.

Class 3	Aromatic compounds: It is one-ring aromatic hydrocarbon, which does not cause condensation and solubility problem such as benzene, toluene, xylene, and styrene.
Class 4	Light poly-aromatic compounds: It is two and three rings aromatic hydrocarbon, which condense at relatively high concentration at moderate temperature, such as indene, naphthalene, phenanthrene and anthracene.
Class 5	Heavy poly-aromatic compounds: It is from four to seven rings aromatic hydrocarbon, which condense at low concentration at high temperature such as pyrene, fluoranthene, chrysene.

3.3.4.1 Wet method

The wet method was utilized to analyze the gravimetric tar (class 1) according to ECN guideline [3.12]. The gravimetric tar was separated from the syngas by the condensation and dissolution. The measuring point consisted of Ai (the gas sampling at the inlet of the scrubber or untreated synthesis gas) and Bi (the gas sampling at the outlet of the scrubber or treated synthesis gas) to compare the gravimetric tar concentration before and after passing the scrubbing. Figure 3.5 illustrates the procedure of the gravimetric tar sampling method. The sampling line is composed of a series of ten impingers, a gas flow meter, a control valve and a suction pump. In order to prevent tar clogging in the workflow, a cotton and an activated carbon filters were connected. Ten impingers were put in a salt, water and ice mixture bath kept at 3°C by a mechanical cooling device and were filled with 100 ml of isopropanol. The gas sampling was done for 60 minutes with the flow rate of 1 l/min. After that, the tar in isopropanol solution was separated by filtering and then evaporating using a rotary evaporator in a water bath kept at 40°C. The residue after evaporation was defined as the gravimetric tar, which was then measured its weight.

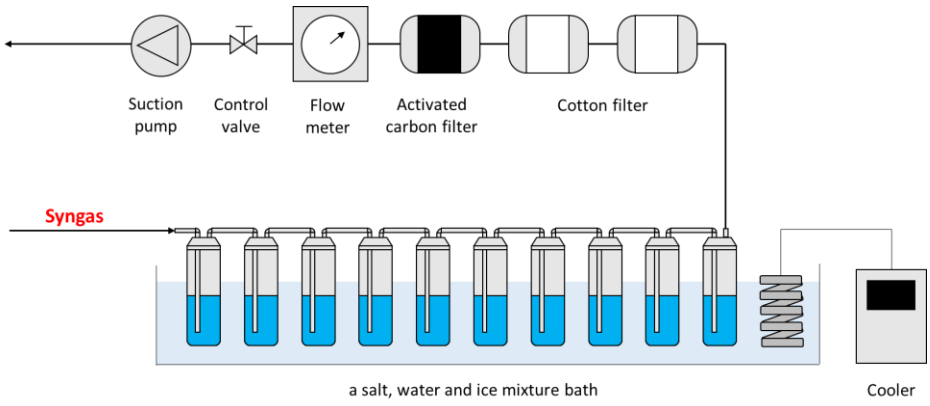

Figure 3.5. Illustration of the gravimetric tar sampling method

3.3.4.2 Dry method

The dry method was utilized to analyze light tars (class 2-5). Figure 3.6 illustrates the procedure of the light tar sampling method. A series of charcoal tube (containing 150g of activated carbon) and silica gel tube (containing 780mg of silica gel) purchased from Sibata Scientific Technology Ltd. were utilized for the sampling. The gas sampling was done for 3 minutes with a flow rate of 0.5 l/min. The measuring points were the same as those used in the wet method. Naphthalene and phenol are highly concerned in this study because of their tendency to become a solid phase at the ambient temperature resulting in the blockage of the piping system. After that, a gas chromatography flame ionization detector (GC-FID) was utilized to detect light tar components and their concentrations. Carbon disulfide and acetone were used as solvents for the charcoal tube and the silica gel tube, respectively.

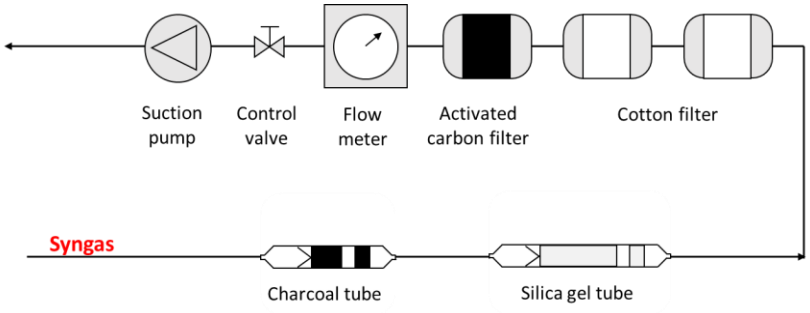

Figure 3.6. Illustration of the light tar sampling method

3.4. Results and discussions

3.4.1 Microbubble formation

3.4.1.1 Microbubble size distribution and mean microbubble diameter

According to various ranges of microbubble size formed by the venturi tube, a suitable method to compare the microbubble size distribution is in the form of the probability density function. The normal distribution function shown in Eq. (3.5) was selected in this research.

$$f(D_{b,i}) = \frac{1}{S.D.\sqrt{2\pi}} exp\left[-\frac{1}{2}\left(\frac{D_{b,i}-D_{10}}{S.D.}\right)^2\right] \quad (3.5)$$

Figure 3.7 illustrates the histograms of the microbubble size distribution, the percentage of the accumulative volume and analytical normal distribution functions at different inverter frequencies

and throat diameter ratios. Both the throat diameter ratio (d/D) and the inverter frequency had a direct influence on the throat velocity of the oil. For d/D = 0.42 and 0.67, the graphs indicated that an increase in the oil throat velocity shifted the microbubble size towards smaller one due to the enhancement of the bubble breakup mechanism. The accumulative distribution of the microbubble size less than or equal to 250 µm was also increased by 26% from 47% to 73% at the oil throat velocity of 1.2 and 5.6 m/s, respectively. However, the undesirable result was observed at d/D = 0.17, where the increase in the oil throat velocity shifted the microbubble size toward larger one and reduced the accumulative distribution from 70% to 36%. Figure 3.8 shows bubble coalescence reduction with an increase in the inverter frequency. A number of large bubbles which could not be measured by the digital microscope were distinctly observed as seen in the red circle due to bubble coalescence at a low d/D. The reduction of bubble coalescence could be done by increasing the oil throat velocity as shown in Figure 3.8. Although the reduction of bubble coalescence has a favorable effect on the number density enhancement as will be discussed further, the size of microbubbles produced due to the effect of bubble coalescence was still much larger than without having this effect.

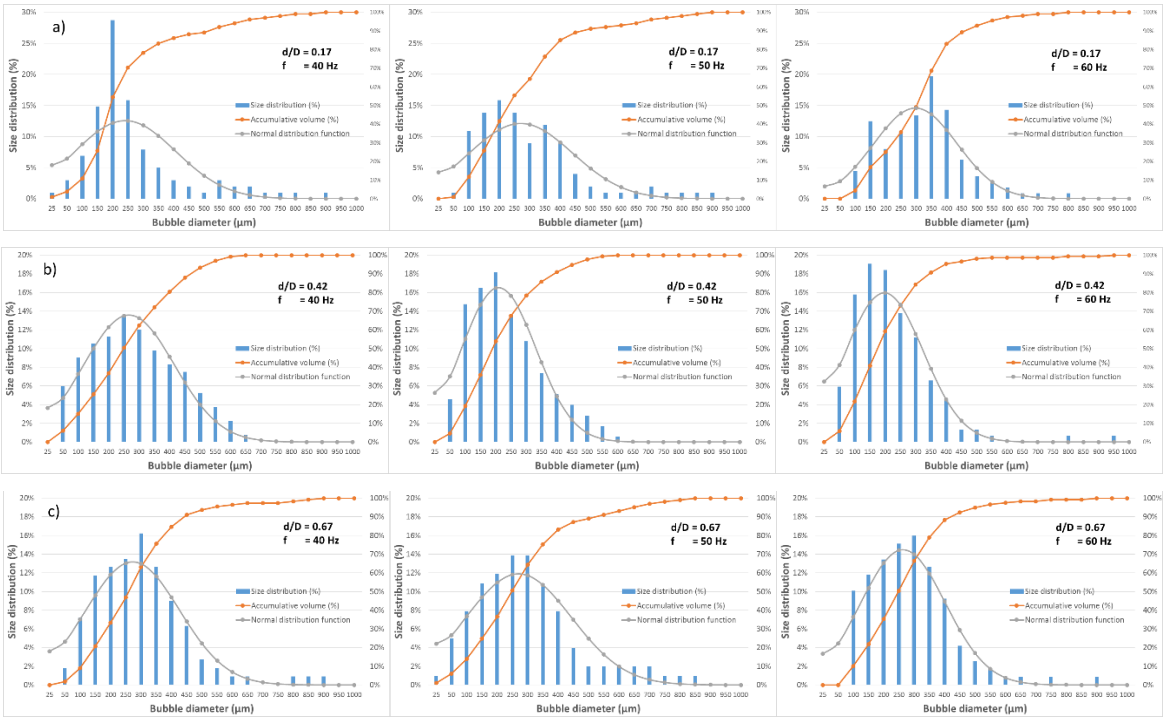

Figure 3.7. Histograms of the microbubble size distribution, the percentage of accumulative volume and analytical normal distribution functions at different inverter frequencies (40, 50 and 60 Hz) and throat diameter ratios; (a) d/D=0.17, (b) d/D=0.42 and (c) d/D=0.67

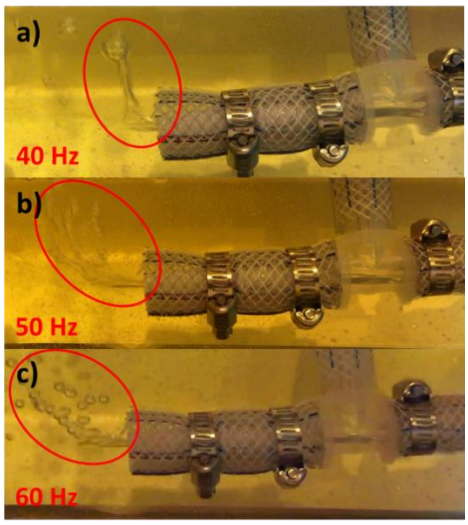

Figure 3.8. Illustration of bubble coalescence reduction with an increase in the inverter frequency; (a) 40 Hz, (b) 50 Hz and (c) 60 Hz, at d/D=0.17

Figure 3.9 summarized the effect of the increase of the oil throat velocity due to the inverter frequency variation on the change of the mean microbubble diameter at different throat diameter ratios. The increase in the oil throat velocity directly decreased the microbubble size, except for d/D = 0.17 due to the bubble coalescence as previously mentioned. The smallest mean microbubble diameter (197 µm) was obtained at d/D = 0.42 with the highest oil throat velocity.

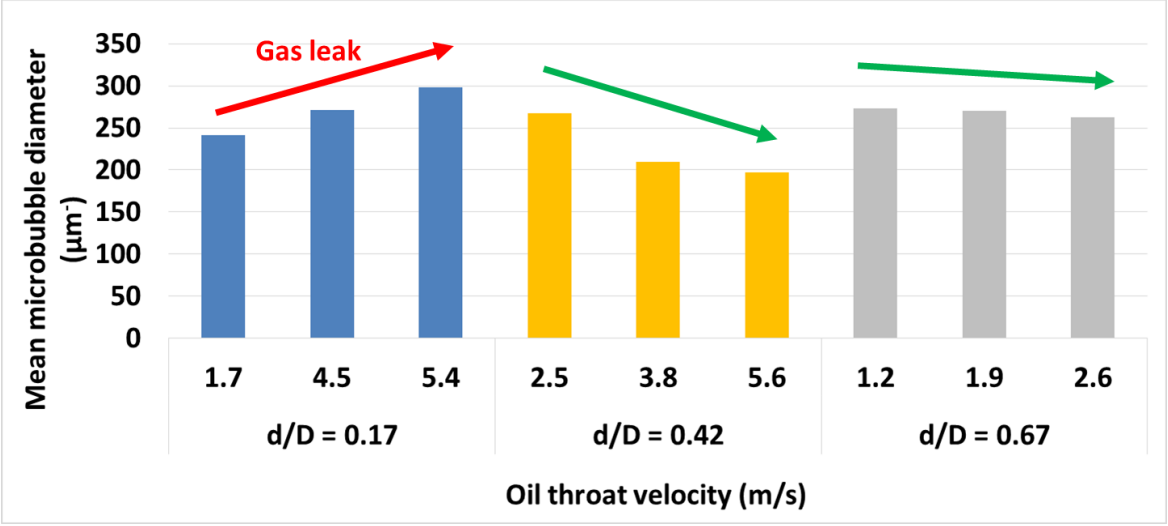

Figure 3.9. Effect of the increase of the oil throat velocity on the mean microbubble diameter at different throat diameter ratios; ● d/D=0.17, ● d/D=0.42 and ● d/D=0.67

3.4.1.2 Number density

The number density is the total number of specified microbubbles per specific unit volume taken by the digital microscope as shown in Figure 3.3c) which implies the number of microbubbles that can be derived from the supplied air. Figure 3.10 illustrated the effect of the increase in the oil throat velocity due to the inverter frequency variation on the number density at different throat diameter ratios. For all cases, an increase in the oil throat velocity also tended to move the number density toward high number density due to bubble breakup mechanisms. However, the number density at d/D = 0.17 was much lower compared to other diameter ratios. This could be explained by the following reason. The bubble coalescence had a negative effect on the number density because all experiments were done by constantly controlling the air flow rate at 1 l/min. This effect caused gas leak obstructing the number density formation at a low d/D ratio, while no significant bubble coalescence was visually observed at d/D = 0.42 and 0.67.

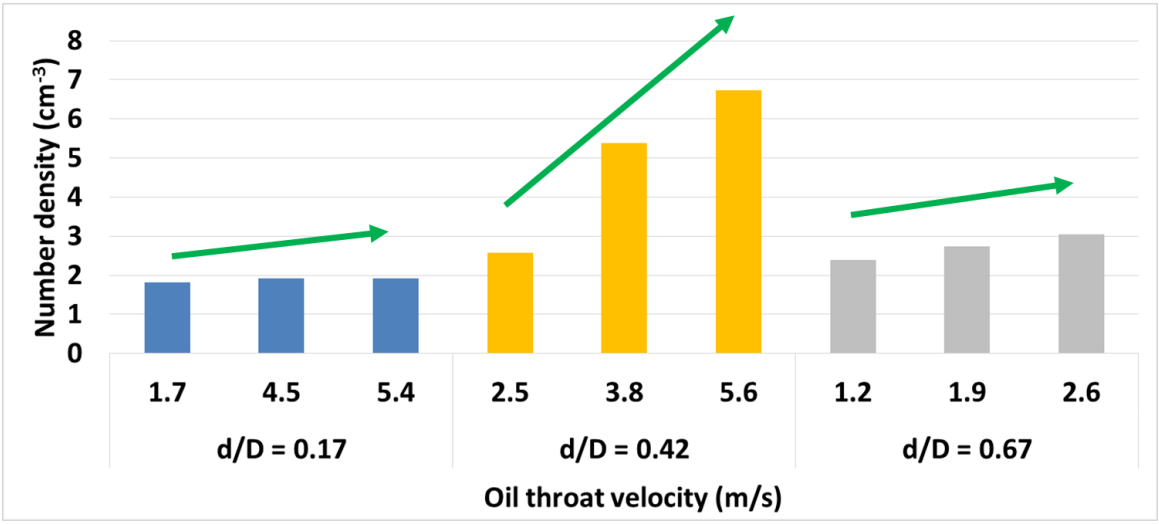

Figure 3.10. Effect of the increase in the oil throat velocity on the number density at different throat diameter ratios; d/D=0.17, 0.42 and 0.67, in all cases

3.4.1.3 Specific absorption surface area

As outlined in the introduction, the relationship between the syngas microbubble formation and the absorption surface area for tar removal was investigated in this study. The specific absorption

surface area increases with an increase in the number density and the decrease in the mean microbubble diameter. Both parameters are the main consideration to enhance the tar removal performance. The specific absorption surface area (A) aims to explain the physical absorption of gas droplets on a liquid surface, which could be determined as shown in Eq. (3.6).

$$A = n\pi D_{10}{}^{2} \quad (3.6)$$

Figure 3.11 shows the specific absorption surface area at different throat diameter ratios of all cases. The specific absorption surface area at d/D = 0.17 was the lowest due to the bubble coalescence while the highest one was achieved at d/D = 0.42 when the oil throat velocity was set to maximum.

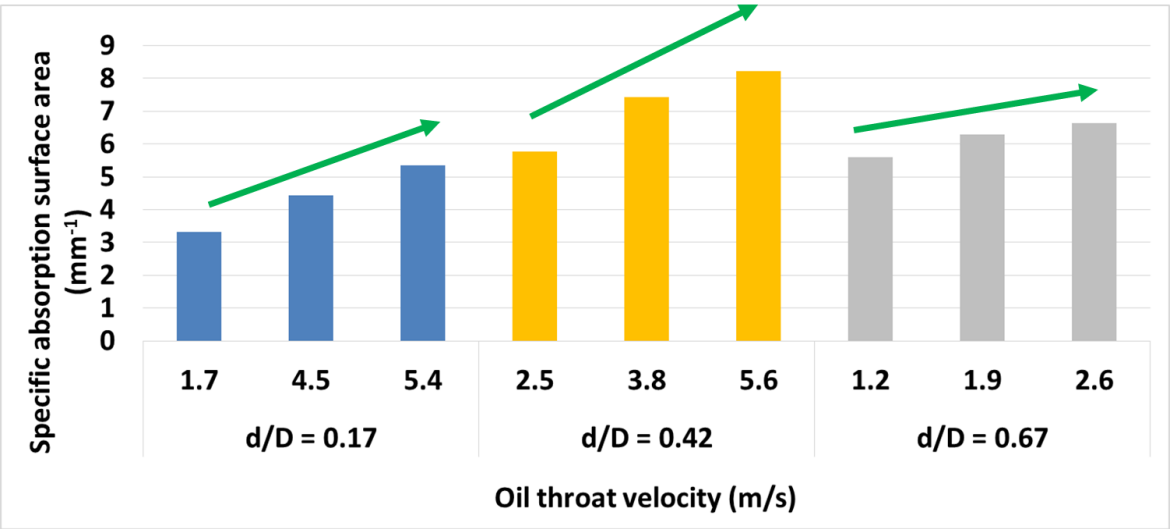

Figure 3.11. Specific absorption surface area at different throat diameter ratios; d/D=0.17, 0.42 and 0.67, in all cases

3.4.2 Laboratory-scale experiment

3.4.2.1 Gravimetric tar removal performance

The gravimetric tar (class 1) is the most dangerous tar for downstream components due to its potential to change from gaseous phase to liquid phase at an operating temperature below 350°C [3.13,3.14]. Its dew point temperature was also higher than that of other classes. The condensation of gravimetric tar leads to clogging, fouling and breakdown of machines and piping in the downstream application. According to the high portion of non-polar compounds in the gravimetric tar, canola oil

was selected as the absorbent for tar removal. In this study, 69.8 g/Nm^3 of gravimetric tar produced by Japanese cedar in the laboratory-scale fixed bed pyrolyzer was constantly supplied to the venturi scrubber. The tar removal efficiency in each experiment was calculated by utilizing Eq. (3.7).

$$\eta_{removal} = \frac{m_{t,i} - m_{t,o}}{m_{t,i}} \times 100 \quad (3.7)$$

Where $m_{t,i}$ is the gravimetric tar concentration before the scrubbing and $m_{t,o}$ is the gravimetric tar concentration after the scrubbing.

Figure 3.12 illustrates the correlation between the tar removal efficiency and the specific absorption surface area. Based on the experimental results, the tar removal efficiency increased linearly with the increase of the specific absorption surface area. At d/D = 0.17, the tar removal efficiency was the lowest among others due to the bubble coalescence resulting in lowering of the specific absorption surface area. The tar removal efficiency was improved from 88.3% to 90.6% due to the increase in the oil throat velocity, which supported the bubble breakup mechanisms as previously discussed. At d/D = 0.42 and 0.67, the tar removal efficiency was higher than in the case of d/D = 0.17 because there was no bubble coalescence visually observed. The tar removal efficiency was between 91.2% and 94.1% in the case of d/D = 0.67, while ranging between 91.9% and 97.7% in the case of d/D = 0.42. However, it can be seen that the tar removal efficiency increased by 5.8% at d/D = 0.42, while by just only 2.9% at d/D = 0.67. This is because a large throat diameter requires more oil flow to increase its throat velocity. The oil throat velocity at d/D = 0.42 and 0.67 were increased by 3.1 and 1.4 m/s, respectively. In conclusion, the tar removal efficiency at the highest inverter frequency in all cases was optimal due to an increase in the oil throat velocity (bubble breakup mechanisms). The best d/D value in this experiment was 0.42 because the bubble coalescence occurred at a low d/D value, while more energy is necessary to enhance the oil throat velocity at a larger d/D value.

Compared to previous study, the tar removal efficiency of the venturi scrubber was much better than the bubbling scrubber. The bubbling scrubber was able to remove the gravimetric tar down to only 14.0 g/Nm^3 with only 80% tar removal efficiency [3.15], while more than 88% could be removed by the venturi scrubber, where in the best case, gravimetric tar was reduced down to 1.6 g/Nm^3 corresponding to the tar removal efficiency of 97.7%. This is because the bubble size produced in the bubbling scrubber was much larger than that in the venturi scrubber resulting in a lower absorption surface area. Although the increase in the turbulent mixing by increasing the stirrer speed also improved the gravimetric tar removal efficiency of the bubbling scrubber up to 89.8% in the previous work [3.16], a low quantity of microbubbles was produced by this technique.

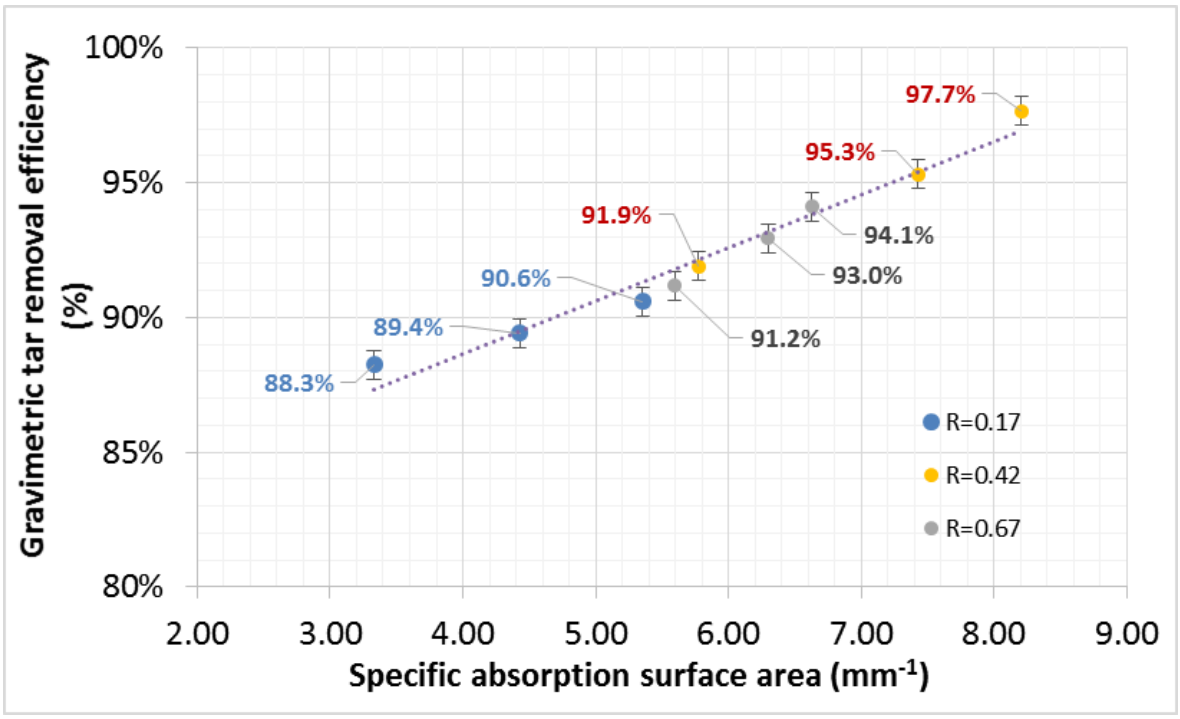

Figure 3.12. Gravimetric tar removal efficiency of the venturi scrubber at different specific absorption surface areas in the laboratory-scale fixed bed pyrolyzer experiment

In addition, there were some evidences to confirm the benefits of producing syngas microbubbles for tar removal. In this study, numerous syngas microbubbles were produced at the venturi throat due to the bubble breakup mechanism. The syngas microbubbles then moved to the storage tank. In the storage tank, the syngas microbubbles were gradually separated from the absorbent material because the retention time of the syngas microbubbles in the absorbent was longer than that of the common syngas bubbles, which improved the tar removal efficiency as well. This could be explained by the model of the overall force balance on a bubble as shown in Eq. (3.8) [3.17].

$$F_B + F_M = F_D + F_\sigma + F_{BA} + F_{I,g} + F_C + F_{I,m} \quad (3.8)$$

$$F_B = \frac{\pi}{6} d_{10}^3 (\rho_l - \rho_g) g \quad (3.9)$$

The force balance involved in this equation consisted of the upward forces (the buoyancy force (F_B) and the gas momentum force (F_M)), the downward resistant forces (the liquid drag force (F_D), the surface tension force (F_σ), the Basset force (F_{BA}), the bubble inertial force ($F_{\mathrm{l,g}}$) and the downward forces from particles effect (the particle-bubble collision (F_{C}) and the suspension inertial ($F_{\mathrm{l,m}}$) forces). The reduction of the mean microbubble diameter directly affected the decrease of the buoyancy force as shown in Eq. (3.9). According to Eq. (3.8), the decrease in the upward forces due to the buoyancy force was effective to increase the gas retention time in the scrubber.

3.4.2.2 Light tar removal performance

Regarding the high tendency of naphthalene and phenol to become solid at the ambient temperature leading to blockages in downstream components, they are also of interest in this study. Approximately only 1.2 and 0.2 g/Nm^3 of naphthalene and phenol were produced at the exit of the reactor. Figure 3.13 illustrates the effect of the specific absorption surface area on the phenol and naphthalene removal efficiency. It can be seen that naphthalene and phenol were completely removed in all cases by the venturi scrubber. Compared to the previous study, the light tar removal efficiency of the venturi scrubber was also higher than the bubbling scrubber with the removal efficiency of 97.9% and 94.6% for naphthalene and phenol, respectively [3.15].

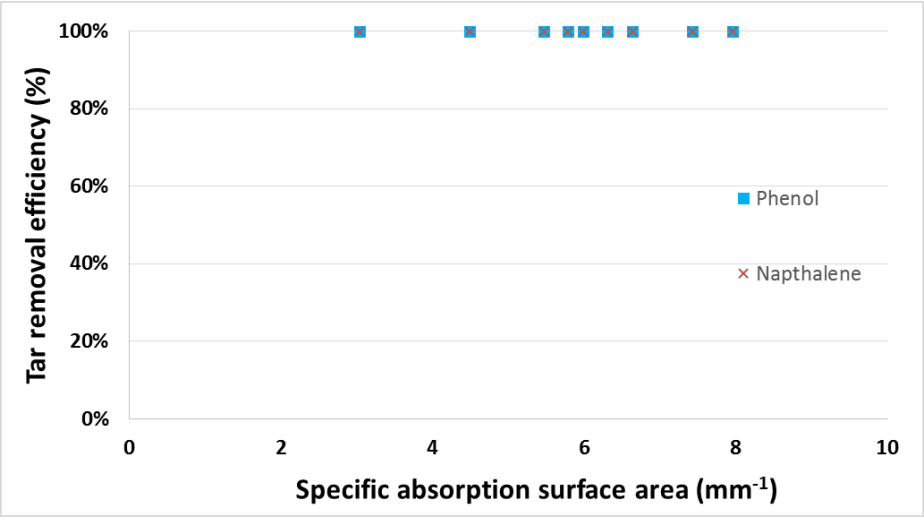

Figure 3.13. Light tar (phenol and naphthalene) removal efficiency of the venturi scrubber at different specific absorption surface areas in the laboratory-scale fixed bed pyrolyzer experiment

3.4.3 Pilot-scale experiment

3.4.3.1 Gravimetric tar removal performance

11.8 g/Nm^3 of gravimetric tar produced by the pilot-scale BFBG was introduced into the gas cleaning system. Afterwards, a series of cyclone, a ceramic filter, an air cooler and two water coolers reduced the gravimetric tar concentration down to an average of 4.3 g/Nm^3 corresponding to 63.6% tar removal efficiency. The remaining tar was then passed through the venturi scrubber. Figure 3.14 shows the gravimetric tar removal efficiency of the venturi scrubber along the 20-hour duration test. In the first two hours of operation, the tar removal efficiency was 91.3%. After the 20th hour, the removal efficiency was slightly dropped to 83.9% due to the absorbent regeneration techniques [3.18]. After cleaning syngas in the scrubber, used oil was fed into the oil regenerative unit by the filtration method in order to trap solid contaminants, which obstructed the dissolution ability. Then, the regenerated oil was returned to the venturi scrubber. The slight drop of the gravimetric tar removal efficiency might require the change of the absorbent in a longer period of operation due to the deterioration of the absorbent. Although the tar measurement is complicated and difficult to implement in a pilot-scale plant, the deterioration of the absorbent could be simply inspected by its viscosity. This is because an accumulation of tar and other contaminants in the absorbent strongly affects the mass transfer between tar and the absorbent. Therefore, tar and other contaminants were continuously collected in the absorbent until reaching the deterioration point, where there was no mass transfer observed. This accumulation of tar and other contaminants in the absorbent causes the increase in the viscosity of the absorbent.

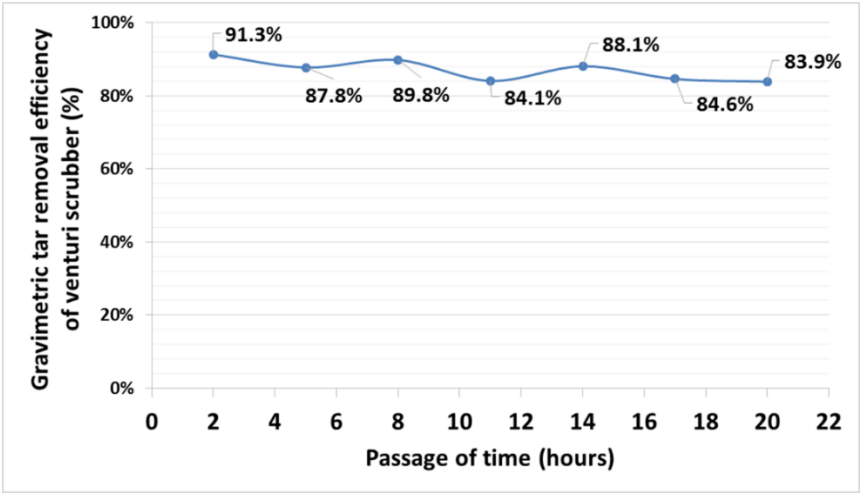

Figure 3.14. Gravimetric tar removal efficiency of the venturi scrubber in the pilot-scale bubbling fluidized bed gasifier along the 20-hour duration test

The overall gravimetric tar removal efficiency of the venturi scrubber was 87.1% along the 20-hour duration test. Compared to the best performance of the laboratory-scale experiment, the tar removal efficiency in the pilot-scale experiment was about 6.4% lower. This could be explained by the following reason. Although the d/D ratios in both the pilot and laboratory scales were similar, the oil throat velocity in the pilot scale was just 0.6 m/s, while it was 5.6 m/s in the best performance case in the laboratory-scale experiment. Therefore, the bubble breakup mechanism in the laboratory-scale experiment was much enhanced and the bubble coalescence was much suppressed than in the pilot-scale experiment. In order to improve the gravimetric tar removal efficiency of the venturi scrubber in the pilot-scale experiment, an increase in the oil throat velocity is required.

In addition, the combination of the gas cleaning system; a series of a cyclone, a ceramic filter, an air cooler, water coolers, the venturi scrubber and the packed bed adsorber, reduced the gravimetric tar concentration down to less than 0.1 g/Nm^3 corresponding to 99.2% tar removal efficiency. Therefore, after passing through the gas cleaning system, syngas is clean enough to be used as gaseous fuel in an internal combustion engine.

3.4.3.2 Light tar removal performance

Approximately only 0.2 and 0.1 g/Nm^3 of naphthalene and phenol were produced by the BFBG. Figure 3.15 illustrates the removal efficiency of naphthalene and phenol. The tendency of naphthalene and phenol removal was similar to the laboratory-scale experiment. It can be seen that phenol was completely removed by a series of a cyclone, a ceramic filter, an air cooler and two water coolers, while naphthalene was completely removed at the exit of the venturi scrubber.

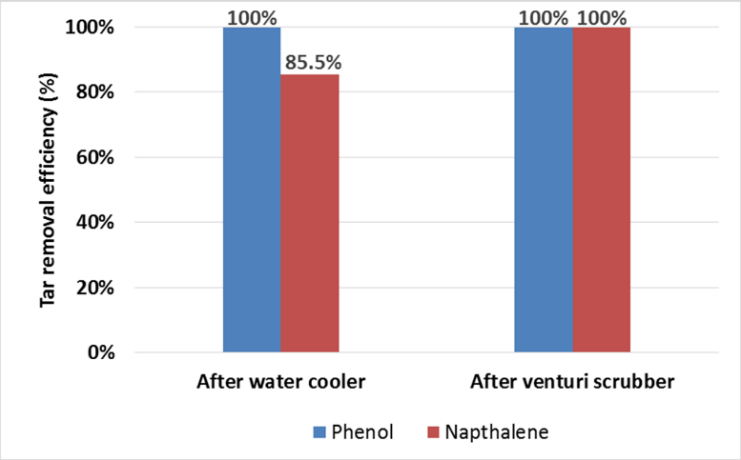

Figure 3.15. Light tar removal efficiency of the water cooler and the venturi scrubber in the pilot-scale bubbling fluidized bed gasifier along the 20-hour duration test

3.5 Conclusion

The objective of this chapter was to investigate the tar removal performance of a venturi scrubber producing syngas microbubbles, which markedly enhanced the absorption surface area compared to a bubbling scrubber. Vegetable oil was used as the absorbent in both laboratory and pilot scale experiments due to its effective absorption performance for tar removal. The syngas containing tar was produced by local biomass and then introduced to the gas cleaning system (venturi scrubber). Several trial products with different throat diameter ratios of the venturi tube were investigated in order to find the best condition for tar removal. This study was divided into three parts; the microbubbles formation, the tar removal performances in laboratory and pilot scale experiments.

For the microbubbles formation, the mean microbubble diameter and the number density could be determined by the images of the microbubbles taken using the digital microscope. The specific absorption surface area was the key parameter to optimize the designing of the venturi scrubber, which could be determined by the mean microbubble diameter and the number density. It was found that the specific absorption surface area at d/D = 0.17 was the lowest due to the bubble coalescence while the highest one was achieved at d/D = 0.42 with the highest oil throat velocity.

In the laboratory-scale experiment, the tar removal efficiency linearly increased with the increase of the specific absorption surface area. The gravimetric tar removal efficiency of the venturi scrubber was higher than that of the bubbling scrubber at all specific absorption surface areas. Only

80% of tar was removed by the bubbling scrubber, while more than 88% was eliminated by the venturi scrubber, where the best performance was 97.7%. Furthermore, naphthalene and phenol were completely removed by the venturi scrubber.

In the pilot-scale experiment, the 20-hour operation of the pilot-scale bubbling fluidized bed gasifier also confirmed that the overall gravimetric tar removal efficiency of the venturi scrubber was 87.1%, while there were no naphthalene and phenol observed at the exit of the venturi scrubber as well. Furthermore, the overall tar removal efficiency was 99.2% by the use of the physical gas cleaning system comprised of the following: a series of a cyclone, a ceramic filter, an air cooler, water coolers, the venturi scrubber and the packed bed adsorber. This could achieve the syngas quality requirement for the safely operation of internal combustion engines.

3.6 Reference

[3.1] Oliveira C, Rodrigues RT, Rubio J. A new technique for characterizing aerated flocs in a flocculation--microbubble flotation system. Int J Miner Process 2010;96:36–44.

[3.2] Chu L-B, Xing X-H, Yu A-F, Sun X-L, Jurcik B. Enhanced treatment of practical textile wastewater by microbubble ozonation. Process Saf Environ Prot 2008;86:389–93.

[3.3] Park J-S, Kurata K. Application of microbubbles to hydroponics solution promotes lettuce growth. Horttechnology 2009;19:212–5.

[3.4] Kotachi A, Miura T, Imai H. Polymorph Control of Calcium Carbonate Films in a Poly (acrylic acid)- Chitosan System. Cryst Growth Des 2006;6:1636–41.

[3.5] Sadatomi M, Kawahara A, Kano K, Ohtomo A. Performance of a new micro-bubble generator with a spherical body in a flowing water tube. Exp Therm Fluid Sci 2005;29:615–23.

[3.6] Fujiwara A, Takagi S, Watanabe K, Matsumoto Y. Experimental study on the new micro-bubble generator and its application to water purification system. ASME/JSME 2003 4th Jt. Fluids Summer Eng. Conf., 2003, p. 469–73.

[3.7] Gadallah AH, Siddiqui K. Bubble breakup in co-current upward flowing liquid using honeycomb monolith breaker. Chem Eng Sci 2015;131:22–40.

[3.8] Thiemann A, Nowak T, Mettin R, Holsteyns F, Lippert A. Characterization of an acoustic

cavitation bubble structure at 230kHz. Ultrason Sonochem 2011;18:595–600.

[3.9] Shintaku H, Imamura S, Kawano S. Microbubble formations in MEMS-fabricated rectangular channels: A high-speed observation. Exp Therm Fluid Sci 2008;32:1132–40.

[3.10] Maeda Y, Hosokawa S, Baba Y, Tomiyama A, Ito Y. Generation mechanism of micro-bubbles in a pressurized dissolution method. Exp Therm Fluid Sci 2015;60:201–7.

[3.11] Kiel JHA, Van Paasen SVB, Neeft JPA, Devi L, Ptasinski KJ, Janssen F, et al. Primary measures to reduce tar formation in fluidised-bed biomass gasifiers. ECN, ECN-C-04-014. 2004.

[3.12] Van Paasen SVB, Kiel JHA, Neeft JPA, Knoef HAM, Buffinga GJ, Zielke U, et al. Guideline for sampling and analysis of tar and particles in biomass producer gases. Energy Res Cent Netherlands, ECN-C-02-090. 2002.

[3.13] Hasler P, Nussbaumer T. Gas cleaning for IC engine applications from fixed bed biomass gasification. Biomass and Bioenergy 1999;16:385–95. doi:10.1016/S0961-9534(99)00018-5.

[3.14] Mondal P, Dang GS, Garg MO. Syngas production through gasification and cleanup for downstream applications—Recent developments. Fuel Process Technol 2011;92:1395–410.

[3.15] Unyaphan S, Tarnpradab T, Takahashi F, Yoshikawa K. Effect of emulsified absorbent for tar removal in biomass gasification process. Biofuels 2016;7:233–43.

[3.16] Paethanom A, Nakahara S, Kobayashi M, Prawisudha P, Yoshikawa K. Performance of tar removal by absorption and adsorption for biomass gasification. Fuel Process Technol 2012;104:144–54.

[3.17] Luo X, Yang G, Lee DJ, Fan L-S. Single bubble formation in high pressure liquid—solid suspensions. Powder Technol 1998;100:103–12.

[3.18] Tarnpradab T, Unyaphan S, Takahashi F, Yoshikawa K. Improvement of the biomass tar removal capacity of scrubbing oil regenerated by mechanical solid--liquid separation. Energy & Fuels 2017.

Chapter 4

Comparative performance of oil and emulsified absorbent in scrubber producing syngas microbubbles

Abstract

This chapter investigated the tar removal performance of vegetable oil and emulsified absorbent in the venturi scrubber enhancing the turbulent mixing by producing syngas microbubbles, where the Reynolds number was the parameter to measure the fluid behavior. The results showed that the increase in the syngas Reynolds number had a favor to the increase in the bubble breakup mechanism and the specific absorption surface area. The gravimetric tar removal efficiency continuously increased with the increase of the syngas Reynolds number of both the vegetable oil and the emulsified absorbent. Moreover, it also confirmed that the gravimetric tar removal efficiency of the emulsified oil was better than the vegetable oil in all experimental conditions. The optimum condition for tar removal was at the highest Reynolds number for both of them, where no gravimetric and light tars were observed in the emulsified absorbent scrubber, while up to 97.7% and 100% of gravimetric tar and light tars were removed by the vegetable oil scrubber. In addition, the mass transfer modelling was also investigated by comparing with the experimental data.

4.1 Background

This chapter investigated the tar removal performance combining two main aspects; the absorbent selection and the scrubber type. For the absorbent selection, previous studies were intensively investigated on the appropriate absorbent for tar removal and found that the tar removal efficiency of oil-based absorbent, especially vegetable oil, was better than water-based absorbent [4.1,4.2]. Moreover, the interesting results in Chapter 2 showed that the emulsified oil (the combination of the hydrophobic and hydrophilic absorbent) enhanced the tar removal efficiency compared to other oil-based absorbent because tar was also composed of both the hydrophobic and hydrophilic tar, where the majority was hydrophobic one [4.3]. For the scrubber type, the tar concentration of treated syngas by the bubbling scrubber and the packed-bed scrubber was still higher than the limitation as previously mentioned in Chapters 2 and 3 [4.4–4.9]. Therefore, in order to completely remove tar by the scrubber, one of the possibility to achieve the target is to increase the turbulent mixing in the venturi scrubber. The increase in the turbulent mixing should make the

syngas bubbles getting smaller until it become microbubbles, which resulted in the increase in the absorption surface area and that gave more area for tar to be absorbed. Previous studies on air microbubble generators in water found that the increase in the turbulent mixing had a favor to decrease the mean gas microbubbles diameter [4.10,4.11]. The similar result was also confirmed in the venturi scrubber, where numerous microbubbles were generated [4.12]. In addition, the interesting results in Chapter 3 showed that up to 97.7% of the gravimetric tar was removed by the vegetable oil in the venturi scrubber producing syngas microbubbles, while all of light tars were not existed. However, the performance of the venturi scrubber for tar removal was still limited and the relationship between the fluid behavior and the tar removal was not clarified as well, where the important parameter to indicate the level of the fluid behavior is “Reynolds number (Re)”.

In this chapter, a venturi scrubber is selected because it is simple to produce various kinds of fluid behavior and also widely used in the commercial scale. The selected absorbents are the vegetable and emulsified oil. The Reynolds number is determined based on the assumption of the multiphase flow of syngas-absorbent, where the Reynolds number of the gas and the liquid phases are separately determined in order to obviously observe the fluid flow. This study first presents a fluid behavior of syngas and absorbent (vegetable and 7.5% emulsified oil) in the bubbling scrubber and the venturi scrubber, where the Reynolds numbers of the syngas, the vegetable oil and the emulsified oil are also presented according to various scrubber designs. Then, the effect of the Reynolds number on the gravimetric and light tar removal performance is determined in the laboratory scale. Finally, the mass transfer modelling is studied to observe the overall volumetric liquid-side mas-transfer coefficient.

4.2 Multiphase flow and syngas microbubble formation

The multiphase flow refers to any fluid flow consisted of more than one of these phases (solid, liquid and gas), for example, the gas-solid flow, the liquid-solid flow or the gas-liquid flow [4.13–4.15]. This study mainly identifies the fluid mechanical phenomena of the gas-liquid flow. The simultaneous flow of gas and liquid in a tube with different fluid properties, flow rates, pressures and so forth contribute several types of flow patterns. Six main types of the gas-liquid flow pattern usually found were shown and summarized in Figure 4.1 and Table 4.1; the bubbly, the dispersed bubbly, the slug, the churn, the annular and the mist flows. The bubbly and dispersed bubbly flow is the main consideration in this study according to a low-pressure and low-temperature operation.

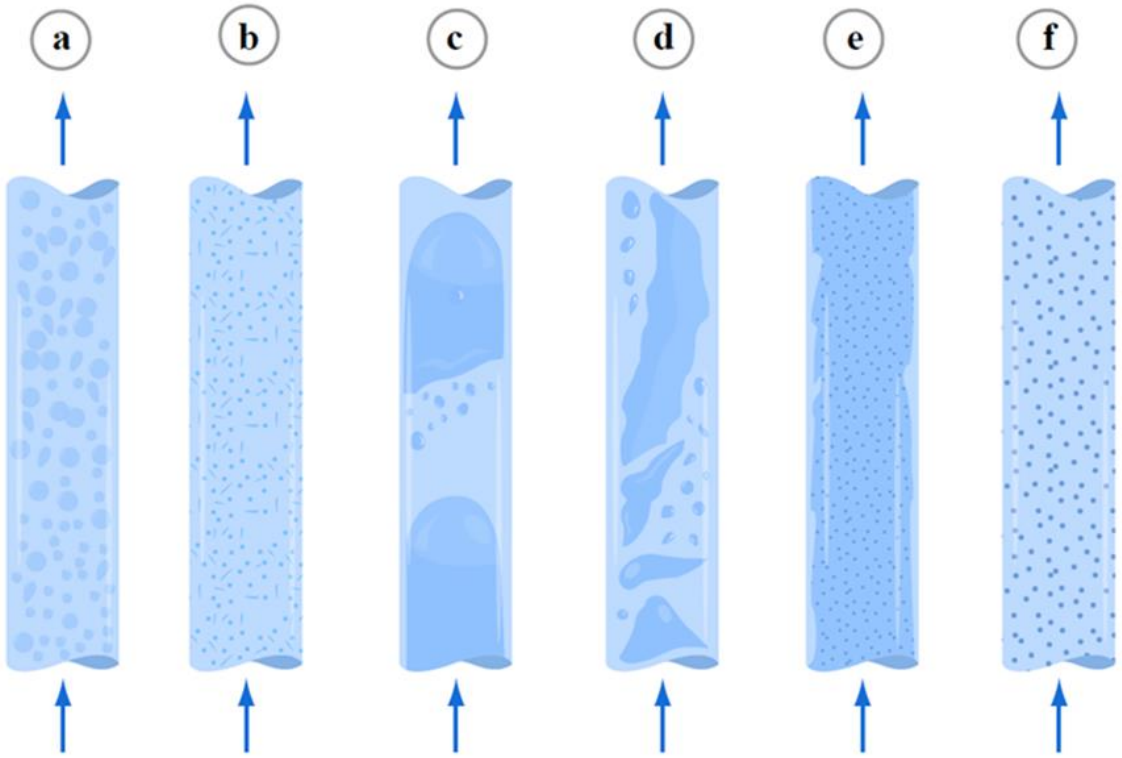

Figure 4.1. Illustration of six main types of gas-liquid flow patterns

Table 4.1. Six main types of gas-liquid flow patterns

Flow quality (Pressure, Temperature)	Flow rate	Flow regime
Low	Low to medium	a) Bubbly flow
	High	b) Dispersed bubbly flow
Intermediate	Low to medium	c) Plug/slug flow
	High	d) Churn flow
High	Low to medium	e) Annular flow
	High	f) Mist flow

In this study, the multiphase flow of the syngas and the absorbent is produced by the venturi scrubber consisted of the convergent, the throat and the divergent part as shown in Figure 4.2. The absorbent is introduced into the convergence part of the venturi tube, while the syngas is sucked into the liquid stream at the throat part due to the conservation equations of mass and energy. The sucked syngas is well-broken into numerous microbubbles by the action of a highly-turbulent shear flow called as “the bubble breakup mechanism” [4.10].

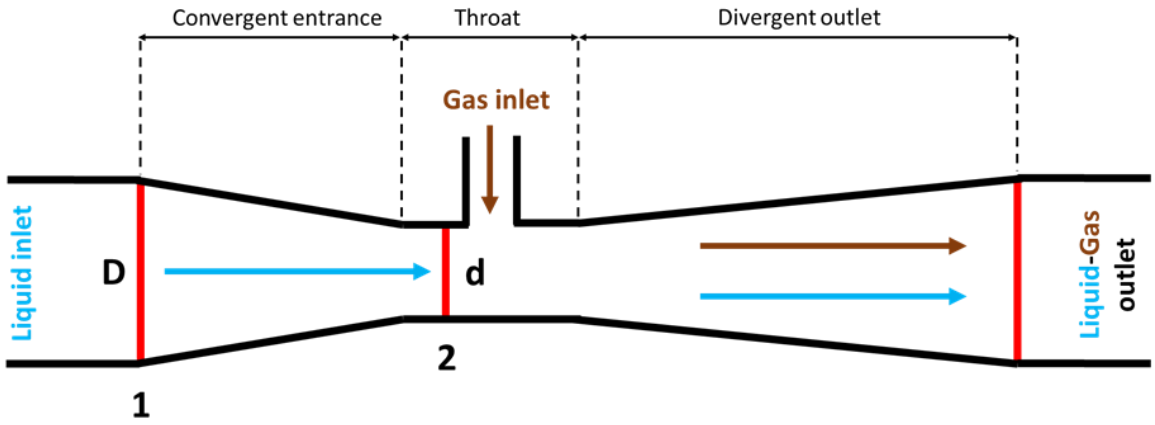

Figure 4.2. Illustration of a common venturi tube

In order to study the fluid behavior of the gas-liquid flow on tar removal, the Reynolds number (Re), which is the dimensionless ratio of the inertial forces to the viscous forces, is an important parameter for guiding the fluid behavior. In the gas-liquid flow, the Reynolds number of the syngas and the absorbent could be separately calculated as shown in Eqs. 4.1 and 4.2 [4.16].

$$Re_{absorbent} = \frac{GxD_h}{\mu_l \alpha} \quad (4.1)$$

$$Re_{syngas} = \frac{G(1-x)D_h}{\mu_g(1-\alpha)} \quad (4.2)$$

Where G is the mass flux, μ is the dynamic viscosity, α is the void fraction and x is the gas-liquid fraction.

4.3 Material and Experimental setup

4.3.1 Raw material

Japanese cedar was utilized as the biomass feedstock for producing real tar from pyrolysis gasification. The preparation of feedstock was done by crushing and sieving with a mesh size from 0.5 mm to 1 mm, drying at 105°C for 10 hours for surface moisture removal and finally storing in an enclosed containers at the room temperature. The characteristic of Japanese cedar was summarized in Table 4.2.

The reactor was made from stainless steel (SUS360) with the inner diameter and the height of 30 mm and 280 mm, respectively. It was heated and controlled to 800°C by an electrical heater and a digital temperature controller, respectively. Before conducting the experiment, the preparation was done by feeding 0.8 l/min of nitrogen as the carrier gas, heating up the reactor, waiting for 30 minutes after reaching the target temperature for isothermal retention time and finally feeding 0.6 g/min of Japanese cedar. Then, the syngas and tar produced by the thermal decomposition were introduced into the venturi scrubber. Finally, the tar concentration before and after the venturi scrubber were analyzed by the wet and dry methods. A schematic diagram of the experimental setup is shown in Figure 4.3.

Table 4.2. Proximate and ultimate analysis of Japanese cedar and vegetable oil

	Japanese cedar	Canola oil
Proximate analysis (wt.% dry basis)		
Volatile matter	84.1	-
Fixed carbon	15.6	-
Ash	0.3	-
LHV (MJ/kg)	16.4	-
Ultimate analysis (wt% dry ash free basis)		
C	50.4	77.5
H	6.3	12.7
N	0.1	0.2
O	43.2	9.6
S	<0.1	<0.1
Cl	<0.1	<0.1

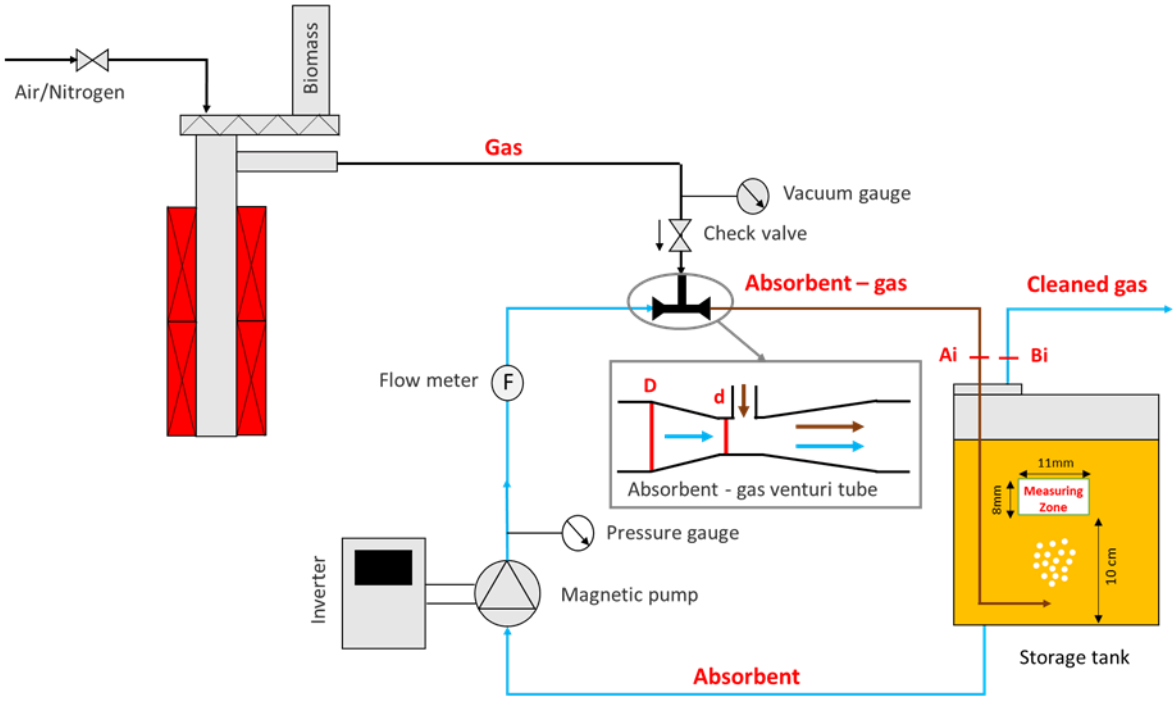

Figure 4.3. Schematic diagram of the experimental setup

4.3.2 Absorbent and venturi scrubber

According to the scrubbing material discussed in Chapter 2 [4.5], 100% of canola oil (vegetable oil, VO) and 7.5% by volume of water in canola oil (7.5% emulsified oil, 7.5%EO) were selected as the scrubbing absorbent. The kinematic viscosity of VO and 7.5%EO at 30°C scrubbing temperature was 66.1 cSt and 63.9 cSt, respectively. The emulsion state of 7.5%EO was produced under “the breakup mechanism” in the venturi tube at the throat part for 30 minutes before conducting the experiment to homogenously control the emulsion state and to assure the uniform distribution of oil and water

Figure 4.3 illustrates a schematic diagram of the venturi scrubber. The absorbents (VO and 7.5%EO) were recirculated by the magnetic pump (SL-20S, As-0ne Co., Ltd., Japan). The flow rate was controlled and measured by an inverter (FR-FS2-0-0.8K, Mitsubishi Electric Co., Ltd., Japan) and a digital flow meter (DigiFlow 6700M, As-0ne Co., Ltd., Japan), respectively. In order to produce various kinds of fluid behavior, the experiments were organized as shown in Table 4.3 in which the throat diameter ratio (d/D) and the inverter frequency were varied at three different levels. A fixed

tube diameter of D=12 mm was tested with different vendturi diameters, d=2, 5 and 8 mm, and different inverter frequencies, f=40, 50 and 60 Hz.

Table 4.3. Experimental procedure

Initial experimental set up		
Feedstock		Japanese cedar
- Feed rate (g/min)		0.6
- Mesh size (mm)		0.5 - 1
Carrier gas		Nitrogen
- Flow rate (l/min)		0.8
Pyrolyzer temperature (°C)		800
Absorbent		VO and 7.5%EO
- Volume (liters)		2
Experimental no.	d/D (-)	Inverter frequency (Hz)
1	0.17	40
2	0.17	50
3	0.17	60
4	0.42	40
5	0.42	50
6	0.42	60
7	0.67	40
8	0.67	50
9	0.67	60

4.3.3 Tar sampling and analysis methods

Many measurement methods of organic contaminants and particles in the syngas from biomass gasification have been standardized by ECN guideline [4.17,4.18]. In this study, the wet method and the dry method were utilized in order to analyze the concentration of the gravimetric and light tars, respectively.

4.3.3.1 Wet method

Figure 4.4 illustrates the procedure of the wet method. It consisted of ten impinger bottles connected in series. Then, the sampling train was arranged in a salt, water and ice mixture kept at 3°C by a mechanical cooling device. Each impinger bottle were filled with 100 ml of isopropanol. The syngas from the sampling point A_i (scrubber inlet or untreated syngas) and B_i (scrubber outlet or treated syngas) was passed through this sampling train by a suction pump with the flow rate of 1

l/min. The gravimetric tar was separated from the syngas by the condensation and dissolution principle. After gas sampling for 60 minutes, the tar in isopropanol solution was filtered and evaporated by a rotary evaporator in a water bath kept at 40°C. The residue after the evaporation was defined as the gravimetric tar, which was measured by the weight.

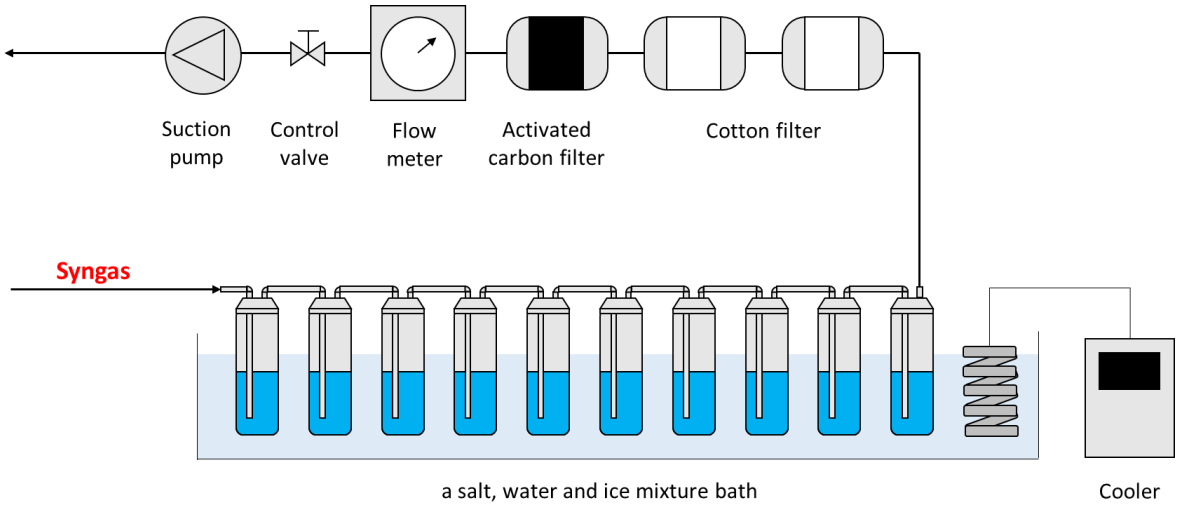

Figure 4.4. Illustration of the wet method

4.3.3.2 Dry method

Figure 4.5 illustrates the procedure of the dry method. A series of charcoal tube and silica gel tube (Standard type, Sibata Scientific Technology Ltd., Japan) was utilized for the gas sampling. The syngas samples from the sampling point A_i and B_i were passed through this sampling by a suction pump with the flow rate of 0.5 l/min for 3 minutes. After that, a gas chromatography flame ionization detector (GC-FID) was utilized to analyze the light tar components and concentrations. Carbon disulfide and acetone were selected as solvents for the charcoal tube and the silica gel tube, respectively. In this study, naphthalene and phenol are mainly concerned due to their possibility to block the piping line at the ambient temperature.

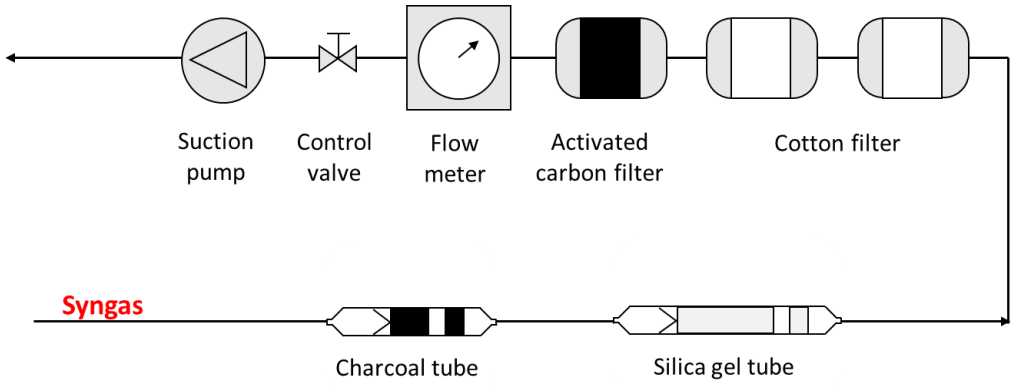

Figure 4.5. Illustration of the dry method

4.4 Mass transfer modeling

The mass transfer of physical absorption in a single phase flow directly depends on the mass transfer coefficient in that phase. Mass can also be transported from one phase to another that called "interphase mass transfer", where the phases are separated by an interface or syngas-absorbent partition in this case. As well as the single phase mass transfer, the overall mass transfer coefficient have an influence on the overall mass transfer rate of a multiphase flow (gas-liquid flow). In this study, the overall volumetric liquid-side mass-transfer coefficients ($K_L a^0$) is a key parameter to present the improvement of the mass transfer rate in each experimental condition which shows the transport of tar from the gas phase to the liquid phase. The multiphase flow of a gas-liquid flow was assumed to be operated under the following conditions; homogenous gas-liquid mixing, no gas back mixing, isothermal process, constant gas flow rate (F_G) between the inlet and the outlet of the scrubber, no chemical reaction (physical absorption) and no radial concentration gradient in both phases.

In order to calculate the overall volumetric liquid-side mass-transfer coefficients ($K_L a^0$), the transport of two phases require a departure from the equilibrium (the breakthrough curve), which have been studied in previous work [4.6]. Figure 4.6 illustrates the calculation procedure of the overall volumetric liquid-side mass-transfer coefficients ($K_L a^0$) developed by P.-F. Biard et al. [4.19]. The numerical resolution by the Excel® solver calculated the concentration gradient (driving force) until the area under the curve of the experimental data and the model was equalized. The numerical calculation procedure was concluded in Appendix B.

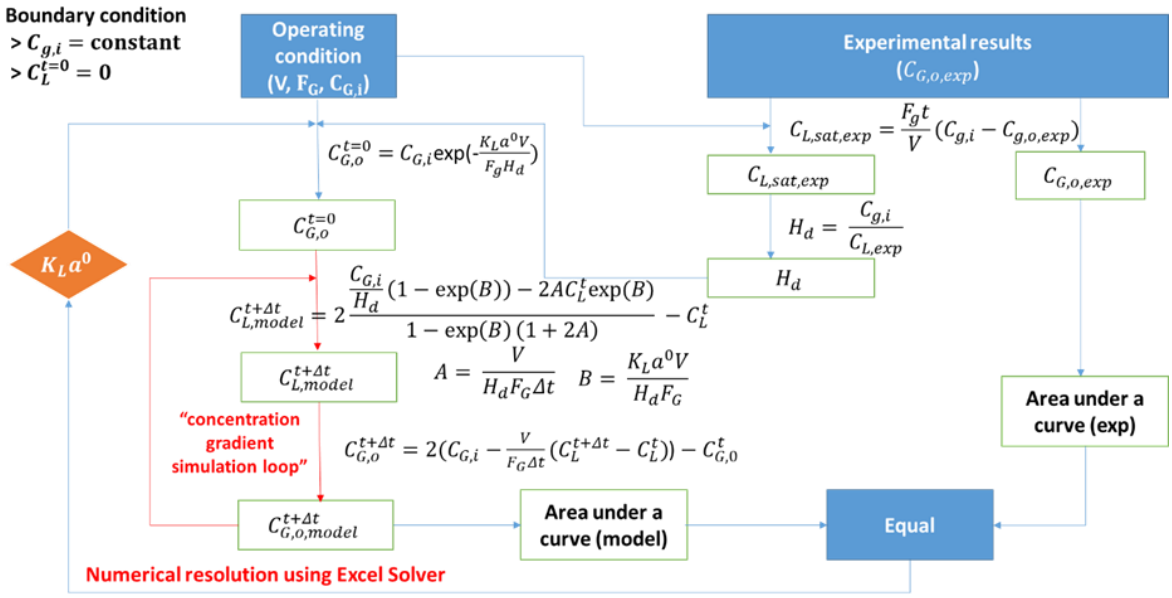

Figure 4.6. Numerical calculation procedure for the $K_L a^0$ determination

4.5 Results and discussions

4.5.1 Reynolds number

Figure 4.7 shows the Reynolds number of VO, 7.5%EO and the syngas at each experimental condition. It can be seen that both the throat diameter ratio (d/D) and the oil throat velocity had a strong influence on the Reynolds number.

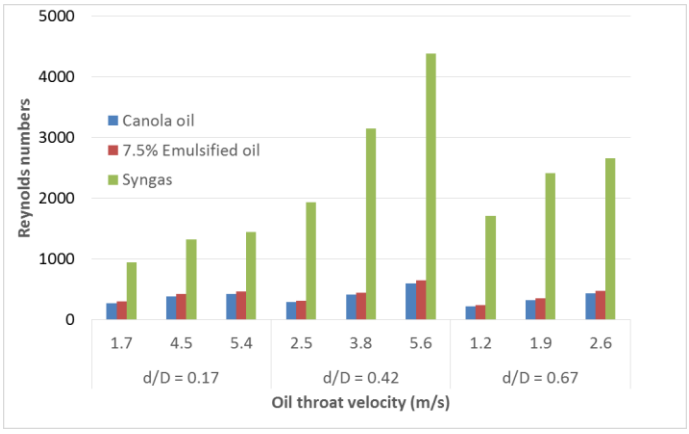

Figure 4.7. Reynolds number of VO, 7.5%EO and syngas at each experimental condition

4.5.1.1 Syngas Reynolds number

For the Reynolds number of syngas, it is obvious to observe the increase in the Reynolds number because the dynamic viscosity of the syngas is much lower than liquid especially oil-based absorbent, where the dynamic viscosity of oil-based absorbent is about 3,000 times higher than the syngas. The lowest Reynolds number started at the lowest d/D and the lowest oil throat velocity. A decrease in the throat diameter enhanced the bubble breakup mechanism, but also increased the pressure drop. Therefore, the highest pressure drop occurred at d/D = 0.17 led to the lowest Reynolds number compared to the other d/D. Comparing between d/D = 0.42 and 0.67, the bubble breakup mechanism of d/D = 0.67 (larger throat diameter) was lower than d/D = 0.42 (smaller throat diameter). Therefore, the Reynolds number at d/D = 0.42 was higher than at d/D = 0.67. The graph also indicated that the Reynold number at d/D = 0.17 increased from 944 to 1449 as a function of the increasing oil throat velocity due to the enhancement of the mass flux. The similar trend was also observed in other d/D (d/D = 0.42, 0.67), where the highest Reynolds number was occurred at d/D=0.42 at the highest throat velocity corresponding to 4,378.

4.5.1.2 Reynolds numbers of VO and 7.5%EO oil

For the Reynolds numbers of VO and 7.5%EO, there was no significant change of the Reynold number due to their high dynamic viscosity property. However, the Reynolds number was slightly increased as a function of the increasing oil throat velocity at each d/D as well. The Reynolds numbers of VO and 7.5%EO were highest at 647 and 594, respectively. The highest Reynolds number was occurred at d/D = 0.42 at the highest oil throat velocity. In addition, it was also observed that the Reynolds number of 7.5%EO was higher than VO because the dynamic viscosity of 7.5%EO (0.0423 Pa-s) was slightly lower than VO (0.0456 Pa-s).

4.5.1.3 Correlation between the Reynolds number and the specific absorption surface area

Based on Chapter 3, Figure 4.8 illustrates the correlation between the Reynolds number (VO, 7.5%EO and syngas) and the specific absorption surface area. The specific absorption surface area is the parameter that aims to explain the physical absorption of gas droplets on a liquid surface. It could be determined by the mean microbubble diameter and the number density. The graph

indicated that the increase in the Reynolds numbers of VO, 7.5%EO and the syngas increased the specific absorption surface area. The strong correlation was confirmed by the syngas Reynolds number. Therefore, it could be concluded that the increase in the syngas Reynolds number had a favor to increase the bubble breakup mechanism and the specific absorption surface area, which are the main consideration parameters to enhance the tar removal performance.

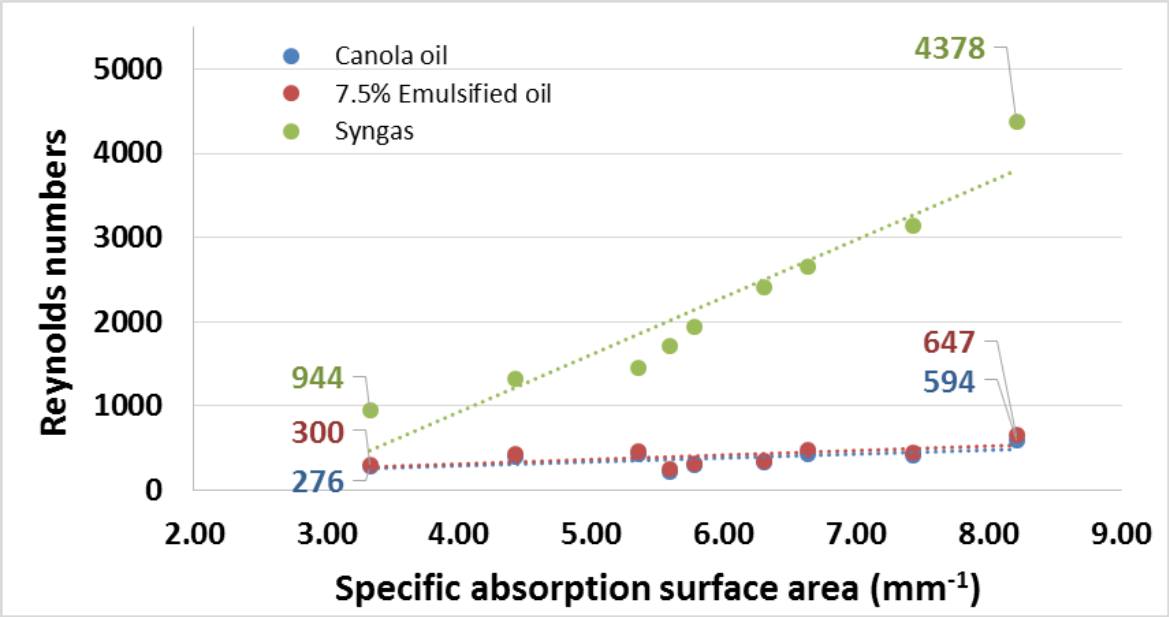

Figure 4.8. Correlation between the Reynolds number of the syngas and the specific absorption surface area

4.5.2 Gravimetric tar removal performance

4.5.2.1 Comparison of the tar removal performance of VO and 7.5%EO in the bubbling scrubber

Due to the tar property, some of them are good-dissolved and removed in non-polar substance like oily materials, while some are in polar one like water. Figure 4.9 presents VO and 7.5%EO scrubbing performance for the gravimetric tar removal in the bubbling scrubber according to Chapter 2 [4.5]. It can be seen that 69.8 g/m^3 of the gravimetric tar contained in the syngas was removed to 14.0 g/m^3 corresponding to 80% gravimetric tar removal efficiency and 8.7 g/m^3 corresponding to 87.6% gravimetric tar removal efficiency by using VO and 7.5%EO, respectively. VO mainly removed the gravimetric non-polar tar, while 7.5%EO improved the gravimetric tar removal

performance by increasing the gravimetric polar tar removal efficiency. Furthermore, the dynamic viscosity of 7.5%EO was lower than VO. For that reason, the diffusivity and the removal efficiency of tar in 7.5%EO was higher than VO.

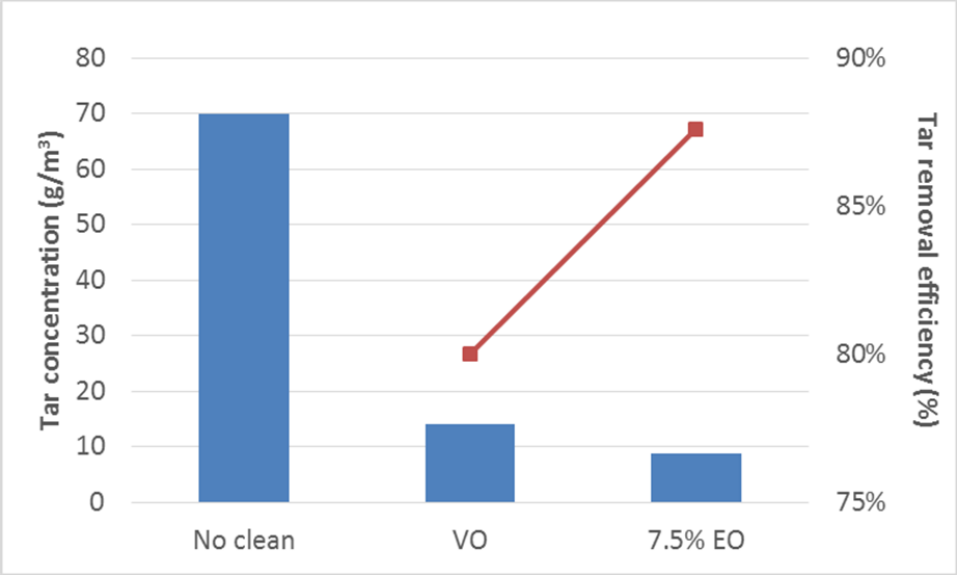

Figure 4.9. VO and 7.5%EO scrubbing performance in the bubbling scrubber

4.5.2.2 Effect of the syngas Reynolds number on the tar removal performance

This study compared the gravimetric tar removal efficiency of VO and 7.5%EO under the same operation conditions as well, but further investigation was done on the venturi scrubber producing syngas microbubbles, which generated the tiny bubbles to increase the absorption surface area. Figure 4.10 illustrates the correlation between the tar removal efficiency and the syngas Reynolds number. The results will be explained as the following.

For the VO scrubber, the gravimetric tar removal efficiency continuously increased with the increase of the syngas Reynolds number. At the beginning, 88.3% of the gravimetric tar was removed by the venturi scrubber at the lowest syngas Reynolds number, while just 80% of the gravimetric tar was removed by the bubbling scrubber. After that, the gravimetric tar removal efficiency continuously increased with the increase in the syngas Reynold number. Finally, the optimum gravimetric tar removal efficiency was achieved at the highest Reynolds number, where tar could be reduced to 1.6 g/m^3 corresponding to 97.7% of the gravimetric tar removal efficiency. These results can be explained by the bubble breakup mechanism. As the syngas Reynolds number increased, the syngas

microbubble diameter was getting smaller resulted in the increase in the absorbent surface area for absorbing tar. Therefore, the gravimetric tar removal efficiency was improved with the increasing in the syngas Reynolds number.

For 7.5%EO scrubber, the tendency of tar removal performance at each syngas Reynolds number was similar to VO. The gravimetric tar removal efficiency was improved from 87.6% (bubbling scrubber) up to 100% (venturi scrubber), where there was no gravimetric tar observed at the highest syngas Reynolds number. This is because the increase in the absorbent surface area for absorbing tar at the highest syngas Reynolds number was the best condition as previously stated.

In addition, comparison between VO and 7.5%EO found that the gravimetric tar removal efficiency of 7.5%EO was better than VO in all experimental conditions. This is because the characteristic of 7.5%EO was better than VO for removing the gravimetric polar tar.

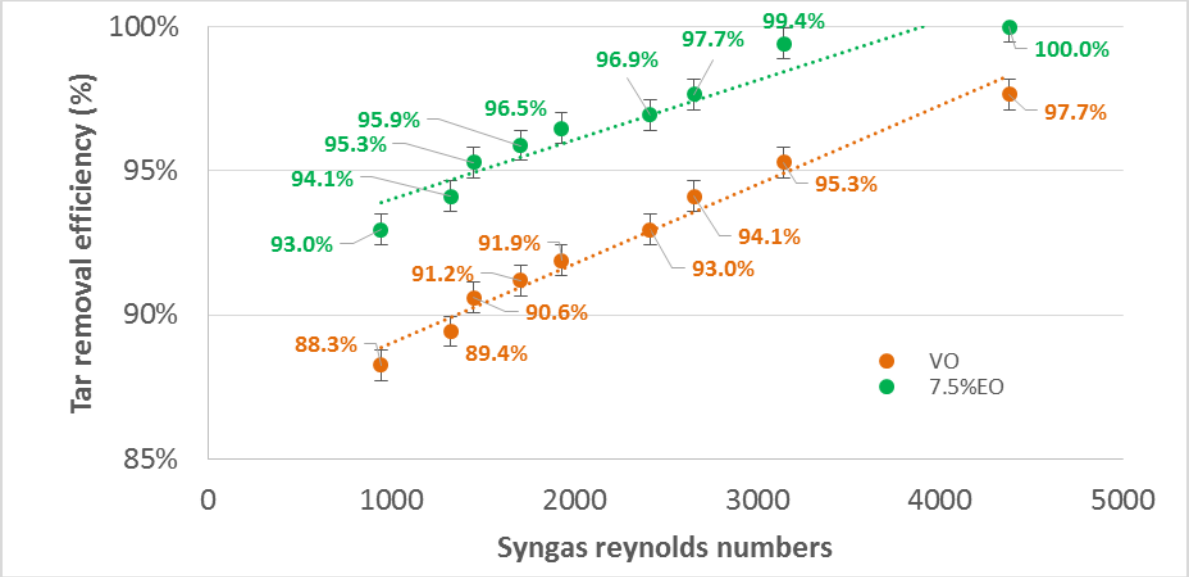

Figure 4.10. Gravimetric tar removal efficiency of VO and 7.5%EO

4.5.3 Light tar removal performance

Figures 4.11 and 4.12 present the scrubbing performances of VO and 7.5%EO for light tar removal. Approximately 0.2 and 0.1 g/m^3 of naphthalene was contained in the syngas at the scrubber inlet. For VO, it could remove 97.9% and 94.6% of napthalene and phenol in the bubbling scrubber, respectively, while those were completely removed in the venturi scrubber even with the lowest

syngas Reynolds number. This is because the venturi scrubber has three times more syngas Reynolds number than the bubbling scrubber at the beginning. The increase of the syngas Reynolds number increased the level of the turbulent mixing and gave the syngas microbubble diameter getting smaller resulted in the increase in the absorbent surface area for absorbing tar as previously mentioned. For 7.5%EO, the similar result was observed. It could remove 97.5% and 96.4% of naphthalene and phenol in the bubbling scrubber, respectively, while those were completely removed in the venturi scrubber as well.

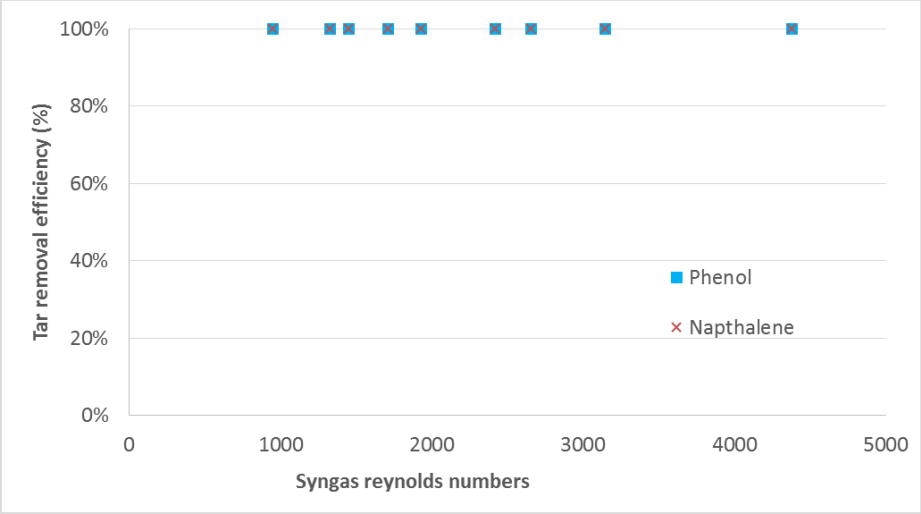

Figure 4.11. Light tar removal efficiency of VO

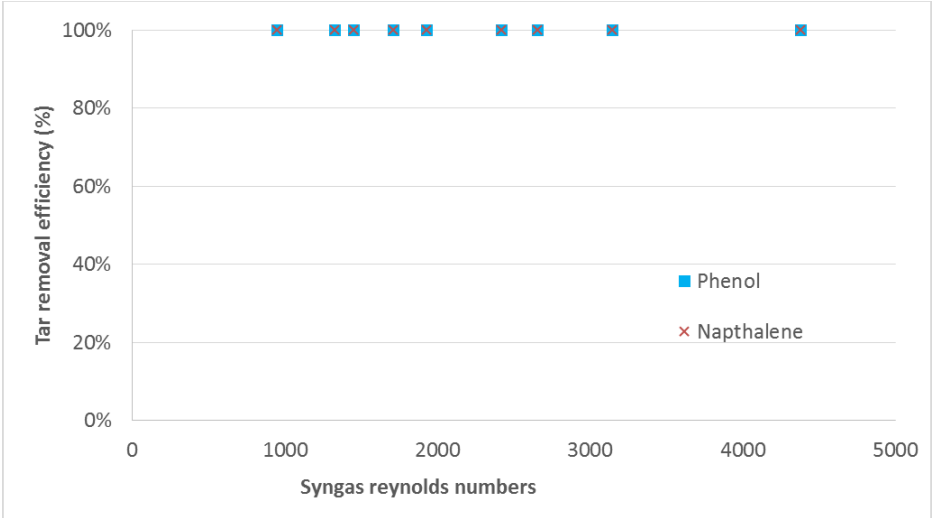

Figure 4.12. Light tar removal efficiency of 7.5%EO

4.5.4 Mass transfer modelling

Based on the experimental data, the mas transfer modelling of the gravimetric tar could be determined in this study, however, the modelling of the light tar could not be done because none of them was observed at the exit of the scrubber in the experiments. Therefore, the concentration gradient of the light tar could not be determined. Figures 4.13, 4.14 and 4.15 illustrated the concentration gradient of the gravimetric tar and the overall volumetric liquid-slide mass-transfer coefficient determined by the numerical resolution procedure, respectively.

4.5.4.1 Concentration gradient of the gravimetric tar in the gas phase (syngas)

Figures 4.13a and 4.13b illustrated the concentration gradient of the gravimetric tar in the gas phase at the exit of the scrubber of VO and 7.5%EO, respectively. The results show that the gravimetric tar concentration in the gas phase of both VO and 7.5%EO was continuously increased with the passage of time for all cases because the accumulated gravimetric tar in the absorbent gradually blocked the absorption surface area between tar and absorbent resulting in the increase of the gravimetric tar contained at the exit of the scrubber. However, the trend of the tar concentration was reduced with the increase of the syngas Reynolds number for both VO and 7.5%EO. This could confirmed that the turbulent mixing effect gave more absorption surface areas of tar for transferring from gas to liquid side. Furthermore, the tar concentration in the syngas at the exit of the scrubber of 7.5%EO was lower than VO as the same as the removal efficiency experiment as well.

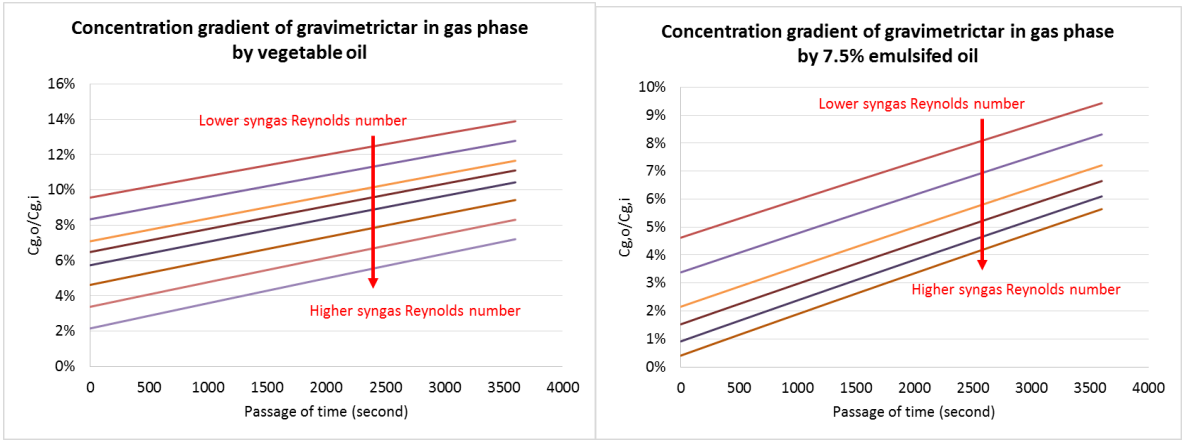

a) **b)**

Figure 4.13. Concentration gradient of the gravimetric tar in the gas phase at the exit of the scrubber a) VO b) 7.5%EO

4.5.4.2 Concentration gradient of the gravimetric tar in the liquid phase (absorbent)

Figures 4.14a and 4.14b illustrated the concentration gradient of the gravimetric tar in VO and 7.5%EO, respectively. The results show that the gravimetric tar concentrations in both VO and 7.5%EO were continuously increased with the passage of time for all cases because the gravimetric tar was continuously accumulated from the gas phase due to the tar removal process. Furthermore, the slope of the tar concentration in the liquid phase increased with the increase in the syngas Reynolds number, which confirmed that more tar was accumulated by increasing of the turbulent mixing.

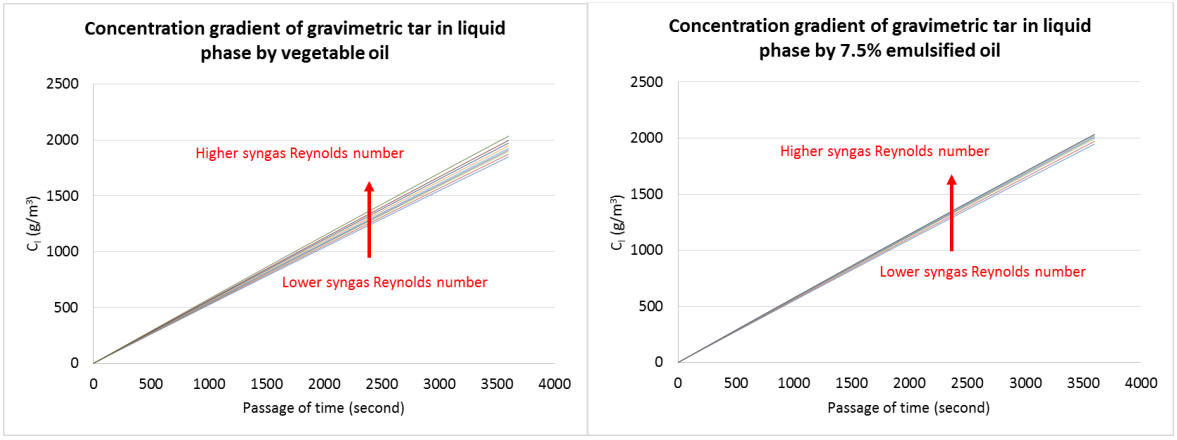

a) **b)**

Figure 4.14. Concentration gradient of the gravimetric tar in the liquid phase at the exit of the scrubber a) VO b) 7.5%EO

4.5.4.3 Overall volumetric liquid-slide mass-transfer coefficient

Figure 4.15 illustrates the overall volumetric liquid-slide mass-transfer coefficient of VO and 7.5%EO. The results show that the overall volumetric liquid-slide mass-transfer coefficient increased with the increase in the syngas Reynolds number for both absorbents. The turbulent mixing enhanced the mass transfer rate from the gas phase (syngas) to the liquid phase (absorbent). Moreover, the overall volumetric liquid-slide mass-transfer coefficient of 7.5%EO was higher than VO at the same syngas Reynolds number, which confirmed that the mass transfer rate of 7.5%EO was better than VO.

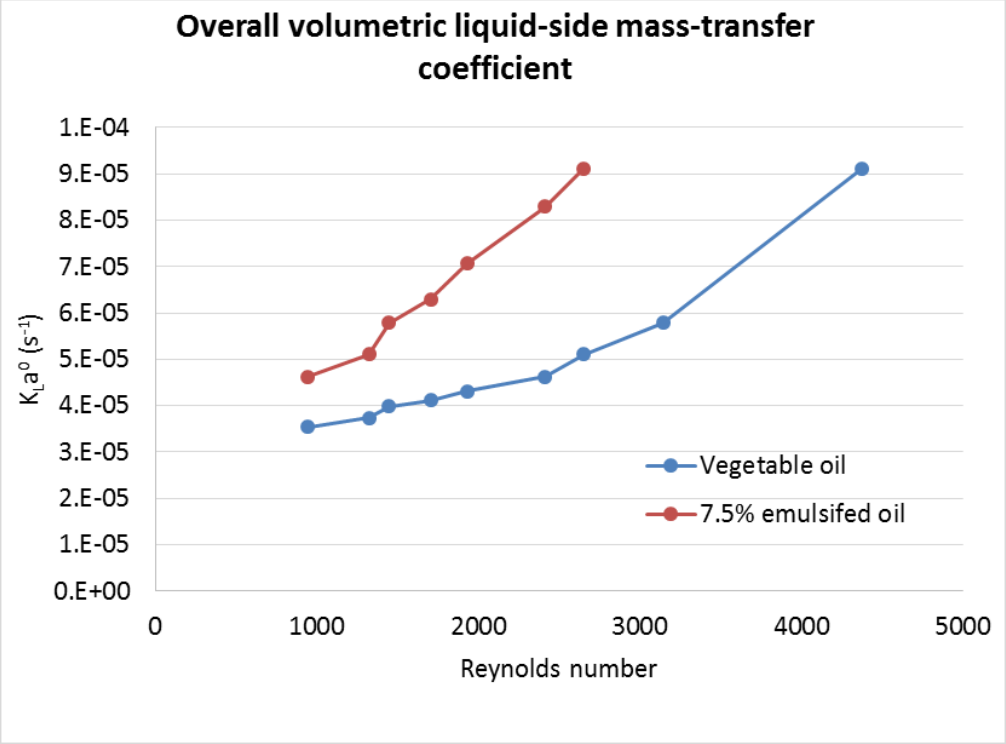

Figure 4.15. Overall volumetric liquid-slide mass-transfer coefficient

4.6 Conclusion

The objective of this study was to investigate the effect of the syngas Reynolds number on the tar removal performance. The increase in the syngas Reynolds number improved the level of the turbulent mixing and the syngas bubbles getting smaller until it became microbubbles, which resulted in the increase in the absorption surface area and that gave more area for tar to be absorbed. VO and 7.5%EO oil were used as the absorbent in both the bubbling and the venturi scrubber according to its absorption performance for tar removal. The real syngas containing tar was introduced to the scrubber, where several trial products produced the different fluid behavior were investigated so as to find the best operational condition. This study was divided into three part; the Reynolds number, the tar removal performance and the mass transfer modelling.

The Reynolds number could be concluded as follow. It is obvious to observe the increase in the Reynolds number in the syngas, while a slight change of the Reynolds number was observed in VO and 7.5%EO Reynolds number because the dynamic viscosity of oil-based absorbent is about

3,000 times higher than the syngas. The study also confirmed that the increase in the syngas Reynolds number had a favor to increase the bubble breakup mechanism and the specific absorption surface area, which are the main parameters to enhance the tar removal performance.

The gravimetric tar removal performance could be concluded as follow. For the scrubber type, the performance of the venturi scrubber was better than the bubbling scrubber. For the absorbent, the tar removal efficiency of 7.5%EO was also better than VO in all experimental conditions. The optimum condition for tar removal was at the highest Reynolds number for both of them. The VO scrubber was able to remove the gravimetric tar down to 1.6 g/m^3 corresponding to 97.7% gravimetric tar removal efficiency, however, there was no gravimetric tar observed at the exit of the 7.5%EO scrubber. This is because the characteristic of 7.5%EO was better than VO for removing the gravimetric polar tar. The light tar removal performance could be concluded as follows. The light tar removal of VO and 7.5%EO showed the similar results in both the bubbling and the venturi scrubber. More than 94% of the light tar was removed in the bubbling scrubber, while there was no light tar observed in the venturi scrubber.

The mass transfer modelling could be concluded as follow. The overall volumetric liquid-slide mass-transfer coefficient increased with the increase in the syngas Reynolds number for both VO and 7.5%EO because the turbulent mixing enhanced the mass transfer rate of the gravimetric tar from the gas phase to the liquid phase. The overall volumetric liquid-slide mass-transfer coefficient of 7.5%EO was higher than VO at the same operating conditions, which confirmed the mass transfer rate of 7.5%EO was better than VO.

In conclusion, the increase in the syngas Reynolds number has a strong influence to improve the absorption surface area and the mass transfer rate for the gravimetric and the light tar removal in both VO and 7.5%EO.

4.7 Reference

[4.1] Phuphuakrat T, Namioka T, Yoshikawa K. Absorptive removal of biomass tar using water and oily materials. Bioresour Technol 2011;102:543–9.

[4.2] Chen H, Namioka T, Yoshikawa K. Characteristics of tar, NOx precursors and their absorption performance with different scrubbing solvents during the pyrolysis of sewage sludge. Appl Energy 2011;88:5032–41.

[4.3] Zambiazi RC, Przybylski R, Zambiazi MW, Mendonca CB. Fatty acid composition of vegetable oils and fats. B Ceppa, Curitiba 2007;25:111–20.

[4.4] Paethanom A, Nakahara S, Kobayashi M, Prawisudha P, Yoshikawa K. Performance of tar removal by absorption and adsorption for biomass gasification. Fuel Process Technol 2012;104:144–54.

[4.5] Unyaphan S, Tarnpradab T, Takahashi F, Yoshikawa K. Effect of emulsified absorbent for tar removal in biomass gasification process. Biofuels 2016;7:233–43.

[4.6] Tarnpradab T, Unyaphan S, Takahashi F, Yoshikawa K. Tar removal capacity of waste cooking oil absorption and waste char adsorption for rice husk gasification. Biofuels 2016;7:401–12.

[4.7] Tarnpradab T, Unyaphan S, Takahashi F, Yoshikawa K. Improvement of the biomass tar removal capacity of scrubbing oil regenerated by mechanical solid--liquid separation. Energy & Fuels 2017.

[4.8] Bhave AG, Vyas DK, Patel JB. A wet packed bed scrubber-based producer gas cooling--cleaning system. Renew Energy 2008;33:1716–20.

[4.9] Bhoi PR, Huhnke RL, Kumar A, Payton ME, Patil KN, Whiteley JR. Vegetable oil as a solvent for removing producer gas tar compounds. Fuel Process Technol 2015;133:97–104.

[4.10] Sadatomi M, Kawahara A, Kano K, Ohtomo A. Performance of a new micro-bubble generator with a spherical body in a flowing water tube. Exp Therm Fluid Sci 2005;29:615–23.

[4.11] Gadallah AH, Siddiqui K. Bubble breakup in co-current upward flowing liquid using honeycomb monolith breaker. Chem Eng Sci 2015;131:22–40.

[4.12] Fujiwara A, Takagi S, Watanabe K, Matsumoto Y. Experimental study on the new micro-bubble generator and its application to water purification system. ASME/JSME 2003 4th Jt. Fluids Summer Eng. Conf., 2003, p. 469–73.

[4.13] Brennen CE. Fundamentals of multiphase flow. Cambridge university press; 2005.

[4.14] Kolev NI. Multiphase flow dynamics: Fundamentals. Springer; 2005.

[4.15] Michaelides E, Feng Z. Fundamentals of Multiphase Flow. Multiph Flow Handbook, Second Ed CRC Press Taylor Fr Gr 2016:1–78.

[4.16] Field BS, Hrnjak PS. Two-phase pressure drop and flow regime of refrigerants and refrigerant-oil mixtures in small channels. 2007.

[4.17] Van Paasen SVB, Kiel JHA, Neeft JPA, Knoef HAM, Buffinga GJ, Zielke U, et al. Guideline for sampling and analysis of tar and particles in biomass producer gases. Energy Res Cent Netherlands, ECN-C-02-090 2002.

[4.18] Kiel JHA, Van Paasen SVB, Neeft JPA, Devi L, Ptasinski KJ, Janssen F, et al. Primary measures to reduce tar formation in fluidised-bed biomass gasifiers. ECN, ECN-C-04-014 2004.

[4.19] Biard P-F, Coudon A, Couvert A, Giraudet S. A simple and timesaving method for the mass-transfer assessment of solvents used in physical absorption. Chem Eng J 2016;290:302–11.

Chapter 5

Performance of absorbent regeneration by a series of filtration and air-blown stripping for tar removal in biomass gasification

Abstract

This chapter investigated the feasibility of a low-cost and highly effective absorbent regeneration technique using a series of the filtration and the air-blown stripping. The operational conditions of the air-blown stripping was firstly evaluated based on various stripping temperatures (75-200°C) and operational times (30-240 minutes) to show that the stripping temperature of 175°C and the operational time of 120 minutes were the optimum conditions. Then, the tar removal efficiency and capacity of a series of the filtration and the air-blown stripping were conducted for 10 hours. It was found that the gravimetric and light tar removal capacity of a series of the filtration and the air-blown stripping was 31.6 g/L, 22.8 g/L, which was 190.6% and 273% higher tar removal capacity compared to non-regenerated oil, respectively. In addition, there was no significant change of the gravimetric and light tar removal efficiency after each regeneration compared to new oil. Therefore, there is a possibility for utilizing regenerated absorbent without changing it to the new one for a longer period of the operation. Furthermore, the air with the stripped gravimetric and light tars could be used as the gasifying agent in gasifiers for energy recycling.

5.1 Background

As it is known that the removal mechanisms of the gravimetric and light tars in a scrubber could be explained by two main principles that are the condensation and the dissolution according to Chapters 2, 3 and 4. However, the accumulation of tar and other contaminants in the absorbent with the passage of time causes the viscous resistive force against the absorbent flow (hydrodynamic drag) and gives less interaction between the syngas and the absorbent by their blocking [5.1–5.3]. There are several methods to maintain the tar removal performance of the absorbent such as periodic making-up of new oil in the scrubber [5.4]. Nevertheless, the massive new oil will be consumed and the waste absorbent will be generated, which is not an economical and environmentally friendly process. Therefore, the absorbent regeneration would be one of the sustainable gas cleaning techniques in order to upgrade and prolong the absorbent lifetime. One possibility to regenerate oil is to remove the contaminants stored in the deteriorated absorbent. Previous researches on the treatment process found that the mechanical separation methods of solids from liquid or liquid from

liquid by the filtration and the centrifugal sedimentation are wildly used to purify liquid media in many industries such as wastewater, drinking water, pharmaceutical, chemical, food, agriculture, and mining industry [5.5–5.8]. In addition, the attractive results for utilizing absorbent regeneration by both the filtration and the centrifugal sedimentation found that 160% and 175% tar removal capacity could be increased by the filtration and the centrifugal sedimentation techniques [5.9]. However, both methods could not effectively remove the light tar especially benzene and toluene. Therefore, the tar removal performance of the absorbent regeneration by the air-blown stripping is investigated in this chapter in order to improve some drawbacks of the previous techniques.

The absorbent regeneration by the air-blown stripping is a physical separation process, where one or more contaminants are removed from liquid stream by a vapor stream. It aims to make the contaminants in the liquid phase transfer to the vapor phase. Stripping could be conducted in tray tower (plate column) [5.10], packed column [5.11–5.13], spray tower [5.14], centrifugal contractor [5.15,5.16] and bubbling column [5.17]. It is widely used in industrial applications such as the removal of volatile organic compounds (VOCs) in drinking water sources and industrial waste waters [5.13]. However, there was few studies on the usage of the air blown stripping for the absorbent regeneration. OLGA tar removal technology presented the general concept process structure of tar removal system consisted of a collector, an absorber and a stripper, respectively [5.18]. According to the controlling temperature in each gas cleaning unit, the gravimetric tar and other contaminants were collected in scrubbing liquid of a collector, while some of the gravimetric tar and most of the light tar were absorbed in an absorbent of an absorber. For the scrubbing oil regeneration, the gravimetric tar was separated from the scrubbing liquid and was returned to the gasifier by the separator. For the absorbent regeneration, some of the gravimetric tar and most of the light tar absorbed in an absorbent were regenerated by a stripper. In case of the air-blown gasification, tar in air after the stripping process could be used as a gasifying agent. Although this technique is attractive, there is no report on the operational conditions and the stripping performance. Therefore, in this chapter, real tar produced from the pyrolysis of Japanese cedar was supplied to a bubbling scrubber, where the gravimetric and light tars were collected in a single bubbling scrubber. Canola oil without any additive was chosen as the absorbent in the bubbling scrubber with the magnetic stirrer speed of 1,000 rpm. The experiments were conducted for 10 hours to investigate the improvement of the tar removal performance without and with the regeneration techniques. A series of the filtration and the air-blown stripping was selected for the absorbent regeneration technique due to the scale up potential [5.18]. The filtration technique aims to remove the gravimetric tars and other contaminants, while the stripping technique aims to remove the remaining gravimetric tar after the filtration and the light tar.

5.2 Material and experimental setup

5.2.1 Material

Real syngas and tar from pyrolysis gasification were produced using Japanese cedar as biomass feedstock. The Japanese cedar was prepared by crushing and sieving with a mesh size between 0.5 and 1 mm. The sample was dried at 105°C for 10 hours to eliminate the moisture content. It was then stored in an enclosed containers at the room temperature and humidity. As for scrubbing absorbent, canola oil was utilized. Its density and kinematic viscosity at 30°C scrubbing temperature was 0.9 g/cm^3 and 50.7 cSt, respectively. The characteristics of Japanese cedar and canola oil are summarized in Table 5.1.

Table 5.1. Proximate and ultimate analysis of Japanese cedar and canola oil

	Japanese cedar	Canola oil
Proximate analysis (wt.% dry basis)		
Volatile matter	84.1	-
Fixed carbon	15.6	-
Ash	0.3	-
LHV (MJ/kg)	16.4	-
Ultimate analysis (wt% dry ash free basis)		
C	50.4	77.5
H	6.3	12.7
N	0.1	0.2
O	43.2	9.6
S	<0.1	<0.1
Cl	<0.1	<0.1

5.2.2 Experimental setup

The experimental setup are divided into three parts that are the syngas and tar generation, the air-blown stripping performance and the tar removal capacity during 10 hours operation.

5.2.2.1 Syngas and tar generation

According to Tarnpradab et al. [5.9], the experiment was conducted using the fixed bed pyrolysis reactor made from stainless steel (SUS306) with an inner diameter and a height of 30 mm and 280 mm, respectively. The reactor was heated to 800°C by an electrical heater. Nitrogen was used as the carrier gas by controlling the flow rate at 0.8 l/min. After an isothermal retention time of 30 minutes, the feedstock was continuously fed into the reactor by a screw feeder at the constant feed rate of 0.3 g/min. Then, the syngas and tar produced by the thermal decomposition were

introduced into the bubbling scrubber. A schematic diagram of the syngas generation part and the gas cleaning unit is shown in Figure 5.1.

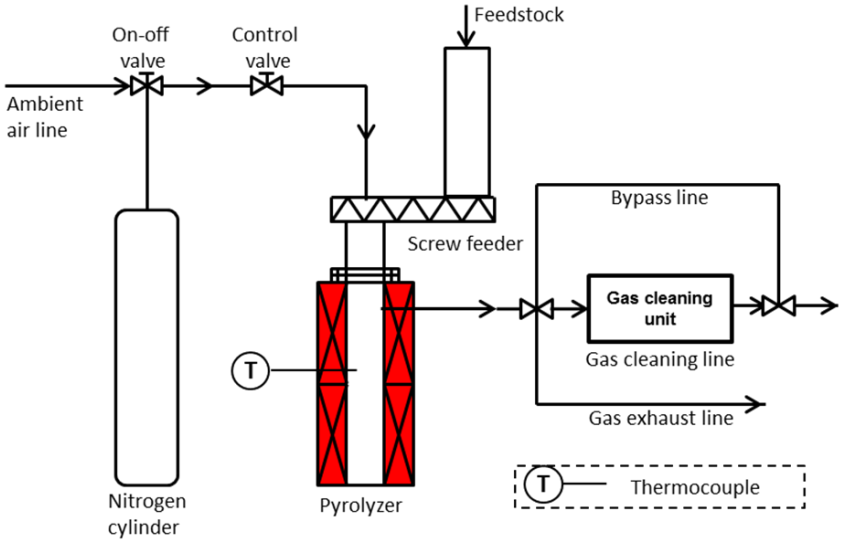

Figure 5.1. Schematic diagram of the syngas generation part and the gas cleaning unit

5.2.2.2 Air-blown stripping performance

In this experiment, it is necessary to firstly produce the deteriorated oil before conducting the air-blown stripping performance experiment. The absorbent which absorbed the gravimetric and light tars until reaching its saturation point were used as the deteriorated absorbent. It was produced by the following procedures. According to Tarnpradab et al. [5.9], the real syngas and tar produced by the fixed bed pyrolysis reactor was continuously introduced into the 500 ml of fresh canola oil in the bubbling scrubber for 10 hours in order to absorb the gravimetric and light tar until reaching the saturation point. The magnetic stirrer was set at the speed of 1,000 rpm, while the temperature of the absorbent was controlled at 30°C. After 10 hours experiment, the canola oil absorbent reached the saturation point and this deteriorated oil will be used for conducting the air-blown stripping regeneration.

In order to effectively utilize this absorbent regeneration technique, the operational conditions of the air-blown stripping were investigated. Two main parameters considering in this experiment are the stripping temperature and the operational time. Air was used as a stripping agent by controlling the flow rate at 1 l/min, while 100 ml of deteriorated oil was used for the stripping process. Both air and deteriorated oil were heated by a mantle heater (MS-ESB5, As-one Co., Ltd., Japan). Air was

introduced into the deteriorated oil so as to transfer the gravimetric and light tar from the deteriorated oil to air. A schematic diagram of the air-blown stripping regeneration is shown in Figure 5.2.

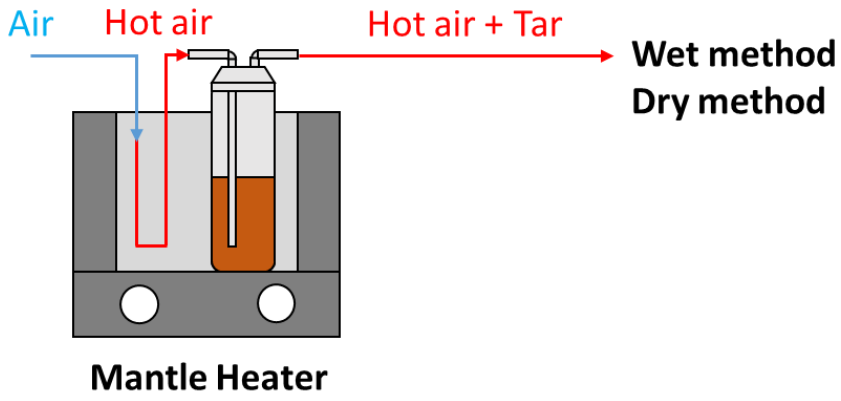

Figure 5.2. Schematic diagram of the air-blown stripping regeneration

For the gravimetric tar stripping performance, it was done by the wet method. The stripping temperature was varied at six different levels and the best stripping temperature condition was varied at three operational times. For the light tar stripping performance, it was done by the dry method. The best stripping temperature from the previous experiment was implemented. The experiments were organized as shown in Table 5.2.

Table 5.2. Experimental setup for the air-blown stripping regeneration

Parameters	RUN1	RUN2	RUN3
Experimental condition of each run			
Absorbent		Deteriorated oil	
Absorbent volume (ml)		100	
Stirring speed (rpm)		1000	
Stripper temperature (°C)	75, 100, 125, 150, 175, 200	175	175
Tar measurement method	Wet	Wet	Dry
Operation period (mins)	60	60,120,180	240

5.2.2.3 Tar removal capacity during 10 hours

In this experiment, the real syngas and tar produced by the fixed bed pyrolysis reactor was introduced into 500 ml of fresh canola oil in the bubbling scrubber for 10 hours with the regeneration technique by a series of the filtration and the air-blown stripping. The magnetic stirrer was set at the speed of 1,000 rpm, while the temperature of the absorbent was controlled at 30°C as well. The gas cleaning unit with the regeneration process is shown in Figure 5.3. For the regeneration process, the used oil for 135 minutes in the scrubber was sent to the regeneration process by using a series of the filtration and the air-blown stripping techniques. The used oil was firstly introduced into the filtration to produce filtrated oil and then air-blown stripping was done to produce regenerated oil, respectively. For the filtration, it was done by a vacuum packed bed filter composed of a packed bed filtration tower, a container and a vacuum pump as shown in Figure 5.4. The packed bed filtration tower contained the 7cm filter bed, the 3cm sand bed, the 7cm filter bed and the 3cm sand bed, respectively. Silica sand with the average size between 0.7-0.9 mm was used as a coarse media in order to prevent rapid increase in the pressure drop while the filter bed was used as a fine media in which the packed bed filtration tower can remove particles with the size greater than 30μm from the used oil. For the air-blown stripping, the operational condition was selected according to the air-blown stripping performance experiment. The experiments were organized as shown in Table 5.3.

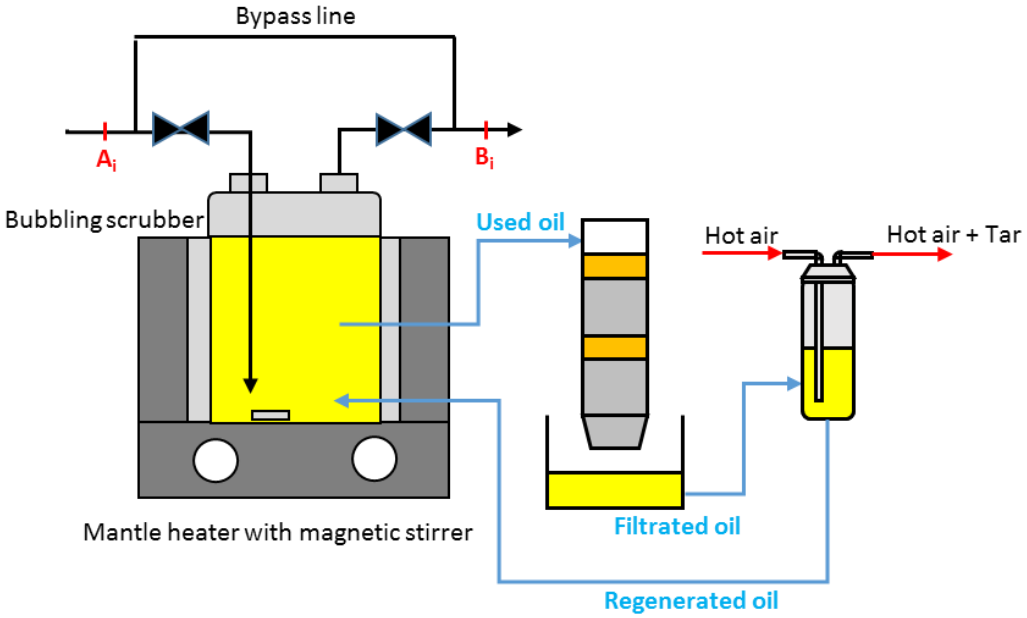

Figure 5.3. Schematic diagram of the bubbling scrubber with the regeneration unit by a series of the filtration and the air-blown stripping

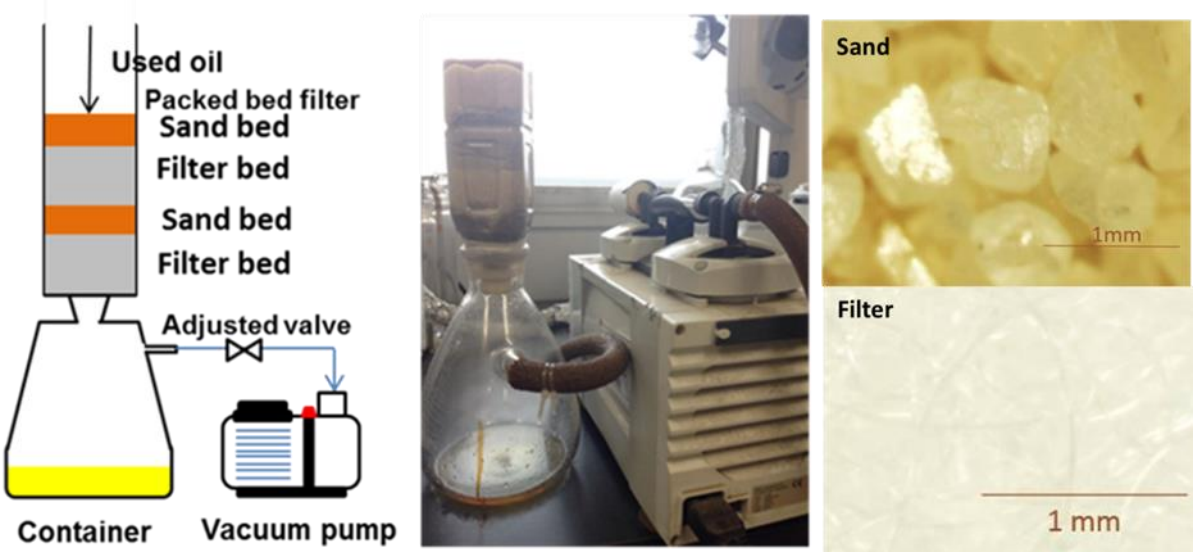

Figure 5.4. Schematic diagram of the oil regeneration setup by the filtration technique

Table 5.3. Experimental setup for the tar removal capacity during 10 hours

Parameters	RUN1	RUN2
Initial experimental set up		
Feedstock	Japanese cedar	
Feedstock size (mm)	0.5-1	
Carrier gas	Nitrogen	
Carrier gas rate (l/min)	0.8	
Pyrolyzer (°C)	800	
Experimental condition of each run		
Absorbent	Canola oil	
Absorbent volume (ml)	500	
Stirring speed (rpm)	1000	
Regeneration technique	Filtration and air-blown stripping	
Regeneration periods (mins)	135	135
Stripper temperature (°C)	175	175
Tar measurement method	Wet	Dry
Operation period (hours)	10	10

5.3 Tar sampling and analysis method

Tar was sampled by both the wet and dry methods for measuring the gravimetric and the light tar concentrations in the syngas, respectively. The details of the tar measurement method used in this research are described below.

5.3.1 Wet method

The wet method was utilized to analyze the gravimetric tar according to ECN guideline [5.19,5.20]. The gravimetric tar was separated from the syngas by the condensation and dissolution. The measuring point consisted of Ai (the gas sampling at the inlet of the scrubber or untreated synthesis gas) and Bi (the gas sampling at the outlet of the scrubber or treated synthesis gas) to compare the gravimetric tar concentration before and after the scrubbing. Figure 5.5 illustrates the procedure of the gravimetric tar sampling method. The sampling line is composed of a series of ten impingers, a gas flow meter, a control valve and a suction pump. In order to prevent tar clogging in the workflow, a cotton and an activated carbon filter were connected. Ten impingers were put in a salt, water and ice mixture bath kept at 3°C by a mechanical cooling device and were filled with 100 ml of isopropanol. 1 l/min of the gas sampling flow rate was adopted for 60 minutes and 15 minutes in the air-blown stripping performance and the tar removal capacity and performance, respectively. After that, the tar in isopropanol solution was separated by filtering and then evaporated using a rotary evaporator in a water bath kept at 40°C. The residue after the evaporation was defined as the gravimetric tar, which was measured by the weight.

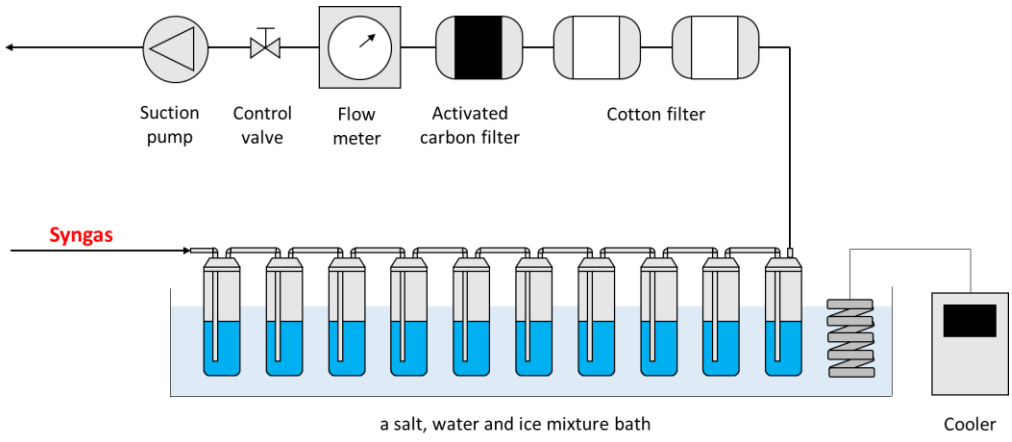

Figure 5.5. Illustration of the gravimetric tar sampling method

5.3.2 Dry method

The dry method was utilized to analyze the light tar. Figure 5.6 illustrates the procedure of the light tar sampling method. A series of charcoal tube (containing 150g of activated carbon) and silica gel tube (containing 780mg of silica gel) purchased from Sibata Scientific Technology Ltd. was utilized for the sampling. The gas sampling was done for 3 minutes with a flow rate of 0.5 l/min. The measuring points were the same as the wet method. Benzene, toluene, naphthalene, phenol and indene are mainly concerned in this study because benzene and toluene in air after the stripping process could be used as a gasifying agent, while the others especially naphthalene and phenol are highly concerned in this study because of their tendency to become a solid phase at the ambient temperature resulting in the blockage of the piping system. After that, a gas chromatography flame ionization detector (GC-FID) was utilized to detect light tar components and their concentrations. Carbon disulfide and acetone were used as solvents for the charcoal tube and the silica gel tube, respectively.

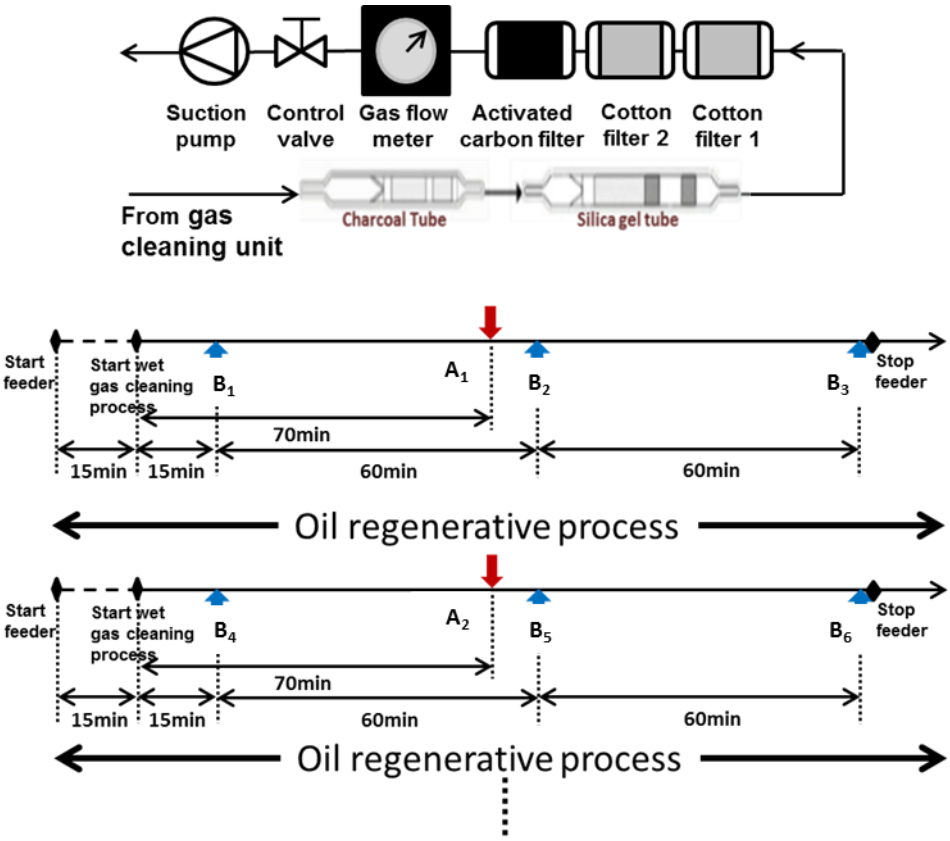

Figure 5.6. Illustration of the light tar sampling method

5.4 Results and discussion

5.4.1 Air-blown stripping performance

5.4.1.1 Gravimetric tar stripping performance

According to Tarnpradab et al [5.9], for the gravimetric tar removal capacity of fresh canola oil during 10 hours without regenerative unit, it was found that 1 litter of non-regenerated oil could absorb 16.6 g of the gravimetric tar. The tar stripping efficiency ($\eta_{stripping}$) in each experiment was calculated by utilizing Eq. (1).

$$\eta_{stripping} = \frac{m_{t,ac}}{m_{t,sat}} \times 100 \quad (1)$$

Where $m_{t,ac}$ is the accumulated tar stripping at each temperature and $m_{t,sat}$ is the tar removal capacity of the deteriorated oil at the saturation point.

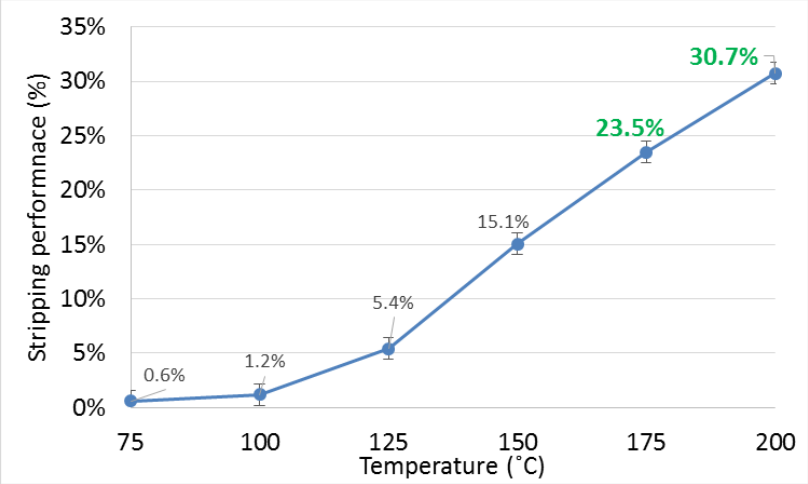

Figure 5.7. Gravimetric tar stripping efficiency of the deteriorated oil at different temperature

Figure 5.7 illustrates the gravimetric tar stripping efficiency at different temperature from 75°C to 200°C. It can be seen that the stripping efficiency at 75°C was the lowest among the others due to the lowest temperature. After that, the stripping efficiency increased with the increase in the stripping temperature. This is because the volatility of the organics like gravimetric tar has a very strong dependence on the temperature. The high stripping temperature allowed for stripping the heavier gravimetric tar. Therefore, there was an increasing trend of the stripping efficiency with the increase in the temperature. The highest stripping efficiency was observed at 200°C corresponding to 30.7%. However, there is a limitation of this techniques due to self-volatilization of the absorbent.

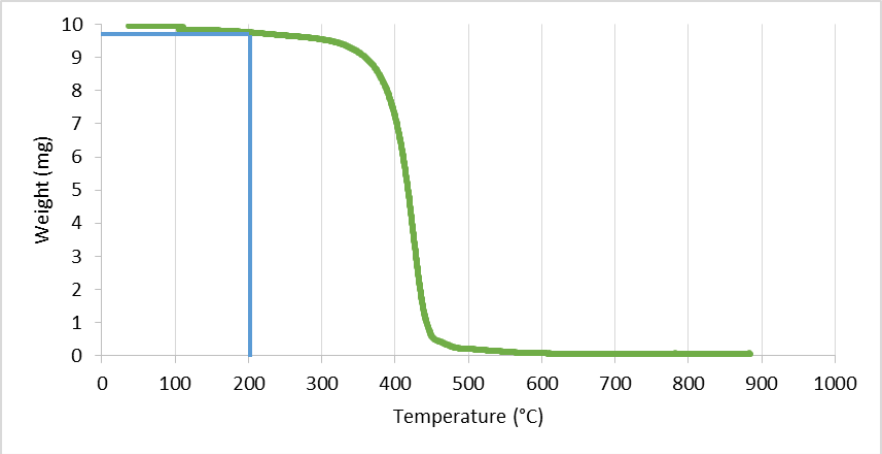

Figure 5.8. Thermogravimetric analysis of canola oil

Figure 5.8 presents the thermogravimetric analysis of canola oil. It indicated that the canola oil starts to evaporate at 200°C, where 0.1% of canola oil was lost by weight. In order to prevent self-volatilization of the absorbent, the stripping temperature was controlled at 175°C corresponding to 23.5% stripping efficiency. In addition, it was observed that the stripping efficiency of the gravimetric tar was relatively low comparing to other techniques. This is because the air-blown stripping was designed to remove the low dew point gravimetric tar. The heavier gravimetric tar could be removed by the filtration technique. Figure 5.9 illustrates the stripping efficiency with the passage of time at 175°C. The stripping efficiency remained constant at around 24%. Therefore, at least 1 hour was required to complete the gravimetric stripping process.

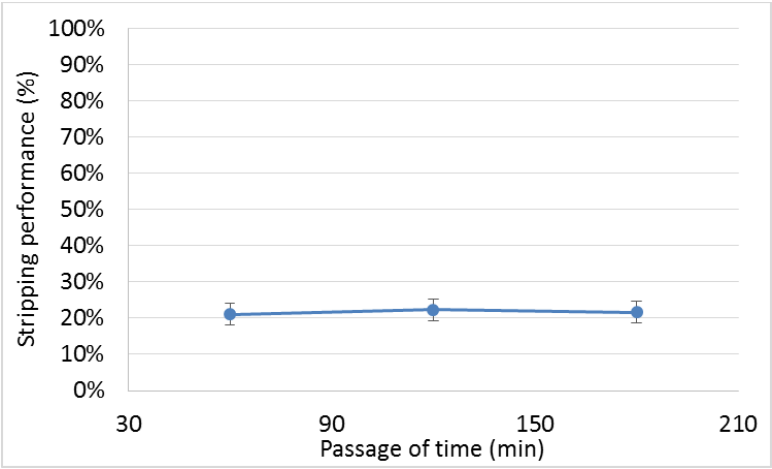

Figure 5.9. Gravimetric tar stripping efficiency of the deteriorated oil with the passage of time at 175°C

5.4.1.2 Light tar stripping performance

According to Tarnpradab et al. [5.9], for the light tar removal capacity of fresh canola oil during 10 hours without regenerative unit, it was found that 1 litter of non-regenerated oil could totally absorb 8.3 g of light tar (2.6, 3.5, 0.6, 1.0 and 0.5 g of benzene, toluene, naphthalene, phenol and Indene, respectively). Figure 5.10 illustrates the proportion of the light tar absorbed in the deteriorated oil at the saturation point. Toluene was in a large proportion among other light tar corresponding to 42.6%. The second was benzene corresponding to 31.1%. The minority was naphthalene, phenol and indene corresponding to 7.6%, 12.3% and 6.4%, respectively.

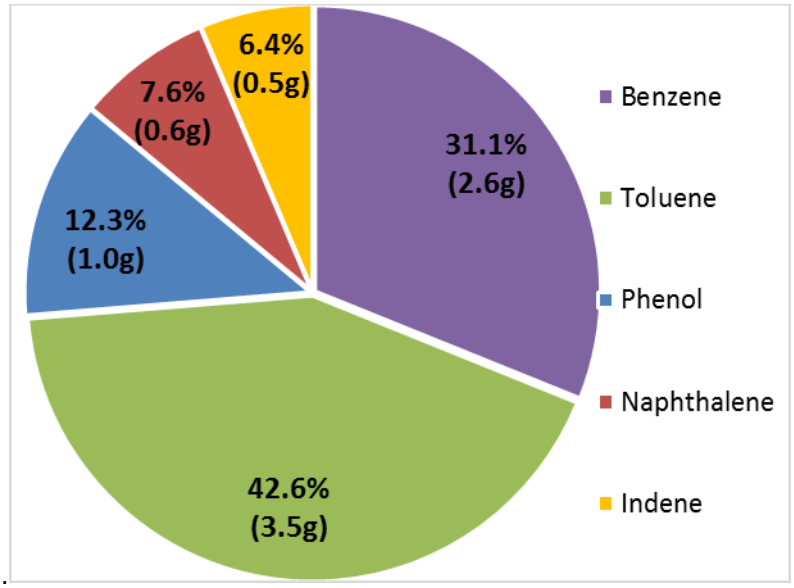

Figure 5.10. Light tar absorbed in the deteriorated oil at the saturation point during 10 hours

Figure 5.11 illustrates the light tar stripping efficiency of the deteriorated oil with the passage of time at 175°C. The tar stripping efficiency in each experiment was also calculated by utilizing Eq. (1). The results showed that the air-blown stripping process at 175°C was very effective to transfer benzene and toluene to the stripping agent, where up to 95.4% and 93.6% of benzene and toluene were transferred from the deteriorated oil to the stripping agent, respectively. However, only 20.3%, 33.2% and 34.8% of naphthalene, phenol and indene were transferred. This is because the dew point temperatures of benzene and toluene were much lower than that of naphthalene, phenol and indene. As previously mentioned, the air-blown stripping effectively desorbed the lower dew point tar. Therefore, the stripping efficiency of benzene and toluene was higher than that of them. Totally, the

overall light tar stripping efficiency was up to 77.4% for 4 hours stripping duration. According to Figure 5.11, after the second hour, the overall light tar stripping efficiency was just slightly increased by 4.9%. Therefore, 2 hours operational time of the air-blown stripping was selected in this study with 72.5% light tar stripping efficiency.

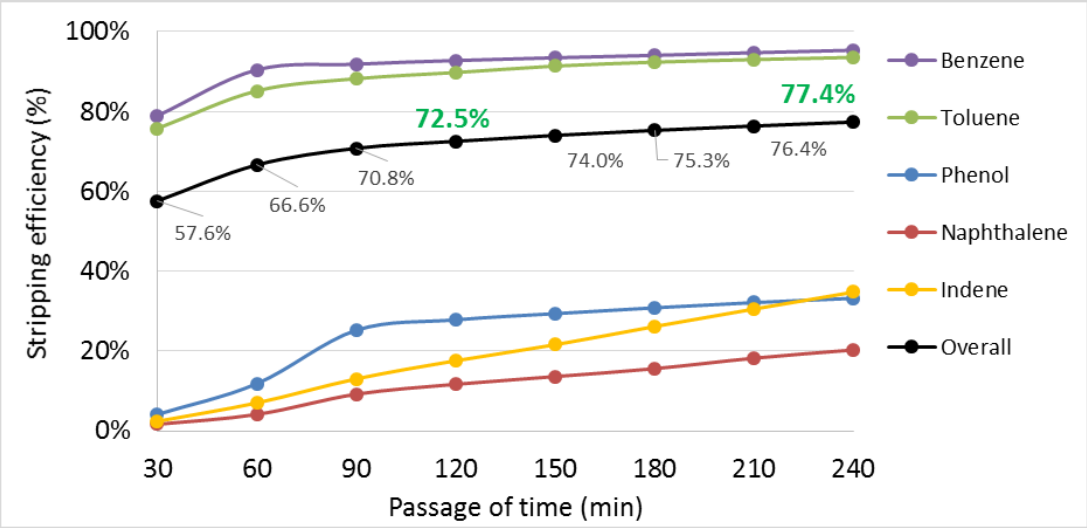

Figure 5.11. Light tar stripping efficiency of the deteriorated oil with the passage of time at 175°C

5.4.2 Performance of oil scrubber by a series of the filtration and the air-blown stripping for absorbent regeneration during 10 hours

5.4.2.1 Gravimetric tar removal performance during 10 hours

According to the large proportion of non-polar components in biomass tars, it is well dissolved in oily materials. The canola oil, which composes of both non-polar group and polar group (-COOH), was used as the absorbent for biomass tar absorption. The constant 30 g/m^3 of the gravimetric tar in the syngas was supplied to the bubbling scrubber. The tar removal efficiency ($\eta_{tar,removal}$) in each experiment was calculated using the Eq. (2).

$$\eta_{tar,removal} = \frac{\int_0^{600} f(x)dx - \int_0^{600} g(x)dx}{\int_0^{600} f(x)dx} \times 100 \qquad (2)$$

Where $f(x)$ and $g(x)$ express the polynomial equation derived from the inlet and outlet data respectively and x is the experimental period (min)

After absorbing tar for 135 minutes, the used oil was firstly introduced into the filtration and then the air-blown stripping for absorbent regeneration was conducted, respectively. For the regeneration of the used oil by the filtration technique, sand and filter were utilized for gravimetric tar and solid particle removal in the absorbent. For the regeneration of the filtrated oil by the air-blown stripping, the filtrated oil and air (stripping agent) was heated at 175°C for 2 hours for gravimetric and light tar removal. Then, the regenerated oil was repeatedly used as an absorbent in the bubbling scrubber. Along 10 hours experiment, the used oil was totally regenerated four times at every 135 minutes by a series of the filtration and the air-blown stripping technique.

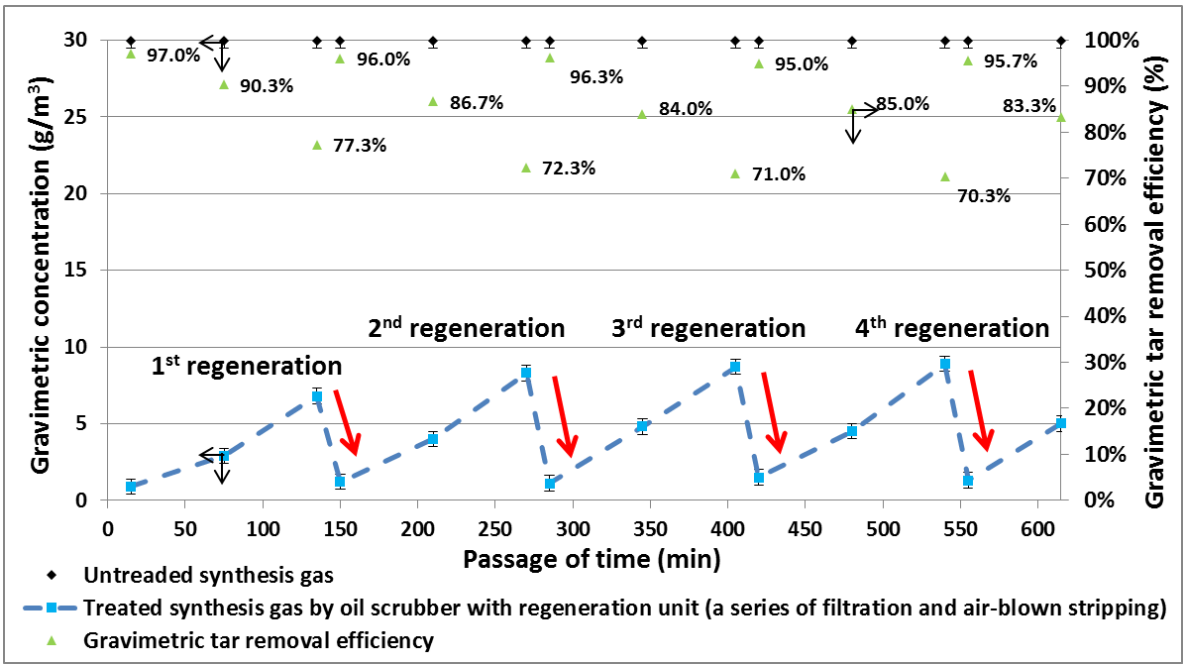

Figure 5.12. Gravimetric tar removal efficiency of the oil scrubber with the regeneration unit by a series of the filtration and the air-blown stripping during 10 hours

At the beginning, the gravimetric tar removal efficiency of fresh canola oil was decreased with the increase of the tar and other contaminants accumulation by 19.7% from 97.0% to 77.3% in the first 135 minutes as shown in Figure 5.12 and Table 5.3. After the first regeneration, the tar removal efficiency could be recovered by 18.7% to 96.0%. A series of the filtration and the air-blown stripping could recover the tar removal efficiency as same as the fresh canola oil performed. After that, the used oil after the absorption process were repeatedly regenerated by the same procedure at every 135 minutes. Table 5.3 indicated that the used oil was regenerated at 270, 405 and 540 minutes for

the 2nd, 3rd and 4th regeneration, respectively. For the second regeneration, the tar removal efficiency could be recovered by 24.0% to 96.3%. The same recovery efficiency was also observed at the 3rd and 4th regenerations, where the recovery efficiency maintained around 23.0% on the average and the tar removal efficiency was recovered to higher than 95%. The gravimetric tar removal efficiency in average during 10 hours was 85.7%. In addition, in every regeneration process, there was no significant drop of the tar removal efficiency. The tar removal efficiency after the regeneration process maintained between 96.3% and 95%. This is because the filtration technique mainly eliminated the gravimetric tar and other solid contaminants, while the air-blown stripping transferred the lower dew point of the gravimetric tar, which could not eliminated by the filtration, into the stripping agent. Therefore, the combination of both regeneration processes performed the desired results to recover the gravimetric removal efficiency. In addition, there was benefit of absorbent regeneration by the air-blown stripping. This is because the stripping agent is air, where the air with the stripped gravimetric tars could be used as the gasifying agent in the gasifier for energy recycling.

Table 5.3. Gravimetric tar removal efficiency of the oil scrubber with the regeneration unit by a series of the filtration and the air-blown stripping during 10 hours

Sampling time(min)	Accumulated volume of the cleaned synthesis gas(liter)	Tar removal amount (g/m^3)	Tar removal Efficiency (%)
0-15	15	29.1	97.0
60-75	75	27.1	90.3
120-135	135	23.2	77.3
135-150	150	28.8	96.0
195-210	210	26.0	86.7
255-270	270	21.7	72.3
270-285	285	28.9	96.3
330-345	345	25.2	84.0
390-405	405	21.3	71.0
405-420	420	28.5	95.0
465-480	480	25.5	85.0
525-540	540	21.1	70.3
540-555	555	28.7	95.7
600-615	615	25.0	83.3

5.4.2.2 Light tar removal performance during 10 hours

For this technique, the filtration only trapped the solid contaminants and gravimetric tar from the used oil, while the light tar still remained in the absorbent. The filtration technique gave no significant improvement for the removal of single aromatic hydrocarbon because the molecule sizes of them are smaller than canola oil. However, the air-blown stripping could effectively remove some gravimetric tar and most of the light tar especially single aromatic hydrocarbon. The Eq. (2) was utilized to calculate the tar removal efficiency of each light tar as well. Figure 5.13 illustrates the light tar concentration before and after the oil scrubber with the regeneration unit by a series of the filtration and the air-blown stripping during 10 hours. In the first 135 minutes, the removal efficiency of benzene, toluene, indene and phenol decreased with an increase of the tar and other contaminants accumulation by 15.7%, 3.8%, 2.9% and 7.3%, respectively, while the naphthalene removal maintained at 100% along 135 minutes. After the first regeneration, the removal efficiency of benzene, toluene, indene and phenol could be recovered by 9.9%, 1.9%, 3.1% and 7.4%, respectively. A series of the filtration and the air-blown stripping could recover the light tar removal efficiency as same as the fresh canola oil performed. After that, the used oil after the absorption process were repeatedly regenerated by the same procedure at every 135 minutes. The desirable recovery efficiency was also observed at the 2^{nd}, 3^{rd} and 4^{th} regeneration, where the recovery efficiency of benzene, toluene, indene and phenol maintained an average of 22.1%, 4.4%, 2.9% and 7.3%, respectively. The overall light tar removal efficiency during 10 hours was 78.0%, where the removal efficiency of benzene, toluene, naphthalene, phenol and indene in average was 70.6%, 95.1%, 100.0%, 85.8% and 97.2%, respectively. In every regeneration process, the same results from the gravimetric tar removal performance were also observed in this experiment because there was no significant drop of light tar removal efficiency. This is because the air-blown stripping transferred the light tar, which could not eliminated by the filtration, into the stripping agent that gave more area for the light tar to be absorbed. In addition, the air with the stripped light tars could be used as the gasifying agent in the gasifier for energy recycling as well.

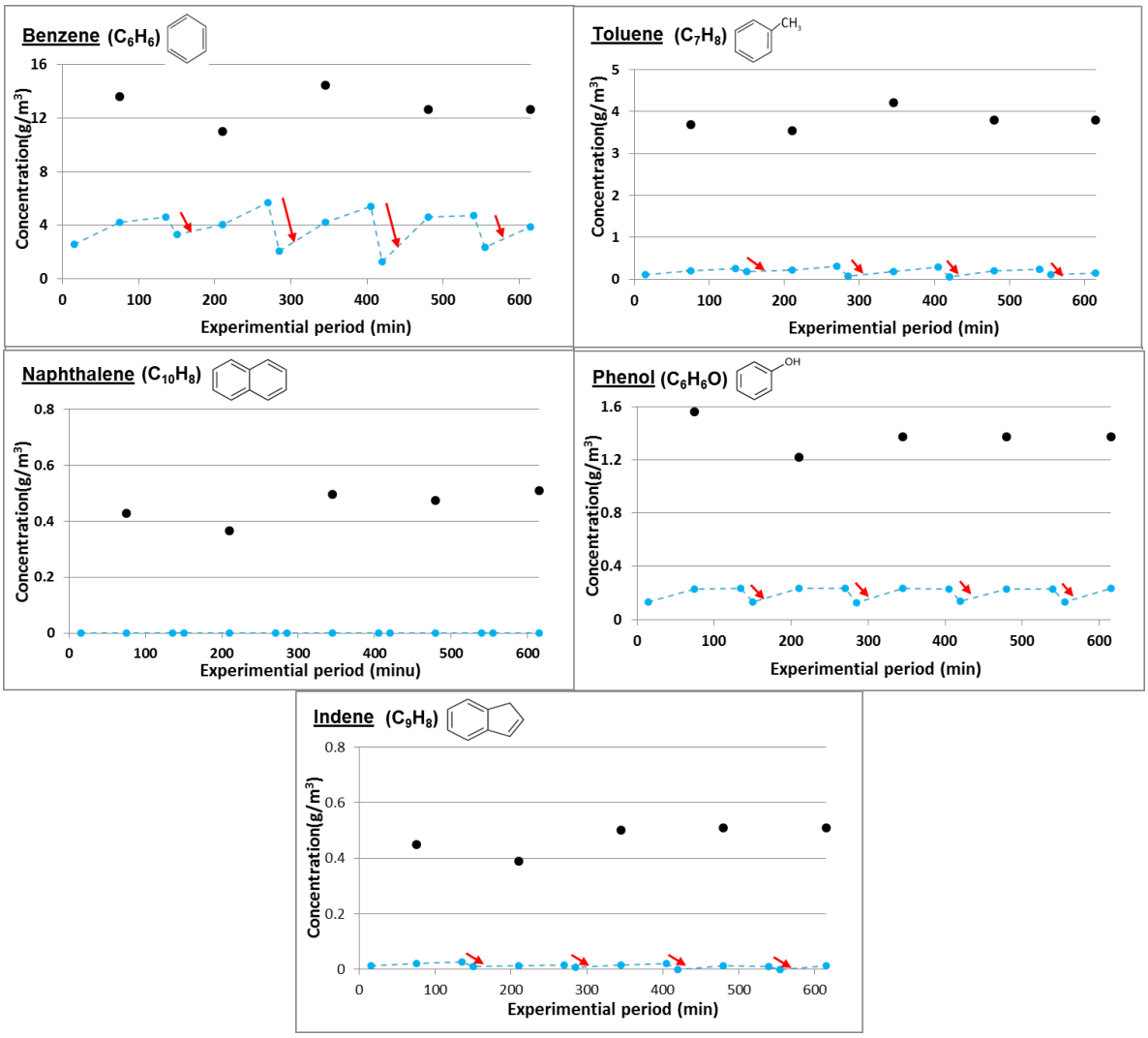

Figure 5.13. Light tar concentration before and after the oil scrubber with the regeneration unit by a series of the filtration and the air-blown stripping during 10 hours

● represents the concentration at the inlet of the scrubber (A_i) ● represents the concentration at the exit of the scrubber (B_i)

5.4.3 Tar removal capacity of a series of the filtration and the air-blown stripping compared with other techniques

5.4.3.1 Gravimetric tar removal capacity during 10 hours

According to the previous research [5.9], the tar removal capacity was investigated based on 10 hour-operation. The accumulated tar in the absorbent was measured by the tar mass balance. Then, the tar removal capacity in all cases was calculated by the following equations.

$$C_{tar,removal} = \frac{m_{tar,removal}}{V_{ab}} \quad (3)$$

$$m_{tar,removal} = \int_0^{600} f(x)dx - \int_0^{600} g(x)dx \quad (4)$$

Where $f(x)$ and $g(x)$express the polynomial equation derived from the inlet and outlet data respectively, x is the experimental period (min) and V_{ab} is the absorbent volume.

Figure 5.14 illustrates the gravimetric tar removal efficiency and the capacity of the absorbent without and with regeneration techniques during 10 hours. According to Tarnpradab et al. [5.9], the tar removal efficiency of non-regenerated oil was the lowest, where only 48.0% of the gravimetric tar was removed during 10 hours. The tar and other contaminants in the non-regenerated oil was the main reasons to obstruct the dissolution ability resulting in the continuous drop of the tar removal efficiency. Therefore, only 16.6 g of the gravimetric tar was absorbed in 1 liter of the non-regenerated oil. However, the utilization of the absorbent regeneration techniques could markedly improve the tar removal efficiency and capacity. The tar and other contaminants could be removed by the absorbent regeneration technique. The tar removal efficiency and capacity of the filtration technique was 78.0% and 26.8 g/L, while those of the centrifugal sedimentation was 83.0% and 28.8 g/L, respectively. However, both techniques could remove only the solid contaminants and the gravimetric tar, whose density was distinctly larger than the absorbent. The gravimetric tar, whose density was similar to or lower than the absorbent, was difficult to separate. The mechanisms of the air-blown stripping technique were different from the previous techniques, where the separation of low boiling point gravimetric tar and light tar was effectively done. Therefore, compared to previous techniques of the non-regenerated and regenerated oil, the absorbent regeneration by a series of the filtration and the air-blown stripping showed the best tar removal efficiency and capacity during 10 hours, where the gravimetric tar removal efficiency and capacity was 85.7% and 31.6 g/L, respectively. Compared to the non-regenerated oil, the gravimetric tar removal capacity of the filtration, the centrifugal sedimentation and a series of the filtration and the air-blown stripping showed 160.0%, 175.0% and 190.6% higher absorption capacity than the non-regenerated oil, respectively.

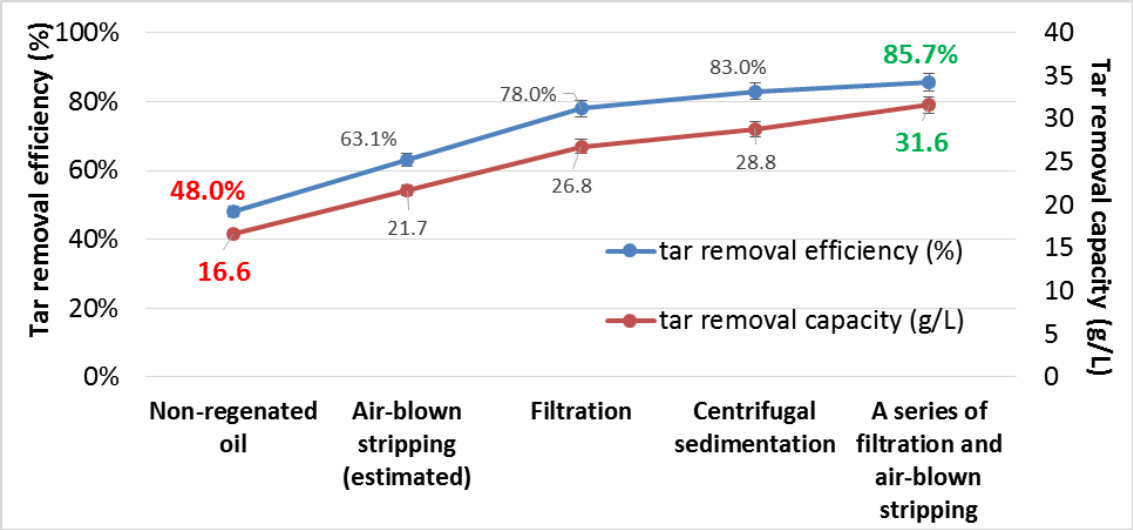

Figure 5.14. Gravimetric tar removal efficiency and capacity of the absorbent without and with the regeneration techniques during 10 hours

In addition, it can be seen that a series of the filtration and the air-blown stripping improved the tar removal capacity by 30.6% compared to the filtration only. It was assumed that the tar removal capacity of the air-blown stripping only was the tar removal capacity difference of a series of the filtration and the air-blown stripping and the filtration only. Therefore, the tar removal capacity of the air-blown stripping technique only might be 130.6% higher absorption capacity than the non-regenerated oil. This led to the lowest gravimetric tar removal capacity by the air-blown stripping technique only compared to other techniques. This could be explained by the following reasons. Most of the gravimetric tars have higher dew point temperature compared to the absorbent (canola oil) and the operational stripping temperature was controlled at 175°C in order to prevent the absorbent transferring to the stripping agent. Therefore, the small amount of the gravimetric tar could be transfer to the stripping agent, while no solid contaminant was removed. The air-blown stripping technique only was not recommended to regenerate absorbent which highly contained the gravimetric tar and solid contaminants. The combination with the filtration or the centrifugal sedimentation was required.

5.4.3.2 Light tar removal capacity during 10 hours

The Eq. (3) and (4) were utilized to calculate the tar removal capacity of each light tar as well. Figure 5.15 illustrates the light tar removal efficiency and the capacity of the absorbent without and

with the regeneration techniques during 10 hours. The light tar removal efficiency of the non-regenerated oil was the lowest, where benzene, toluene, naphthalene, phenol and indene were removed with the efficiency of13.1%, 60.5%, 90.6%, 48.4% and 73.1%, respectively. The light tar removal efficiency and capacity was just 28.5% and 8.3 g/L, respectively. The removal efficiency of the light tar could be improved with the absorbent regeneration techniques. The tar removal efficiency and the capacity of the filtration technique was 34.1% and 9.9 g/L, while the centrifugal sedimentation was 40.5% and 11.8 g/L, respectively. Compared to the non-regenerated oil, the tar removal capacity of the filtration and the centrifugal sedimentation showed 119.5% and 142.1% higher absorption capacity than the non-regenerated oil, respectively. It can be seen that the light tar removal efficiency and capacity of both techniques was not much improved according to the following reasons. The majority of light tars absorbed in the absorbent was benzene and toluene, whose molecular sizes are smaller than the canola oil molecule. Therefore, benzene and toluene were passed though the filter media, while benzene and toluene could not be sediment at the bottom by the centrifugal sedimentation because their density were lower than the absorbent (canola oil). Therefore, benzene and toluene removal efficiency and capacity were almost similar to the non-regenerated oil. The light tar removal efficiency and capacity of both techniques were slightly improved for naphthalene, phenol and indene removal due to the heavier molecular weight of phenol and indene. However, a series of the filtration and the air-blown stripping markedly improved the light tar removal capacity. The light tar removal efficiency of the air-blown stripping was 78.0%, while the light tar removal capacity was 22.8 g/L. Compared to the non-regenerated oil, the light tar removal capacity of a series of the filtration and the air-blown stripping showed 273.4% higher absorption capacity than the non-regenerated oil, respectively. This is because the air-blown stripping technique effectively removed the lower boiling point light tar. It can be seen that the benzene and toluene removal efficiency was 70.6% and 95.1%, which is much higher than the previous techniques. The phenol and indene removal efficiency was also higher than the previous techniques, while the naphthalene removal efficiency was similar to the centrifugal sedimentation technique performed. Therefore, the air-blown stripping technique only was recommended to regenerate absorbent which highly contains light tar especially single aromatic hydrocarbon (benzene and toluene). The combination with the filtration or the centrifugal sedimentation was not necessary.

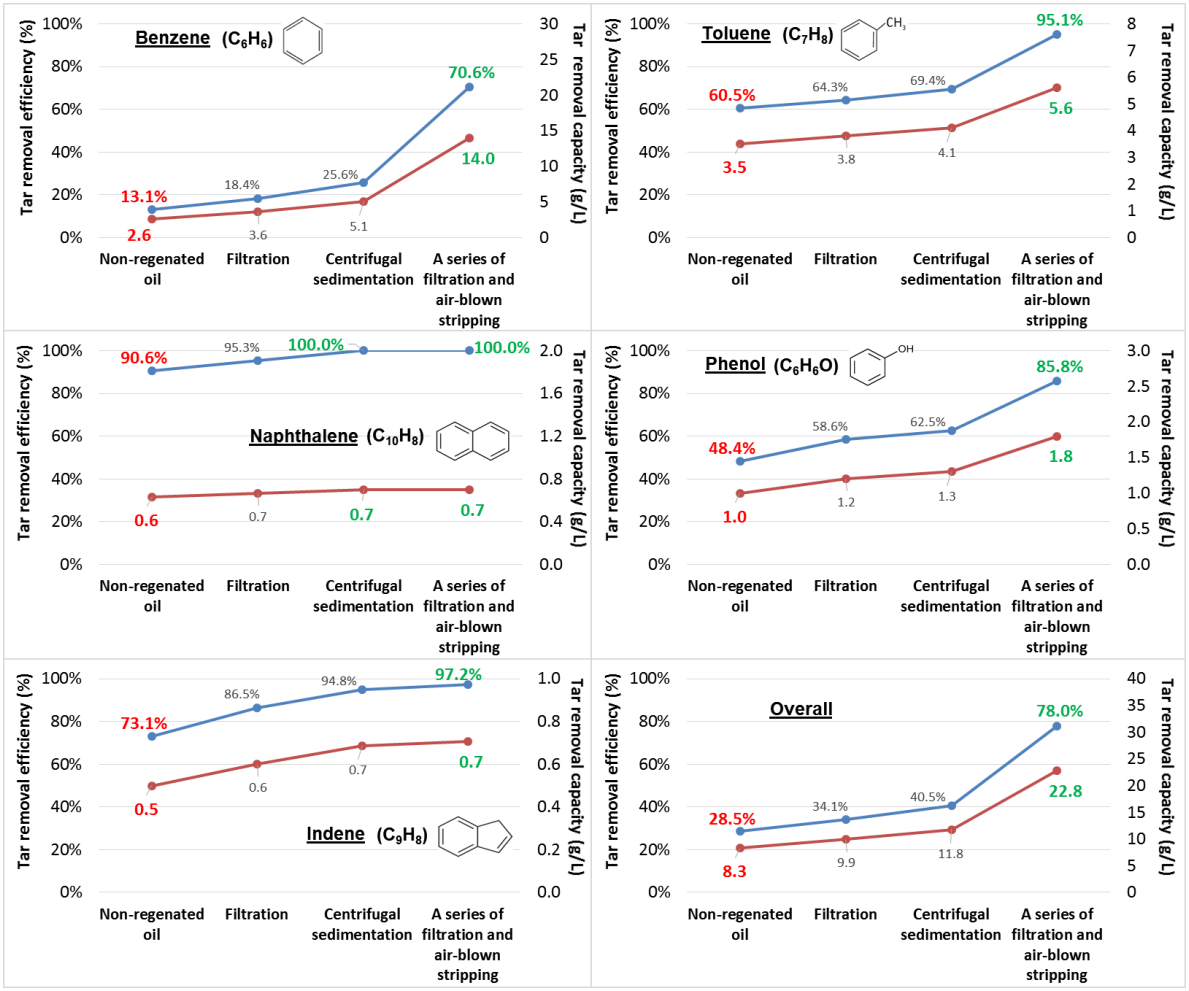

Figure 5.15. Light tar removal efficiency and capacity of the absorbent without and with the regeneration techniques during 10 hours

● represents the tar removal efficiency (%) ● represents the tar removal capacity (g/L)

5.5 Conclusion

The objective of this chapter was to investigate the tar removal efficiency and capacity of the bubbling scrubber with the regeneration technique by a series of the filtration and the air-blown stripping compared to without and with the regeneration techniques by the filtration and the centrifugal sedimentation. Canola oil was selected as an absorbent in this study. The syngas containing the gravimetric and light tar produced by the pyrolysis of Japanese cedar was introduced into the bubbling

scrubber during 10-hour experiment. The absorbent was regenerated by a series of the filtration and the air-blown stripping every 135 minutes for 10 hours. The tar in the syngas was measured before and after the scrubbing by both the wet and the dry methods. This chapter was divided into two parts; the air-blown stripping performance and the performance of the oil scrubber by a series of the filtration and the air-blown stripping for the absorbent regeneration during 10 hours.

For the air-blown stripping performance, the operational conditions of the air-blown stripping were investigated in order to effectively utilize this technique. Two main parameters considering in this experiment are the stripping temperature and the operational time. According to the limitation of the self-volatilization in the absorbent, 175°C stripping temperature and 2 hours operational time were selected in this study with 23.5% and 72.5% of the gravimetric and light tar stripping efficiency. The air-blown stripping was designed to remove the low dew point gravimetric tar, while the filtration was designed to remove the heavier tar and solid contaminants.

For the performance of the oil scrubber by a series of the filtration and the air-blown stripping for the absorbent regeneration during 10 hours, the gravimetric tar removal efficiency of the air-blown stripping was 85.7%, while the gravimetric tar removal capacity was 31.6 g/L. Compared to other techniques, the tar removal capacity of a series of the filtration and the air-blown stripping was the highest, which could be ranked in the following order; a series of the filtration and the air-blown stripping (190.6%) > the centrifugal sedimentation (175.0%) > the filtration (160.0%) > the air-blown stripping (130.6%). Therefore, the air-blown stripping technique only was not recommended to regenerate the absorbent which highly contained the gravimetric tar and solid contaminants. The combination with the filtration or the centrifugal sedimentation was required. For the light tar, removal efficiency of the air-blown stripping was 78.0%, while the gravimetric tar removal capacity was 22.8 g/L. The light tar removal capacity could be ranked in the following order; a series of the filtration and the air-blown stripping (273.4%) > the centrifugal sedimentation (142.1%) > the filtration (119.5%). Therefore, the air-blown stripping technique only was enough to regenerate the absorbent which highly contained light tar especially single aromatic hydrocarbon. The combination with the filtration or the centrifugal sedimentation was not necessary.

In summary, this chapter shows attractive results for utilizing oil regeneration by a series of the filtration and the air-blown stripping. The gravimetric and light tar removal efficiency and capacity markedly improved compared to other regeneration techniques. In addition, there was no significant change of the gravimetric and light tar removal efficiency after each regeneration compared to new oil. Therefore, there is a possibility for utilizing regenerated absorbent without changing it to the new one for a longer period of the operation. Furthermore, the air with the stripped gravimetric and light tars could be used as the gasifying agent in the gasifier for energy recycling.

5.6 Reference

[5.1] Jin H, Yang S, He G, Liu D, Tong Z, Zhu J. Gas--liquid mass transfer characteristics in a gas--liquid--solid bubble column under elevated pressure and temperature. Chinese J Chem Eng 2014;22:955–61.

[5.2] Ferreira A, Ferreira C, Teixeira JA, Rocha F. Temperature and solid properties effects on gas--liquid mass transfer. Chem Eng J 2010;162:743–52.

[5.3] Yoon S, Kang YT. Mass transfer enhancement in non-Brownian particle suspension under a confined shear. Int J Heat Mass Transf 2013;60:114–24.

[5.4] Tarnpradab T, Unyaphan S, Takahashi F, Yoshikawa K. Tar removal capacity of waste cooking oil absorption and waste char adsorption for rice husk gasification. Biofuels 2016;7:401–12.

[5.5] Cancino-Madariaga B, Aguirre J. Combination treatment of corn starch wastewater by sedimentation, microfiltration and reverse osmosis. Desalination 2011;279:285–90.

[5.6] Sutherland K. Pharmaceuticals: Filtration plays key role in pharmaceuticals and biotechnology. Filtr Sep 2011;48:16–9.

[5.7] Fu P, Wang F, Ma L, Yang X, Wang H. Fine particle sorting and classification in the cyclonic centrifugal field. Sep Purif Technol 2016;158:357–66.

[5.8] Roush DJ, Lu Y. Advances in primary recovery: centrifugation and membrane technology. Biotechnol Prog 2008;24:488–95.

[5.9] Tarnpradab T, Unyaphan S, Takahashi F, Yoshikawa K. Improvement of the biomass tar removal capacity of scrubbing oil regenerated by mechanical solid--liquid separation. Energy & Fuels 2017.

[5.10] Sadeghifar H. Simple and rapid determination of effective Murphree component efficiencies for operating absorbers, strippers and distillation columns filled with any type of trays. Sep Purif Technol 2015;139:104–8.

[5.11] Gao J, Yin J, Zhu F, Chen X, Tong M, Kang W, et al. Orthogonal test design to optimize the operating parameters of CO 2 desorption from a hybrid solvent MEA-Methanol in a packing stripper. J Taiwan Inst Chem Eng 2016;64:196–202.

[5.12] Zhang X, Fu K, Liang Z, Rongwong W, Yang Z, Idem R, et al. Experimental studies of regeneration heat duty for CO 2 desorption from diethylenetriamine (DETA) solution in a stripper column packed with Dixon ring random packing. Fuel 2014;136:261–7.

[5.13] Ghoreyshi AA, Sadeghifar H, Entezarion F. Efficiency assessment of air stripping packed towers for removal of VOCs (volatile organic compounds) from industrial and drinking waters. Energy 2014;73:838–43.

[5.14] Stirling TE, Ackerman JR. Air stripping of liquids using high intensity turbulent mixer 1991.

[5.15] Singh SP, Wilson JH, Counce RM, Lucero AJ, Reed GD, Ashworth RA, et al. Removal of volatile organic compounds from groundwater using a rotary air stripper. Ind Eng Chem Res 1992;31:574–80.

[5.16] Kundu A, SenGupta B, Hashim MA, Redzwan G. Taguchi optimisation approach for chromium removal in a rotating packed bed contractor. J Taiwan Inst Chem Eng 2015;57:91–7.

[5.17] Valdés FJ, Hernández MR, Catalá L, Marcilla A. Estimation of CO 2 stripping/CO 2 microalgae consumption ratios in a bubble column photobioreactor using the analysis of the pH profiles. Application to Nannochloropsis oculata microalgae culture. Bioresour Technol 2012;119:1–6.

[5.18] Bergman PCA, van Paasen SVB, Boerrigter H. The novel “OLGA” technology for complete tar removal from biomass producer gas. Pyrolysis Gasif. biomass waste, Expert Meet. Strasbourg, Fr., vol. 30, 2002.

[5.19] Kiel JHA, Van Paasen SVB, Neeft JPA, Devi L, Ptasinski KJ, Janssen F, et al. Primary measures to reduce tar formation in fluidised-bed biomass gasifiers. ECN, ECN-C-04-014 2004.

[5.20] Van Paasen SVB, Kiel JHA, Neeft JPA, Knoef HAM, Buffinga GJ, Zielke U, et al. Guideline for sampling and analysis of tar and particles in biomass producer gases. Energy Res Cent Netherlands, ECN-C-02-090 2002.

Chapter 6

Conclusion and recommendation

6.1 Conclusion

This research focuses on the physical tar removal using oil-based absorption in a scrubber for biomass gasification. The study on the tar removal by the absorption technique is divided into three main aspects that is the absorbent selection, the scrubber type and the absorbent regeneration. The physical gas cleaning techniques and developments were investigated based on the gasification temperature of 800°C, which is an operation condition of both the laboratory and pilot-scale experiment.

For the absorbent selection, Chapter 2 first investigated the characteristics of tar in syngas and found that the majority of tar was ranked in the following order; non-polar tar (60%) > condensable tar (25%) and polar tar (15%). Then, the tar removal performance of pure vegetable oil was compared to the emulsified oil. It was found that the emulsified oil performs better tar removal than pure vegetable oil in all water content proportions. The emulsified oil mainly enhanced the gravimetric tar removal performance by increasing the polar tar removal efficiency with no significant decrease of the light tar removal efficiency. The choice of the absorbent for biomass tar removal can be ranked in the following order; 7.5% emulsified oil > vegetable oil > waste cooking oil > water.

For the scrubber type, Chapter 3 first investigated a fundamental study on the microbubbles formation utilizing a venturi scrubber in order to optimize the operational condition at the best absorption surface area. It was found that the specific absorption surface area at d/D = 0.17 was the lowest due to the bubble coalescence while the highest one was achieved at d/D = 0.42 with the highest oil throat velocity. Then, the tar removal performance of venturi scrubber were investigated and found that the tar removal efficiency linearly increased with the increase of the specific absorption surface area. The gravimetric removal efficiency of the venturi scrubber was higher than that of the bubbling scrubber at all specific absorption surface areas, while there was no light tar observed. The feasibility of the venturi scrubber for tar removal has been proved at the pilot-scale gasifier by the use of physical gas cleaning system comprised of the following; a series of a cyclone, a ceramic filter, an air cooler, water coolers, the venturi scrubber and the packed bed adsorber. This system could achieve the syngas quality requirement for internal combustion engines. In Chapter 4, the investigation on the venturi scrubber was further studied, where the relationship between the

Reynolds number and the tar removal performance was focused. It could be concluded that the performance of the venturi scrubber was also better than the bubbling scrubber at all values of the Reynold numbers. The optimum condition for tar removal was at the highest Reynolds number for both of vegetable oil and emulsified oil. Furthermore, the overall volumetric liquid-slide mass-transfer coefficient also increased with the increase in the syngas Reynolds number. The performance of the scrubber for biomass tar removal can be ranked in the following order; venturi scrubber > bubbling scrubber with mixing stirrer > packed-bed scrubber.

For the absorbent regeneration, Chapter 5 studied the tar removal efficiency and capacity of the oil scrubber combining the regeneration unit (a series of the filtration and the air-blown stripping) in order to upgrade and prolong the absorbent lifetime and then compared to other techniques (non-regeneration, filtration and centrifugal sedimentation). The gravimetric and light tar removal efficiency and capacity of a series of the filtration and the air-blown stripping markedly improved compared to other regeneration techniques. In addition, there was no significant change of the gravimetric and light tar removal efficiency after each regeneration compared to new oil. Therefore, there is a possibility for utilizing regenerated absorbent without changing it to the new one for a longer period of the operation. Furthermore, the air with the stripped gravimetric and light tars could be used as the gasifying agent in the gasifier for energy recycling. The performance of the absorbent regeneration technique can be ranked in the following order; a series of the filtration and the air-blown stripping > the centrifugal sedimentation > the filtration > non-regeneration.

6.2 Recommendation

In the pilot-scale experiment, the physical gas cleaning system could reduce the tar concentration lower than 0.1 g/Nm^3, which met the requirement for internal combustion engines. The flow diagram and the operational condition of the low-cost and effective physical gas cleaning unit in a commercial-scale gasifier should be designed as seen in Figure 6.1 and Table 6.1, respectively. It consisted of a series of a cyclone, a ceramic filter, an air cooler, a cooking oil based venturi scrubber with a regenerative unit (a series of the filtration/centrifuge and the air-blown stripping) and a packed bed adsorber, respectively. Soot and particles are trapped by the cyclone and the ceramic filter. Then, some of the gravimetric and light tar are condensed when passing through the air cooler. Finally, all of the gravimetric and light tar are absorbed and adsorbed by the venturi scrubber and the packed bed adsorber, respectively. The used absorbent is regenerated by using a series of the filtration unit/centrifuge and the air-blow stripping unit to prolong the absorbent lifetime. The advantage of filtration unit is uncomplicated and low-cost, which is appropriate to utilize in rural area. However, this

technique might cause the periodic cleaning or changing of the filtration media due to the accumulation of tar in the filtration media, which can be simply inspected by the increase in the pressure drop between the inlet and the outlet of the filtration unit. To prevent this running cost, the optional technique is the centrifugal sedimentation by centrifuge, which could be utilized instead of the filtration, because the performance and the removal mechanism of both techniques are similar. The hot air from the air cooler process could be used as the stripping agent in the air-blown stripping unit.

In addition, in case of pure cooking oil, the air with the stripped gravimetric and light tars could be used as the gasifying agent in the gasifier for energy recycling. In case of emulsified oil, according to the operational condition of the air-blown stripping (175°C, 2 hours), all water in the emulsified oil will be evaporated. Therefore, water make-up is necessary to maintain the 7.5% water content in oil. The by-product after the air-blown stripping of emulsified oil, which is composed of hot air, tar and steam, could be used as the gasifying agent in the gasifier for the energy recycling as well. However, there is a possibility that the remaining tar in the water phase of the emulsified oil after the air-blown stripping of the emulsified oil might be dissolved in the oil phase due to the water evaporation, which might cause the decrease of the tar removal performance of the regenerated emulsified oil. Therefore, the performance of the air-blown stripping in the emulsified oil should be further investigated.

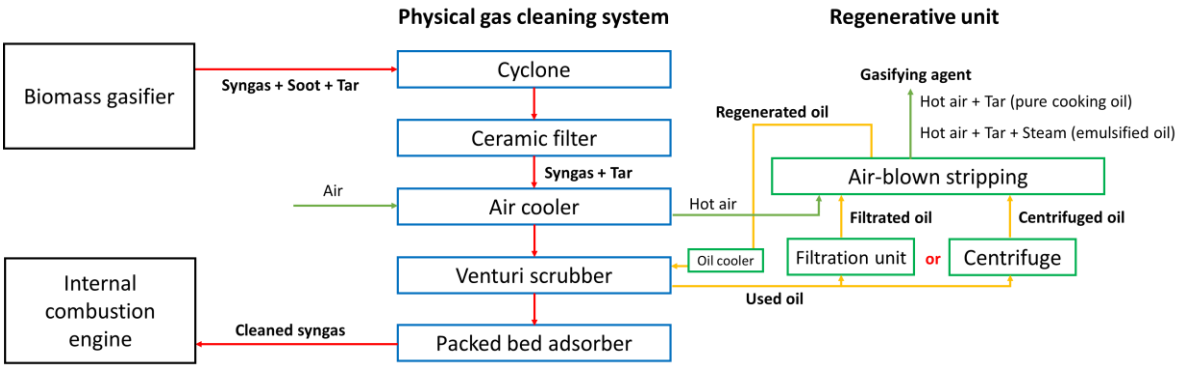

Figure 6.1. Recommended flow diagram of the gas cleaning system using only physical method with the regeneration unit in a commercial-scale gasifier

Table 6.1. Operational condition of the gas cleaning system using only physical method with the regeneration unit in a commercial-scale gasifier

Unit	Operational condition
1. Gasifier (Bubbling fluidized bed gasifier)	
- Under bed temperature	800°C
- Bed temperature	850°C
- Bed material	silica sand
- Preheated fuel	natural gas
- Feed stock	biomass (260 kg/h, 16.4 MJ/kg)
- Gasifying agent	air (375 Nm^3/h)
- Equivalent ratio	0.35
- Syngas heating value	4 MJ/m^3
- Tar concentration	12 g/Nm^3
2. Cyclone	
- Cyclone temperature	>350°C
3. Ceramic filter	
- Ceramic filter temperature	>350°C
4. Air cooler	
- Air inlet temperature	ambient temperature (30°C)
- Air outlet temperature	175°C
5. Venturi scrubber	
- Absorbent material	pure cooking oil or 7.5% emulsified oil
- Absorbent volume	50 litter
- Absorbent temperature	50°C
- Throat ratio	0.42
- Oil throat velocity	>4 m/s
6. Filtration unit (packed bed filtration)	
- Filtration media	filter bed and sand bed
7. Centrifuge	
- Rotation speed	10,000 rpm
8. Air-blown stripping (bubbling type)	
- Stripping agent	Hot air from air cooler
- Stripping temperature	175°C
- Holding time	2 hours
9. Oil cooler	
- Oil inlet temperature	175°C
- Oil outlet temperature	50°C
10. Packed bed adsorber	
- Adsorber material	Gasified char (by-product)
- Adsorber amount	15 kg
- Adsorber temperature	30°C
11. Internal combustion engine	
- Syngas heating value	4 MJ/m^3
- Tar concentration	<100 mg/Nm^3

Appendix **A**

The saturation and deterioration point of non-regenerated oil for tar removal

There were two essential points for the analysis; the saturation point (the point at which the passage of time does not affect the tar removal efficiency) and the breakpoint (the point at which the deterioration of non-regenerated oil starts and the change to new oil is required). Figure A1 shows the absorption capacity when the non-regenerated oil was continuously absorbing tar until reaching its saturation point in 7th of the experiment which is 29% of the tar removal efficiency. In 8th, 9th and 10th hour of the experiment, the tar removal efficiency was 29% 29% and 31%, respectively. Between 7th and 10th hour of the experiment, the difference percentage of the tar removal efficiency was only 2%. Therefore, 7th hour of the experiment was the saturation point of the non-regenerated oil in this study, where the removed tar was from the condensation of the low-dew-point tar. For the breakpoint from the breakthrough curve, there was a large change of the performance from one to three hours into the experiment. A total of 20% and 22% of the tar removal efficiency were different in every hour from this period of the experiment which, in total, was 42% of the performance drop indicating that it was the timing that non-regenerated reached the breakpoint and should be changed to the new one. Therefore, it can be seen that non-regenerated oil reached the breakpoint in the 2nd hour of the experiment due to the huge percentage drop in this period.

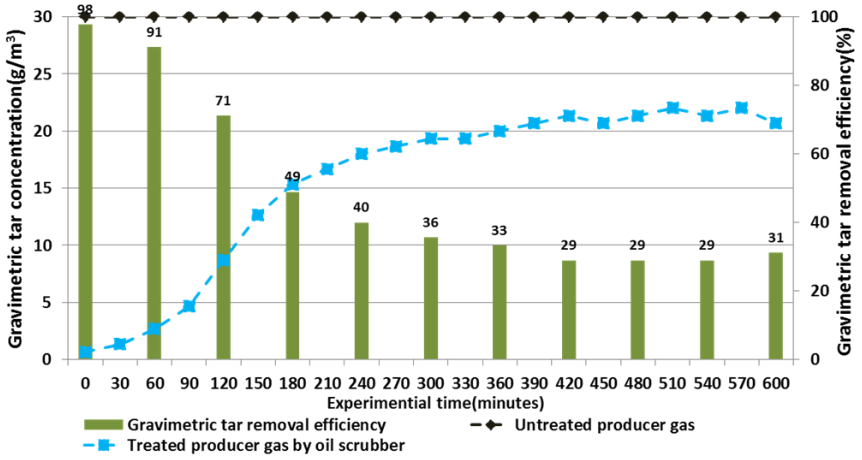

Figure A1. Gravimetric tar concentration and the gravimetric tar removal efficiency over 600 minutes of the experiment period

Appendix **B**

Numerical calculation procedure for the K_La^0 determination

The multiphase flow of syngas-absorbent was assumed to be operated under the following conditions.

1. The syngas and absorbent are perfectly mixed (homogenous gas-liquid mixing)
2. The gas back mixing is negligible.
3. The process is isothermal and atmospheric pressure.
4. The gas flow rate (F_G) is constant between the inlet and outlet of the scrubber.
5. No chemical reaction happens in the liquids phase (physical absorption).
6. There is no radial concentration gradient in both phases.

The boundary and initial conditions are:

1. C_G at the inlet = $C_{G,i}$ = constant
2. C_L at t_0 = $C_{L,0}$= 0
3. Absorbent volume (V) = constant

Where C_G is tar concentration at the inlet of scrubber, $C_{L,0}$ is tar concentration in fresh oil

The variables are:

1. C_G at the outlet = $C_{G,o}$ = *f*(t)
2. C_L at any time = C_L^t

Where $C_{G,o}$ is tar concentration at the outlet of scrubber and C_L^t is tar concentration in oil at any time

Mass balance

The mass balance can be written:

Gas inlet = Gas outlet + transfer

$$F_G C_{G,i} = F_G C_{G,o} + V\frac{dC_L}{dt} \quad \text{(B1)}$$

$$F_G\left(C_{G,i} - C_{G,o}\right) = V\frac{dC_L}{dt} \quad \text{(B2)}$$

Eq. (B2) can be integrated over time proceeding by discretization considering a small time interval (Δt):

$$F_G(C_{G,i} - \bar{C}_{G,o}) = \frac{V}{\Delta t}(C_L^{t+\Delta t} - C_L^t) \quad \text{(B3)}$$

Where $\bar{C}_{G,o}$ is the average gravimetric tar concentration at the outlet measured during (Δt)

$$\bar{C}_{G,o} = \frac{C_{G,o}^{t+\Delta t} + C_{G,o}^t}{2} \quad \text{(B4)}$$

It leads to

$$C_L^{t+\Delta t} = C_L^t + F_G\frac{\Delta t}{V}(C_{G,i} - \bar{C}_{G,o}) \quad \text{(B5)}$$

The liquid concentration over time can be calculated through Eq. (B6)

$$C_L^t = \frac{F_G}{V}\sum_{j=1}^{n}\Delta t(C_{G,i} - \frac{C_{G,o}^{t+\Delta t} + C_{G,o}^t}{2}) \quad \text{(B6)}$$

Where j is the number of time interval

Mass transfer rate equation

The mass transfer rate (*dJ*) per section (S) of gas-liquid contractor (mol s^{-1} m^{-2}) is calculated through Eq. (B7)

$$\frac{dJ}{S} = F_G\frac{dC_G}{S} = K_L a^0\left(C_L^{eq} - C_L\right)dz \quad \text{(B7)}$$

Where K_L is the overall liquid-side mass-transfer coefficient (m s^{-1}), a^0 is the interfacial area relative to the liquid volume V (m^{-1}), C_L^{eq} is the liquid concentration (mol m^{-3}) at the gas–liquid interface at the equilibrium with the gas concentration. It can be easily calculated for dilute solutions using the Henry's law (Eq. (B8))

$$C_L^{eq} = \frac{C_G}{H_d} \quad \text{(B8)}$$

H_d is the dimensionless Henry's law constant of the treated VOC in the selected solvent (partition coefficient). It leads to:

$$F_G dC_G = K_L a^0 \left(\frac{C_G}{H_d} - C_L\right) S dz \quad \text{(B9)}$$

After integration during a time-interval Δt:

$$F_G \int_{C_{G,i}}^{\bar{C}_{G,o}} dC_G = K_L a^0 \int_0^Z \left(\frac{C_G}{H_d} - C_L\right) S dz \quad \text{(B10)}$$

The left-hand term can be easily integrated whereas the right-hand term must be solved using a variable modification. The solution is well-known and can be found in many book dealing with gas–liquid mass-transfer. It involves the logarithmic average concentration assuming a gas plug flow and a perfectly mixed liquid phase:

$$F_G\left(C_{G,i} - \bar{C}_{G,o}\right) = K_L a^0 V \frac{\left(\frac{C_{G,i}}{H_d} - \bar{C}_L\right) - \left(\frac{\bar{C}_{G,o}}{H_d} - \bar{C}_L\right)}{ln\frac{\left(\frac{C_{G,i}}{H_d} - \bar{C}_L\right)}{\left(\frac{\bar{C}_{G,o}}{H_d} - \bar{C}_L\right)}} \quad \text{(B11)}$$

Where $\bar{C}_L$ is the average liquid concentration during a time-interval Δt:

$$\bar{C}_L = \frac{C_L^{t+\Delta t} + C_L^t}{2} \quad \text{or } C_L^{t+\Delta t} = 2\bar{C}_L - C_L^t \quad \text{(B12)}$$

After mathematical resolution, the liquid and outlet gas concentrations at t + Δt are calculated through Eq. (B13) and (B14), respectively.

$$C_L^{t+\Delta t} = 2\frac{\frac{C_{G,i}}{H_d}(1-\exp(B)) - 2AC_L^t \exp(B)}{1-\exp(B)(1+2A)} - C_L^t \quad \text{(B13)}$$

Where $A = \frac{V}{H_d F_G \Delta t}$ and $B = AK_L a^0 \Delta t = \frac{K_L a^0 V}{H_d F_G}$

$$C_{G,o}^{t+\Delta t} = 2\bar{C}_{G,o} - C_{G,o}^t = 2\left(C_{G,i} - \frac{V}{F_G \Delta t}\left(C_L^{t+\Delta t} - C_L^t\right)\right) - C_{G,o}^t \quad \text{(B14)}$$

To initialize the resolution, $C_{G,o}$ at t = 0 must be calculated. In this case, Eq. (B11) can be rewritten considering that $C_L = 0$:

$$F_G\left(C_{G,i} - C_{G,o}^{t=0}\right) = \frac{K_L a^0 V}{H_d} \frac{\left(C_{G,i} - C_{G,o}^{t=0}\right)}{ln\frac{C_{G,i}}{C_{G,o}^{t=o}}} \quad \text{(B15)}$$

$$C_{G,o}^{t=0} = C_{G,i} \exp\left(-\frac{K_L a^0 V}{F_G H_d}\right) \quad \text{(B16)}$$

Henry's law constant determination

H_d can be deduced from the liquid concentration at the plateau of the breakthrough curve corresponding to the gas–liquid equilibrium.

$$H_d = \frac{C_{G,i}}{C_{L,saturation}} \quad \text{(B17)}$$

K_La^0 determination

In order to calculate the overall volumetric liquid-side mass-transfer coefficients (K_La^0), Figure 4.6 illustrates the calculation procedure of the overall volumetric liquid-side mass-transfer coefficients (K_La^0). The simulation of the concentration gradient of the gravimetric tar was done as following. First, the area under the curve of the experimental results was calculated for 1 hour-operation. After that, K_La^0 was trialed to simulate the concentration gradient of the gravimetric tar for 1 hour-operation as seen in the concentration gradient simulation loop. Then, the numerical resolution using the Excel Solver was utilized to find the corrected K_La^0. The numerical resolution finishes when the area under the curve of the experimental data and the model is equalized.

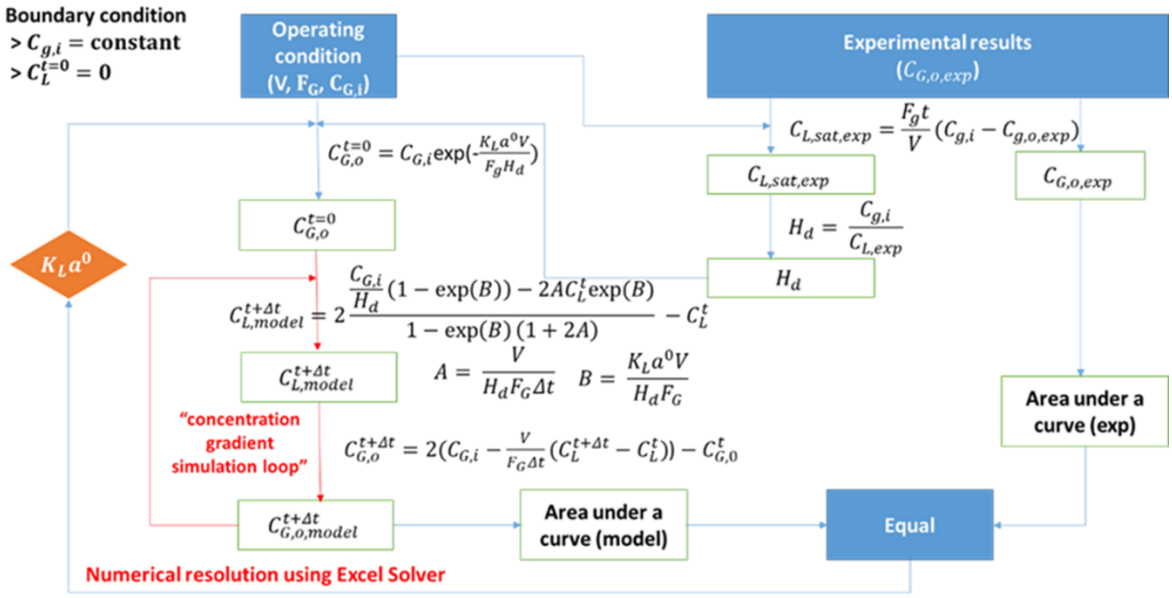

Figure B1. Numerical calculation procedure for the K_La^0 determination